UNIVERSIDAD DE CONCEPCIÓN

Centro de Investigación en Ingeniería Matemática (CI^{2}MA)

A posteriori error analysis of two mixed formulations for a coupled Brinkman–Forchheimer and convection-diffusion-reaction system

Alonso J. Bustos, Sergio Caucao

PREPRINT 2026-15

SERIE DE PRE-PUBLICACIONES

A posteriori error analysis of two mixed formulations for a coupled Brinkman–Forchheimer and convection-diffusion-reaction system*

Alonso J. Bustos† Sergio Caucao‡

Abstract

In this paper, we consider the mixed-primal and fully-mixed Banach spaces-based formulations recently proposed for the coupling of the stationary Brinkman–Forchheimer and convection-diffusion-reaction equations, and develop reliable and efficient residual-based *a posteriori* error estimators for both two- and three-dimensional versions of the associated mixed finite element schemes. For the reliability analysis, we employ the global inf-sup conditions associated with each uncoupled problem, combined with appropriate small data assumptions, stable Helmholtz decompositions in nonstandard Banach spaces, and the local approximation properties of the Raviart–Thomas and Clément interpolants. Efficiency is established using inverse inequalities, bubble-function localization in local L^p-spaces, and auxiliary estimates available in the literature. Finally, several numerical experiments are presented, confirming the theoretical properties of the proposed estimators and illustrating the performance of the corresponding adaptive algorithms, including the recovery of optimal convergence rates and the ability to handle challenging physical regimes.

Key words: Brinkman–Forchheimer, convection-diffusion-reaction, pseudostress-velocity formulation, mixed finite element methods, *a posteriori* error analysis

Mathematics subject classifications (2020): 65N30, 65N12, 65N15, 35Q79, 80A19, 76R50, 76D07

1 Introduction

Recently, in [6], two Banach spaces-based mixed finite element methods for the transport of chemical species in a saturated porous medium were introduced and analyzed. In this model, the velocity field is governed by the stationary Brinkman–Forchheimer (BF) equations, which in turn drives the evolution of the concentration via a convection-diffusion-reaction (CDR) equation. Within that framework, a pseudostress-velocity mixed formulation was proposed for the BF equations, while two distinct strategies were developed for the CDR equation. Specifically, the first approach consists of a mixed-primal formulation for the coupled problem, whereas the second one introduces the diffusion vector as an additional unknown, resulting in a fully-mixed formulation in a Banach space setting. A key distinction

*This research was partially supported by ANID-Chile through Centro de Modelamiento Matemático (FB210005) and Fondecyt project 1250937; by Grupo de Investigación en Análisis Numérico y Cálculo Científico (GIANuC^2), Universidad Católica de la Santísima Concepción; and by Centro de Investigación en Ingeniería Matemática (CI^{2}MA), Universidad de Concepción.

†GIANuC^2 and Departamento de Matemática y Física Aplicadas, Universidad Católica de la Santísima Concepción, Casilla 297, Concepción, Chile, and CI^{2}MA, Universidad de Concepción, Casilla 160-C, Concepción, Chile, email: alonso.bustos@ucsc.cl.

‡GIANuC^2 and Departamento de Matemática y Física Aplicadas, Universidad Católica de la Santísima Concepción, Casilla 297, Concepción, Chile, email: scaucao@ucsc.cl.

between these strategies lies in the treatment of the boundary conditions: whereas the mixed-primal approach enforces the Dirichlet condition for the concentration via a suitable Lagrange multiplier, the fully-mixed formulation circumvents this requirement entirely, incorporating it naturally as a functional on the right-hand side of the weak formulation. The resulting schemes are recast as fixed-point equations, whose well-posedness is established by employing recently developed solvability results for perturbed saddle-point problems in Banach spaces, the Babuška–Brezzi theory, the Banach–Nečas–Babuška theorem, and the Banach fixed-point theorem. Regarding the finite element discretization, the proposed schemes utilize Raviart–Thomas elements for both the pseudostress tensor and the diffusion vector, and discontinuous polynomial elements for the velocity field. For the concentration, Lagrange finite elements are employed in the mixed-primal approach, while discontinuous polynomials are used in the fully-mixed case.

Although stability, convergence, and optimal *a priori* error estimates were also derived in [6], it is well known that the discretization of nonlinear problems on complex geometries, as well as the approximation of solutions exhibiting singularities or steep gradients, poses significant numerical challenges and often deteriorates the theoretically optimal convergence rates. Adaptive algorithms driven by *a posteriori* error estimates provide a key mechanism to recover optimal convergence rates in standard Galerkin discretizations, including finite element and mixed finite element methods, and their analysis has been extensively studied in the literature. Foundational contributions include the pioneering works [2, 9, 10], which established the theoretical framework for residual-based *a posteriori* error estimation for saddle-point and mixed problems, and [39], which provided a comprehensive treatment of adaptive mesh-refinement techniques. These ideas were subsequently extended to augmented mixed and pseudostress-based methods [31, 15, 28, 22], as well as to coupled fluid flow and transport problems [24, 4, 16, 29]. In the context of the CDR equation, *a posteriori* error analysis has also received considerable attention, particularly for convection-dominated regimes. Seminal contributions in this direction are due to Verfürth [38], later refined to yield estimates that are fully robust with respect to convection dominance and uniform with respect to the magnitude of the zero-order reaction term [40]. More recently, a mixed formulation for the CDR equation was considered in [25], where suitable residual-based *a posteriori* error estimators were derived. Specifically, the authors introduce a diffusion-type vector as an additional unknown, present centered and upwind-weighted mixed schemes, and develop the *a posteriori* error analysis via postprocessing techniques, thereby avoiding Helmholtz decompositions and dual arguments. Nevertheless, the analysis therein is restricted to the lowest-order case, and the error estimates are measured only in the L^2-norm of both the diffusion vector and the concentration.

It should be noted that most of the aforementioned works are set within standard Hilbert space frameworks, where nonlinearities are typically handled via augmentation techniques. In contrast, working in Banach space settings avoids such augmented formulations, but makes the derivation of reliability and efficiency estimates substantially more involved, as classical tools such as orthogonality arguments and the Riesz representation theorem are no longer directly available. First steps in this direction were taken in [13] and [7], where the authors derived reliable and efficient residual-based *a posteriori* error estimators for the mixed finite element method applied to the Navier–Stokes/Darcy–Forchheimer coupled model and to the Navier–Stokes model, respectively. Key contributions of these works include novel Helmholtz decompositions adapted to the Banach space framework for the reliability analysis, as well as inverse inequalities and bubble function techniques for the efficiency bounds. These tools have since become cornerstones for the *a posteriori* error analysis of mixed finite element methods in Banach spaces and have subsequently inspired, for example, the development of estimators for Boussinesq-type models [30] and for the coupled Brinkman–Forchheimer and double-diffusion equations [14].

In the context of flows in porous media, *a posteriori* error analysis has been investigated in both Hilbert and Banach space settings across a range of models, including the Darcy–Forchheimer [35], Brinkman–Darcy [5], and Brinkman–Darcy–Forchheimer [34] problems, as well as coupled formulations such as the Brinkman–Navier–Stokes system with an advection-diffusion equation [3], the Brinkman–Forchheimer system with double-diffusive convection [12], and the Brinkman–Forchheimer/Darcy problem [18]. Most closely related to the present work are [11], where the tools of [13, 7] were employed to derive a residual-based *a posteriori* error estimator for a Banach spaces-based mixed formulation of the stationary convective Brinkman–Forchheimer equations, and [37], where an *a posteriori* error analysis was developed for the coupling of the Darcy–Forchheimer problem with the CDR equation. Of particular relevance is also [12], where a reliable and efficient estimator is proposed for the Brinkman–Forchheimer equations coupled with a double-diffusive convection system. However, the formulation therein differs from the one adopted in [6]: in [12], the velocity gradient and the pseudostress tensor are introduced as additional unknowns for the BF system, while the double-diffusion equations are handled via vectors involving the temperature/concentration, their gradients, and the velocity. In our formulation, by contrast, the velocity gradient is not introduced as an unknown, and the CDR equation is handled, in the fully-mixed approach, through the classical diffusion vector.

In light of the above discussion, in this paper we propose residual-based *a posteriori* error estimators for the BF equations coupled with the CDR equation, considering both the mixed-primal and fully-mixed formulations studied in [6]. Drawing upon the techniques of [13, 7, 39, 38] and building on the approach of [11], we analyze the proposed estimators within our Banach space setting, rigorously establishing their reliability and efficiency in two- and three-dimensional domains. More precisely, we derive global estimators expressed in terms of computable local indicators Θ_K defined on each element K of a given mesh $\mathcal{T}_h$, which are then employed to drive an adaptive mesh refinement algorithm. In particular, we prove that each estimator Θ is reliable and efficient, meaning that there exist positive constants C_{eff} and C_{rel}, independent of the mesh sizes, such that

$$C_{\mathrm{eff}}\,\Theta + \mathtt{h.o.t.} \leqslant \|\,\mathrm{error}\,\| \leqslant C_{\mathrm{rel}}\,\Theta + \mathtt{h.o.t.}\,,$$

where `h.o.t.` denotes one or more terms of higher order.

The rest of this paper is organized as follows. The remainder of this section is devoted to standard notation and functional spaces. In Sections 2 and 3, we recall from [6] the model problem and its continuous formulations based on the mixed-primal and fully-mixed approaches, along with the two discrete schemes. Subsequently, Section 4 deals with the derivation and analysis of a residual-based *a posteriori* error estimator for the mixed-primal formulation, establishing its reliability and efficiency. Section 5 then addresses the analogous analysis for the fully-mixed formulation. In Section 6, we present several numerical examples illustrating the performance of the proposed estimators and the associated adaptive algorithm, confirming the recovery of optimal convergence rates in the presence of singularities, steep gradients, and challenging physical scenarios with and without manufactured solutions. Finally, auxiliary results employed in the reliability and efficiency analyses are collected in Appendices A and B, respectively.

Preliminary notations

Let $\Omega \subset \mathrm{R}^n, n \in \{2,3\}$, be a bounded domain with polyhedral boundary Γ, and let $\mathbf{n}$ be the outward unit normal vector on Γ. Standard notation will be adopted for Lebesgue spaces $\mathrm{L}^p(\Omega)$ and Sobolev spaces $\mathrm{W}^{s,p}(\Omega)$, with $s \in \mathrm{R}$ and $p > 1$, whose corresponding norms, either for the scalar, vectorial, or tensorial case, are denoted by $\|\cdot\|_{0,p;\Omega}$ and $\|\cdot\|_{s,p;\Omega}$, respectively. In particular, given a non-negative integer m, $\mathrm{W}^{m,2}(\Omega)$ is also denoted by $\mathrm{H}^m(\Omega)$, and the notations of its norm and seminorm are

simplified to $\|\cdot\|_{m,\Omega}$ and $|\cdot|_{m,\Omega}$, respectively. In addition, $\mathrm{H}^{1/2}(\Gamma)$ is the space of traces of functions of $\mathrm{H}^1(\Omega)$, and $\mathrm{H}^{-1/2}(\Gamma)$ denotes its dual. On the other hand, given any generic scalar functional space S, we let $\mathbf{S}$ and $\mathbb{S}$ be the corresponding vectorial and tensorial counterparts, whereas $\|\cdot\|$, with no subscripts, will be employed for the norm of any element or operator whenever there is no confusion about the space to which they belong. For any normed vector space V, we denote its topological dual space by V', which is a Banach space when endowed with the norm

$$\|F\|_{V'} := \sup_{0\neq v\in V} \frac{|F(v)|}{\|v\|_V} \qquad \forall\, F \in V' \,.$$

Also, $|\cdot|$ denotes the Euclidean norm in both R^n and $\mathrm{R}^{n\times n}$, and as usual, $\mathbb{I}$ stands for the identity tensor in $\mathrm{R}^{n\times n}$. In turn, for any vector field $\mathbf{v} = (v_i)_{i=1}^n$, we set the gradient and divergence, as

$$\nabla \mathbf{v} := \left(\frac{\partial v_i}{\partial x_j}\right)_{i,j=1}^n \quad \text{and} \quad \mathrm{div}(\mathbf{v}) := \sum_{j=1}^n \frac{\partial v_j}{\partial x_j} \,,$$

whereas for any tensor fields $\boldsymbol{\tau} = (\tau_{ij})_{i,j=1}^n$ and $\boldsymbol{\zeta} = (\zeta_{ij})_{i,j=1}^n$, we let $\mathbf{div}(\boldsymbol{\tau})$ be the divergence operator div acting along the rows of $\boldsymbol{\tau}$, and define the transpose, the trace, the deviatoric tensor, and the tensor inner product, respectively, as

$$\boldsymbol{\tau}^{\mathrm{t}} := (\tau_{ji})_{i,j=1}^n \,, \quad \mathrm{tr}(\boldsymbol{\tau}) := \sum_{i=1}^n \tau_{ii} \,, \quad \boldsymbol{\tau}^{\mathrm{d}} := \boldsymbol{\tau} - \frac{1}{n}\,\mathrm{tr}(\boldsymbol{\tau})\,\mathbb{I} \,, \quad \text{and} \quad \boldsymbol{\tau} : \boldsymbol{\zeta} := \sum_{i,j=1}^n \tau_{ij}\,\zeta_{ij} \,.$$

Furthermore, for each $t \in [1, +\infty)$ we introduce the Banach spaces

$$\mathbf{H}(\mathrm{div}_t;\Omega) := \left\{ \mathbf{v} \in \mathbf{L}^2(\Omega) : \quad \mathrm{div}(\mathbf{v}) \in \mathrm{L}^t(\Omega) \right\}, \quad \text{and}$$

$$\mathbb{H}(\mathbf{div}_t;\Omega) := \left\{ \boldsymbol{\tau} \in \mathbb{L}^2(\Omega) : \quad \mathbf{div}(\boldsymbol{\tau}) \in \mathbf{L}^t(\Omega) \right\},$$

endowed with the natural norms

$$\|\mathbf{v}\|_{\mathrm{div}_t;\Omega} := \|\mathbf{v}\|_{0,\Omega} + \|\mathrm{div}(\mathbf{v})\|_{0,t;\Omega} \quad \forall\, \mathbf{v} \in \mathbf{H}(\mathrm{div}_t;\Omega) \,, \quad \text{and}$$

$$\|\boldsymbol{\tau}\|_{\mathbf{div}_t;\Omega} := \|\boldsymbol{\tau}\|_{0,\Omega} + \|\mathbf{div}(\boldsymbol{\tau})\|_{0,t;\Omega} \quad \forall\, \boldsymbol{\tau} \in \mathbb{H}(\mathbf{div}_t;\Omega) \,.$$

In addition, we consider the canonical injections $i_{p,q} : \mathrm{L}^p(\Omega) \to \mathrm{L}^q(\Omega)$ for all $p, q \in [1, +\infty)$, $p \geqslant q$, and $i_p : \mathrm{H}^1(\Omega) \to \mathrm{L}^p(\Omega)$ for all $p \in [1, +\infty)$ when $n = 2$, and for all $p \in [1, 6]$ when $n = 3$, which are continuous with norms depending on the domain. In particular, we have

$$\|i_{p,q}\| \leqslant |\Omega|^{(p-q)/(pq)} \,. \tag{1.1}$$

In turn, we let $\boldsymbol{i}_{p,q}$ and $\boldsymbol{i}_p$ be the corresponding vector or tensor counterparts of $i_{p,q}$ and i_p, respectively. Note that the norm of $\boldsymbol{i}_{p,q}$ also achieves the bound (1.1). Additionally, we recall that, proceeding as in [27, eq. (1.43), Section 1.3.4] (see also [8, Section 4.1]), one can prove that for $t \in \begin{cases} (1, +\infty] \text{ in } \mathrm{R}^2 \,, \\ [\frac{6}{5}, +\infty] \text{ in } \mathrm{R}^3 \,, \end{cases}$ there hold

$$\langle \boldsymbol{\xi}\cdot\mathbf{n}, \varphi\rangle = \int_\Omega \left\{ \boldsymbol{\xi}\cdot\nabla\varphi + \varphi\,\mathrm{div}(\boldsymbol{\xi}) \right\} \quad \forall\, (\boldsymbol{\xi}, \varphi) \in \mathbf{H}(\mathrm{div}_t;\Omega) \times \mathrm{H}^1(\Omega) \,, \quad \text{and} \tag{1.2}$$

$$\langle \boldsymbol{\tau}\mathbf{n}, \mathbf{v}\rangle = \int_\Omega \left\{ \boldsymbol{\tau} : \nabla\mathbf{v} + \mathbf{v}\cdot\mathbf{div}(\boldsymbol{\tau}) \right\} \quad \forall\, (\boldsymbol{\tau}, \mathbf{v}) \in \mathbb{H}(\mathbf{div}_t;\Omega) \times \mathbf{H}^1(\Omega) \,, \tag{1.3}$$

where $\langle\cdot,\cdot\rangle$ in (1.2) and (1.3) denotes the duality pairing between $\mathrm{H}^{-1/2}(\Gamma)$ and $\mathrm{H}^{1/2}(\Gamma)$, and between $\mathbf{H}^{-1/2}(\Gamma)$ and $\mathbf{H}^{1/2}(\Gamma)$, respectively.

Finally, we use the letters C or c to denote generic constants that are independent of mesh sizes and may vary from line to line. We only indicate their precise dependencies if they depend on physical parameters of the model problem.

2 The model problem

We consider the physical process of fluid flow and reactive transport in a saturated porous medium occupying the region Ω. The fluid flow is governed by the Brinkman–Forchheimer equations (cf. [19], [23], [17]), characterized by the velocity $\mathbf{u}$ and the pressure p. In addition, following the approach in [36], the scalar field ϕ denotes the concentration of a chemical species transported by the fluid and modeled by a convection-diffusion-reaction equation. As a result, the coupled model of interest is described by the following system of partial differential equations:

$$-\,\mathbf{div}\big(\nu\,\nabla\mathbf{u}\big)\;+\;\mathtt{D}\,\mathbf{u}\;+\;\mathtt{F}\,|\mathbf{u}|^{\rho-2}\,\mathbf{u}\;+\;\nabla p=\mathbf{f}(\phi)\quad\text{in}\quad\Omega\,,\tag{2.1a}$$

$$\mathrm{div}(\mathbf{u})=f\qquad\text{in}\quad\Omega\,,\tag{2.1b}$$

$$-\kappa\,\Delta\,\phi\;+\;\mathbf{u}\cdot\nabla\phi\;+\;\eta\,\phi=g\qquad\text{in}\quad\Omega\,,\tag{2.1c}$$

where $\nu>0$ is the Brinkman coefficient (or effective viscosity), $\mathtt{D}>0$ is the Darcy coefficient, $\mathtt{F}>0$ is the Forchheimer coefficient, $\rho\in[3,4]$ is a given number representing the inertial power, $\kappa>0$ is the diffusion coefficient, and $\eta>0$ is the reaction coefficient. We assume that ν, $\mathtt{D}$, and $\mathtt{F}$ may vary spatially and are bounded in terms of positive constants $\nu_0,\nu_1,\mathtt{D}_0,\mathtt{D}_1,\mathtt{F}_0$, and $\mathtt{F}_1$ satisfying

$$\nu_0\;\leqslant\;\nu(\mathbf{x})\;\leqslant\;\nu_1\,,\quad\mathtt{D}_0\;\leqslant\;\mathtt{D}(\mathbf{x})\;\leqslant\;\mathtt{D}_1\,,\quad\text{and}\quad\mathtt{F}_0\;\leqslant\;\mathtt{F}(\mathbf{x})\;\leqslant\;\mathtt{F}_1\,,\qquad\forall\,\mathbf{x}\in\Omega\,.\tag{2.2}$$

The source terms f and g belong to suitable function spaces to be specified later. In addition, the external force $\mathbf{f}(\phi)$ is defined by

$$\mathbf{f}(\phi)\;:=\;-(\phi-\phi_{\mathtt{r}})\,\mathbf{g}\,,\tag{2.3}$$

where $\mathbf{g}$ represents the gravitational acceleration of potential type, and $\phi_{\mathtt{r}}$ is the reference concentration of the solute.

Equations (2.1) are complemented with Dirichlet boundary conditions for the velocity and concentration fields, namely,

$$\mathbf{u}\;=\;\mathbf{u}_{\mathrm{D}}\quad\text{and}\quad\phi\;=\;\phi_{\mathrm{D}}\quad\text{on}\quad\Gamma\,,\tag{2.4}$$

with given data $\mathbf{u}_{\mathrm{D}}\in\mathbf{H}^{1/2}(\Gamma)$ and $\phi_{\mathrm{D}}\in\mathrm{H}^{1/2}(\Gamma)$. Due to condition (2.1b) and the Dirichlet boundary condition for $\mathbf{u}$, the datum $\mathbf{u}_{\mathrm{D}}$ must satisfy the compatibility condition

$$\int_{\Gamma}\mathbf{u}_{\mathrm{D}}\cdot\mathbf{n}\;=\;\int_{\Omega}f\,.$$

Additionally, to ensure uniqueness of the pressure p in (2.1a), we seek p in the space

$$\mathrm{L}^2_0(\Omega)\;:=\;\left\{q\in\mathrm{L}^2(\Omega):\quad\int_{\Omega}q=0\right\}.$$

3 Continuous and discrete mixed formulations

In this section, we recall the mixed-primal and fully-mixed formulations of the model problem (2.1), together with their corresponding Galerkin discretizations based on conforming finite element spaces. We also summarize the associated well-posedness results. Further details are provided in [6, Sections 3 and 4].

3.1 Mixed-primal approach

We briefly recall from [6, Section 3.1] the derivation of the mixed-primal formulation for the coupled problem (2.1). Following the approach proposed in [17] and [21], we introduce the pseudostress tensor $\boldsymbol{\sigma}$ as an additional unknown, which is defined by

$$\boldsymbol{\sigma} := \nu \nabla \mathbf{u} - p\,\mathbb{I} \quad \text{in} \quad \Omega\,, \tag{3.1}$$

and observe that, by taking the matrix trace and using the fact that $\mathrm{tr}(\nu\nabla\mathbf{u}) = \nu\,\mathrm{div}(\mathbf{u}) = \nu f$, we obtain

$$p = -\frac{1}{n}\mathrm{tr}(\boldsymbol{\sigma}) + \frac{\nu}{n} f \quad \text{in} \quad \Omega\,. \tag{3.2}$$

Then, applying the divergence to $\boldsymbol{\sigma}$ in (3.1) and replacing the result into (2.1a), together with using (3.2) in (3.1), leads to an equivalent representation of the system (2.1): Find $\boldsymbol{\sigma}$, $\mathbf{u}$ and ϕ, in suitable spaces to be indicated below, such that

$$\frac{1}{\nu}\,\boldsymbol{\sigma}^{\mathrm{d}} - \nabla\mathbf{u} \;=\; -\frac{1}{n}\,f\,\mathbb{I} \quad \text{in} \quad \Omega\,, \tag{3.3a}$$

$$-\mathbf{div}\big(\boldsymbol{\sigma}\big) \;+\; \mathtt{D}\,\mathbf{u} \;+\; \mathtt{F}\,|\mathbf{u}|^{\rho-2}\,\mathbf{u} \;=\; \mathbf{f}(\phi) \quad \text{in} \quad \Omega\,, \tag{3.3b}$$

$$-\kappa\,\Delta\,\phi \;+\; \mathbf{u}\cdot\nabla\phi \;+\; \eta\,\phi \;=\; g \quad \text{in} \quad \Omega\,, \tag{3.3c}$$

$$\mathbf{u} \;=\; \mathbf{u}_{\mathrm{D}}, \quad \phi \;=\; \phi_{\mathrm{D}} \quad \text{on} \quad \Gamma\,, \tag{3.3d}$$

$$\int_{\Omega}\Big\{\mathrm{tr}(\boldsymbol{\sigma}) - \nu\,f\Big\} \;=\; 0\,. \tag{3.3e}$$

Notice that p was eliminated from the system, and it can subsequently be recovered through a post-processing step via (3.2). We remark that (3.3e) represents the uniqueness condition of the pressure $\int_\Omega p = 0$.

We now set $\ell := \rho/(\rho-1) \in [4/3, 3/2]$ as the Hölder conjugate of ρ, and recall the decomposition $\mathbb{H}(\mathbf{div}_\ell;\Omega) = \mathbb{H}_0(\mathbf{div}_\ell;\Omega) \oplus \mathrm{R}\,\mathbb{I}$, where

$$\mathbb{H}_0(\mathbf{div}_\ell;\Omega) := \left\{\boldsymbol{\tau} \in \mathbb{H}(\mathbf{div}_\ell;\Omega) : \quad \int_\Omega \mathrm{tr}(\boldsymbol{\tau}) = 0\right\}.$$

Then, we note that, by looking for $\boldsymbol{\sigma}$ in $\mathbb{H}(\mathbf{div}_\ell;\Omega)$, there exist unique components $\boldsymbol{\sigma}_0 \in \mathbb{H}_0(\mathbf{div}_\ell;\Omega)$ and $d_{\boldsymbol{\sigma}} \in \mathrm{R}$ such that $\boldsymbol{\sigma} = \boldsymbol{\sigma}_0 + d_{\boldsymbol{\sigma}}\,\mathbb{I}$. Moreover, using (3.3e), we deduce that the $\mathrm{R}\,\mathbb{I}$-component can be computed as

$$d_{\boldsymbol{\sigma}} = \frac{1}{n\,|\Omega|}\int_\Omega \mathrm{tr}(\boldsymbol{\sigma}) = \frac{1}{n\,|\Omega|}\int_\Omega \nu\,f\,. \tag{3.4}$$

Certainly, by employing this decomposition in (3.3a) and (3.3b), the system remains unaltered, with only $\boldsymbol{\sigma}$ replaced by $\boldsymbol{\sigma}_0$. In this context, we simply seek $\boldsymbol{\sigma}_0$ and compute the complete pseudostress tensor using (3.4). For simplicity, we shall denote $\boldsymbol{\sigma}_0$ by $\boldsymbol{\sigma}$.

To derive a weak formulation of (3.3), we first test (3.3a) and (3.3b) against functions in $\mathbb{H}_0(\mathbf{div}_\ell;\Omega)$ and $\mathbf{L}^\rho(\Omega)$, respectively, and integrate by parts the second term in (3.3a) using the Dirichlet boundary condition $\mathbf{u} = \mathbf{u}_{\mathrm{D}}$ (cf. (2.4)). In turn, we test the convection-diffusion-reaction equation (cf. (2.1c)) against functions in $\mathrm{H}^1(\Omega)$, and integrate by parts the first term. In this case, it is necessary to introduce a normal flux-type variable λ, defined by

$$\lambda := -\kappa\,\nabla\phi\cdot\mathbf{n} \quad \text{on} \quad \Gamma\,, \tag{3.5}$$

and enforce the Dirichlet boundary condition $\phi = \phi_{\mathrm{D}}$ (cf. (2.4)) weakly.

Thus, denoting $\mathcal{H} := \mathbb{H}_0(\mathbf{div}_\ell;\Omega)$ and $\mathcal{Q} := \mathbf{L}^\rho(\Omega)$, the weak mixed-primal formulation of (2.1) reads: Find $(\boldsymbol{\sigma},\mathbf{u}) \in \mathcal{H}\times\mathcal{Q}$ and $(\phi,\lambda)\in \mathrm{H}^1(\Omega)\times\mathrm{H}^{-1/2}(\Gamma)$ such that

$$\begin{array}{rcll} \mathbf{a}(\boldsymbol{\sigma},\boldsymbol{\tau}) + \mathbf{b}(\boldsymbol{\tau},\mathbf{u}) & = & \mathbf{F}(\boldsymbol{\tau}) & \forall\,\boldsymbol{\tau}\in\mathcal{H}\,,\\ \mathbf{b}(\boldsymbol{\sigma},\mathbf{v}) - \mathbf{c}_{\mathbf{u}}(\mathbf{u},\mathbf{v}) & = & \mathbf{G}_\phi(\mathbf{v}) & \forall\,\mathbf{v}\in\mathcal{Q}\,,\\ a_{\mathbf{u}}(\phi,\psi) + b(\psi,\lambda) & = & \mathrm{F}(\psi) & \forall\,\psi\in\mathrm{H}^1(\Omega)\,,\\ b(\phi,\xi) & = & \mathrm{G}(\xi) & \forall\,\xi\in\mathrm{H}^{-1/2}(\Gamma)\,, \end{array} \tag{3.6}$$

where the bilinear forms $\mathbf{a}:\mathcal{H}\times\mathcal{H}\to\mathrm{R}$, $\mathbf{b}:\mathcal{H}\times\mathcal{Q}\to\mathrm{R}$, and $\mathbf{c}_{\mathbf{z}}:\mathcal{Q}\times\mathcal{Q}\to\mathrm{R}$, for each $\mathbf{z}\in\mathcal{Q}$, and the linear functionals $\mathbf{F}:\mathcal{H}\to\mathrm{R}$ and $\mathbf{G}_\varphi:\mathcal{Q}\to\mathrm{R}$, for each $\varphi\in\mathcal{H}$, are defined as

$$\mathbf{a}(\boldsymbol{\chi},\boldsymbol{\tau}) := \int_\Omega \frac{1}{\nu}\,\boldsymbol{\chi}^{\mathrm{d}} : \boldsymbol{\tau}^{\mathrm{d}}\,, \qquad \mathbf{b}(\boldsymbol{\tau},\mathbf{v}) := \int_\Omega \mathbf{v}\cdot\mathbf{div}(\boldsymbol{\tau})\,, \tag{3.7}$$

$$\mathbf{c}_{\mathbf{z}}(\mathbf{w},\mathbf{v}) := \int_\Omega \mathtt{D}\,\mathbf{w}\cdot\mathbf{v} + \int_\Omega \mathtt{F}\,|\mathbf{z}|^{\rho-2}\mathbf{w}\cdot\mathbf{v}\,, \tag{3.8}$$

$$\mathbf{F}(\boldsymbol{\tau}) := \langle\boldsymbol{\tau}\,\mathbf{n},\mathbf{u}_{\mathrm{D}}\rangle - \frac{1}{n}\int_\Omega f\,\mathrm{tr}(\boldsymbol{\tau})\,, \qquad \mathbf{G}_\varphi(\mathbf{v}) := -\int_\Omega \mathbf{f}(\varphi)\cdot\mathbf{v}\,, \tag{3.9}$$

while the bilinear forms $a_{\mathbf{z}}:\mathrm{H}^1(\Omega)\times\mathrm{H}^1(\Omega)\to\mathrm{R}$ and $b:\mathrm{H}^1(\Omega)\times\mathrm{H}^{-1/2}(\Gamma)\to\mathrm{R}$, and linear functionals $\mathrm{F}:\mathrm{H}^1(\Omega)\to\mathrm{R}$ and $\mathrm{G}:\mathrm{H}^{-1/2}(\Gamma)\to\mathrm{R}$, are given by

$$a_{\mathbf{z}}(\varphi,\psi) := \kappa\int_\Omega \nabla\varphi\cdot\nabla\psi + \int_\Omega (\mathbf{z}\cdot\nabla\varphi)\,\psi + \eta\int_\Omega \varphi\,\psi\,, \tag{3.10}$$

$$b(\psi,\xi) := \langle\xi,\psi\rangle_\Gamma\,, \quad \mathrm{F}(\psi) := \int_\Omega g\,\psi \quad \text{and} \quad \mathrm{G}(\xi) := \langle\xi,\phi_{\mathrm{D}}\rangle_\Gamma\,. \tag{3.11}$$

In order to introduce a Galerkin scheme for (3.6), let us consider a regular family of triangulations $\{\mathcal{T}_h\}_{h>0}$ of $\bar\Omega$ made up of triangles K (when $n=2$) or tetrahedra K (when $n=3$) of diameter h_K, and set $h := \max\{h_K : K\in\mathcal{T}_h\}$. Given an integer $l\geqslant 0$ and a subset S of R^n, we denote by $\mathrm{P}_l(S)$ the space of polynomials of total degree at most l defined on S, and $\mathbf{P}_l(S)$ its vectorial counterpart. In turn, for each integer $k\geqslant 0$ and $K\in\mathcal{T}_h$, we define the local Raviart–Thomas spaces of order k as $\mathbf{RT}_k(K) := \mathbf{P}_k(K)\oplus\widetilde{\mathrm{P}}_k(K)\,\mathbf{x}$, where $\mathbf{x} := (x_1,\ldots,x_n)^{\mathrm{t}}$ is a generic vector of R^n and $\widetilde{\mathrm{P}}_k(K)$ is the space of polynomials of total degree equal to k defined on K. Furthermore, define $\mathbb{RT}_k(K)$ as the tensor space in which each row lies in $\mathbf{RT}_k(K)$.

To handle the boundary variable λ, we introduce an independent partition of Γ, consisting of straight segments when $n=2$ and flat triangles when $n=3$, denoted by $\{\Gamma_1,\Gamma_2,\ldots,\Gamma_m\}$, and we set

$\widetilde{h} := \max_{j\in\{1,\ldots,m\}} |\Gamma_j|$. Under this notation, we define the following finite element subspaces:

$$\begin{aligned}
\mathbb{H}_h^{\boldsymbol{\sigma}} &:= \left\{ \boldsymbol{\tau}_h \in \mathbb{H}_0(\mathbf{div}_\ell;\Omega) : \quad \boldsymbol{\tau}_h\big|_K \in \mathbb{RT}_k(K) \quad \forall\, K \in \mathcal{T}_h \right\}, \\
\mathbf{H}_h^{\mathbf{u}} &:= \left\{ \mathbf{v}_h \in \mathbf{L}^\rho(\Omega) : \quad \mathbf{v}_h\big|_K \in \mathbf{P}_k(K) \quad \forall\, K \in \mathcal{T}_h \right\}, \\
\mathrm{H}_h^{\phi} &:= \left\{ \psi_h \in C(\overline{\Omega}) : \quad \psi_h|_K \in \mathrm{P}_{k+1}(K) \quad \forall\, K \in \mathcal{T}_h \right\}, \\
\mathrm{H}_{\widetilde{h}}^{\lambda} &:= \left\{ \xi_{\widetilde{h}} \in \mathrm{L}^2(\Gamma) : \quad \xi_{\widetilde{h}}|_{\Gamma_j} \in \mathrm{P}_k(\Gamma_j) \quad \forall\, j \in \{1,\ldots,m\} \right\}.
\end{aligned} \tag{3.12}$$

Thus, the Galerkin scheme associated with (3.6) reads: Find $(\boldsymbol{\sigma}_h, \mathbf{u}_h) \in \mathbb{H}_h^{\boldsymbol{\sigma}} \times \mathbf{H}_h^{\mathbf{u}}$ and $(\phi_h, \lambda_{\widetilde{h}}) \in \mathrm{H}_h^{\phi} \times \mathrm{H}_{\widetilde{h}}^{\lambda}$ such that

$$\begin{aligned}
\mathbf{a}(\boldsymbol{\sigma}_h, \boldsymbol{\tau}_h) + \mathbf{b}(\boldsymbol{\tau}_h, \mathbf{u}_h) &= \mathbf{F}(\boldsymbol{\tau}_h) && \forall\, \boldsymbol{\tau}_h \in \mathbb{H}_h^{\boldsymbol{\sigma}}, \\
\mathbf{b}(\boldsymbol{\sigma}_h, \mathbf{v}_h) - \mathbf{c}_{\mathbf{u}_h}(\mathbf{u}_h, \mathbf{v}_h) &= \mathbf{G}_{\phi_h}(\mathbf{v}_h) && \forall\, \mathbf{v}_h \in \mathbf{H}_h^{\mathbf{u}}, \\
a_{\mathbf{u}_h}(\phi_h, \psi_h) + b(\psi_h, \lambda_{\widetilde{h}}) &= \mathrm{F}(\psi_h) && \forall\, \psi_h \in \mathrm{H}_h^{\phi}, \\
b(\phi_h, \xi_{\widetilde{h}}) &= \mathrm{G}(\xi_{\widetilde{h}}) && \forall\, \xi_{\widetilde{h}} \in \mathrm{H}_{\widetilde{h}}^{\lambda}.
\end{aligned} \tag{3.13}$$

The well-posedness of (3.6) and (3.13) was established in [6, Sections 3.2 and 3.3], respectively, by means of a fixed-point argument. In particular, the solvability of the Galerkin scheme was proved for arbitrary finite element spaces satisfying suitable assumptions. In the present work, we restrict the analysis to the specific finite element spaces given in (3.12), which were also considered as a particular example in [6, Section 3.5].

For later use, let us recall some notation from the solvability analysis. Let c_P denote the Poincaré constant (cf. [6, eq. (38)]), and let $s := 2\rho/(\rho-2) \in [4,6]$. In addition, following [6, Lemmas 1 and 2], let $\delta > 0$, set $\delta_0 := \frac{1}{2}\,\|i_s\|^{-1}\,\kappa\, c_P$, and define $r_0 := \min\{\delta, \delta_0\}$, so that $r \in (0, r_0]$. Then, we define the continuous and discrete balls

$$\mathbf{W}(r) := \left\{ \mathbf{z} \in \mathcal{Q} : \quad \|\mathbf{z}\|_{0,\rho;\Omega} \leqslant r \right\} \quad \text{and} \quad \mathbf{W}_h(r) := \left\{ \mathbf{z}_h \in \mathbf{H}_h^{\mathbf{u}} : \quad \|\mathbf{z}_h\|_{0,\rho;\Omega} \leqslant r \right\}, \tag{3.14}$$

and denote by $(\boldsymbol{\sigma}, \mathbf{u}, \phi, \lambda) \in \mathcal{H} \times \mathcal{Q} \times \mathrm{H}^1(\Omega) \times \mathrm{H}^{-1/2}(\Gamma)$, with $\mathbf{u} \in \mathbf{W}(r)$, the unique solution to (3.6), and by $(\boldsymbol{\sigma}_h, \mathbf{u}_h, \phi_h, \lambda_{\widetilde{h}}) \in \mathbb{H}_h^{\boldsymbol{\sigma}} \times \mathbf{H}_h^{\mathbf{u}} \times \mathrm{H}_h^{\phi} \times \mathrm{H}_{\widetilde{h}}^{\lambda}$, with $\mathbf{u}_h \in \mathbf{W}_h(r)$, the unique solution to (3.13). Furthermore, we recall from [6, Theorem 1] that there exist $\mathcal{C}_1 > 0$ depending only on r, ρ, ν_0, ν_1, $\mathtt{D}_1$, $\mathtt{F}_1$, $\|i_s\|$, β (cf. [6, eq. (34)]), and $|\Omega|$, and $\mathcal{C}_2 > 0$ depending only on κ, η, $\widetilde{\beta}$ (cf. [6, Lemma 2]), and $|\Omega|$, such that the following *a priori* estimates hold:

$$\|(\boldsymbol{\sigma}, \mathbf{u})\|_{\mathcal{H}\times\mathcal{Q}} \leqslant \mathcal{C}_1\, \Psi_1(\mathbf{u}_{\mathrm{D}}, f, \mathbf{g}, g, \phi_{\mathrm{D}}, \phi_{\mathbf{r}}) \tag{3.15}$$

$$\text{and} \quad \|(\phi, \lambda)\|_{\mathrm{H}^1(\Omega)\times\mathrm{H}^{-1/2}(\Gamma)} \leqslant \mathcal{C}_2\, \Psi_2(g, \phi_{\mathrm{D}}), \tag{3.16}$$

where Ψ_1 and Ψ_2 are defined as

$$\Psi_1(\mathbf{u}_{\mathrm{D}}, f, \mathbf{g}, g, \phi_{\mathrm{D}}, \phi_{\mathbf{r}}) := \|\mathbf{u}_{\mathrm{D}}\|_{1/2,\Gamma} + \|f\|_{0,\Omega} + \|\mathbf{g}\|_{0,\Omega} \left(\|g\|_{0,\Omega} + \|\phi_{\mathrm{D}}\|_{1/2,\Gamma} + \|\phi_{\mathbf{r}}\|_{0,s;\Omega} \right) \tag{3.17}$$

$$\text{and} \quad \Psi_2(g, \phi_{\mathrm{D}}) := \|g\|_{0,\Omega} + \|\phi_{\mathrm{D}}\|_{1/2,\Gamma}. \tag{3.18}$$

Moreover, from [6, Theorem 2], there exist $\mathcal{C}_{1,\mathtt{d}} > 0$, depending only on r, ρ, ν_0, ν_1, $\mathtt{D}_1$, $\mathtt{F}_1$, $\|i_s\|$, $\beta_{\mathtt{d}}$ (cf. [6, eq. (60)]), and $|\Omega|$, and $\mathcal{C}_{2,\mathtt{d}} > 0$, depending only on κ, η, $\widetilde{\beta}_{\mathtt{d}}$ (cf. [6, eq. (62)]), and $|\Omega|$, such that

$$\|(\boldsymbol{\sigma}_h, \mathbf{u}_h)\|_{\mathcal{H}\times\mathcal{Q}} \leqslant \mathcal{C}_{1,\mathtt{d}}\, \Psi_1(\mathbf{u}_{\mathrm{D}}, f, \mathbf{g}, g, \phi_{\mathrm{D}}, \phi_{\mathbf{r}}) \tag{3.19}$$

$$\text{and} \quad \|(\phi_h, \lambda_{\widetilde{h}})\|_{\mathrm{H}^1(\Omega)\times\mathrm{H}^{-1/2}(\Gamma)} \leqslant \mathcal{C}_{2,\mathtt{d}}\, \Psi_2(g, \phi_{\mathrm{D}})\,. \tag{3.20}$$

Additionally, given $\mathbf{z} \in \mathcal{Q}$ and $\varphi \in \mathrm{H}^1(\Omega)$, we introduce the bilinear form $\mathbf{A}_{\mathbf{z}} : (\mathcal{H}\times\mathcal{Q})\times(\mathcal{H}\times\mathcal{Q}) \to \mathrm{R}$ and the linear functional $\mathbf{R}_{\varphi} : \mathcal{H}\times\mathcal{Q} \to \mathrm{R}$, defined as

$$\mathbf{A}_{\mathbf{z}}\big((\boldsymbol{\chi}, \mathbf{w}), (\boldsymbol{\tau}, \mathbf{v})\big) := \mathbf{a}(\boldsymbol{\chi}, \boldsymbol{\tau}) + \mathbf{b}(\boldsymbol{\tau}, \mathbf{w}) + \mathbf{b}(\boldsymbol{\chi}, \mathbf{v}) - \mathbf{c}_{\mathbf{z}}(\mathbf{w}, \mathbf{v})$$
$$\text{and} \quad \mathbf{R}_{\varphi}(\boldsymbol{\tau}, \mathbf{v}) := \mathbf{F}(\boldsymbol{\tau}) + \mathbf{G}_{\varphi}(\mathbf{v})\,,$$

for all $(\boldsymbol{\chi}, \mathbf{w}), (\boldsymbol{\tau}, \mathbf{v}) \in \mathcal{H}\times\mathcal{Q}$, and we observe that the first two rows in (3.6) can be written equivalently as

$$\mathbf{A}_{\mathbf{u}}\big((\boldsymbol{\sigma}, \mathbf{u}), (\boldsymbol{\tau}, \mathbf{v})\big) = \mathbf{R}_{\phi}(\boldsymbol{\tau}, \mathbf{v}) \qquad \forall\, (\boldsymbol{\tau}, \mathbf{v}) \in \mathcal{H}\times\mathcal{Q}\,. \tag{3.21}$$

Then, it is possible to establish the global inf-sup condition (cf. [6, eq. (37)])

$$\sup_{\mathbf{0}\neq(\boldsymbol{\tau},\mathbf{v})\in\mathcal{H}\times\mathcal{Q}} \frac{\mathbf{A}_{\mathbf{z}}\,((\boldsymbol{\chi}, \mathbf{w}), (\boldsymbol{\tau}, \mathbf{v}))}{\|(\boldsymbol{\tau}, \mathbf{v})\|_{\mathcal{H}\times\mathcal{Q}}} \geqslant \alpha_{\mathbf{A}}\, \|(\boldsymbol{\chi}, \mathbf{w})\|_{\mathcal{H}\times\mathcal{Q}} \qquad \forall\, (\boldsymbol{\chi}, \mathbf{w}) \in \mathcal{H}\times\mathcal{Q}\,, \tag{3.22}$$

for all $\mathbf{z} \in \mathcal{Q}$ satisfying $\|\mathbf{z}\|_{0,\rho;\Omega} \leqslant r$, where $\alpha_{\mathbf{A}}$ is a positive constant depending only on r, ρ, ν_0, ν_1, $\mathtt{D}_1$, $\mathtt{F}_1$, β (cf. [6, eq. (6)]), and $|\Omega|$, and thus independent of h and $\widetilde{h}$.

Although we did not mention in [6] that a global inf-sup condition associated with the uncoupled CDR equations can also be obtained, this result will be useful in the forthcoming analysis. Indeed, having established the well-posedness of the uncoupled problem associated with the last two rows in (3.6), by invoking the Babuška–Brezzi Theorem (cf. [26, Theorem 2.34]), one establishes the existence of a positive constant $\alpha_{\mathtt{CDR}}$, depending only on κ, η, $\widetilde{\beta}$ (cf. [6, Lemma 2]), and $|\Omega|$, and thus independent of h and $\widetilde{h}$, such that

$$\sup_{\mathbf{0}\neq(\psi,\xi)\in\mathrm{H}^1(\Omega)\times\mathrm{H}^{-1/2}(\Gamma)} \frac{a_{\mathbf{z}}(\varphi, \psi) + b(\psi, \varsigma) + b(\varphi, \psi)}{\|(\psi, \xi)\|_{\mathrm{H}^1(\Omega)\times\mathrm{H}^{-1/2}(\Gamma)}} \geqslant \alpha_{\mathtt{CDR}}\, \|(\varphi, \varsigma)\|_{\mathrm{H}^1(\Omega)\times\mathrm{H}^{-1/2}(\Gamma)}\,, \tag{3.23}$$

for all $(\varphi, \varsigma) \in \mathrm{H}^1(\Omega)\times\mathrm{H}^{-1/2}(\Gamma)$ and $\mathbf{z} \in \mathcal{Q}$ satisfying $\|\mathbf{z}\|_{0,\rho;\Omega} \leqslant r$.

3.2 Fully-mixed approach

We now recall from [6, Section 4.1] the fully-mixed formulation of (2.1). We still employ a pseudostress mixed formulation for the Brinkman–Forchheimer equations, which consists of the first two equations in (3.6). To derive a mixed formulation for the CDR equation, we introduce the diffusion vector $\boldsymbol{\vartheta}$, defined by

$$\boldsymbol{\vartheta} := \kappa\, \nabla\phi \quad \text{in} \quad \Omega\,. \tag{3.24}$$

Applying the divergence operator to $\boldsymbol{\vartheta}$ in (3.24) and substituting back into (2.1c), we deduce that the mixed strong formulation of the CDR equation reads:

$$\kappa^{-1}\, \boldsymbol{\vartheta} \,-\, \nabla\phi = \mathbf{0} \quad \text{in} \quad \Omega\,, \tag{3.25a}$$

$$\mathrm{div}\big(\boldsymbol{\vartheta}\big) \,-\, \kappa^{-1}\mathbf{u}\cdot\boldsymbol{\vartheta} \,-\, \eta\,\phi = -\,g \quad \text{in} \quad \Omega\,, \tag{3.25b}$$

$$\phi = \phi_{\mathrm{D}} \quad \text{on} \quad \Gamma\,. \tag{3.25c}$$

In this case, it is not necessary to introduce the normal flux-type variable defined in (3.5), since the boundary condition for the concentration (cf. (3.25c)) now becomes natural. As rigorously explained in [6, Section 4.1], we test (3.25a) and (3.25b) against functions in $\mathbf{H}(\mathrm{div}_t;\Omega)$ and $\mathrm{L}^s(\Omega)$, respectively,

where s and t are Hölder conjugates suitably defined below, and integrate by parts the second term in (3.25a) using the Dirichlet datum (3.25c), which allows us to seek $\boldsymbol{\vartheta} \in \mathbf{H}(\mathrm{div}_t;\Omega)$ and $\phi \in \mathrm{L}^s(\Omega)$. Bearing in mind that $\rho \in [3,4]$, we recall the index ℓ already introduced in the mixed-primal approach, and define the two new parameters s and t:

$$\ell := \frac{\rho}{\rho-1} \in \left[\frac{4}{3},\frac{3}{2}\right], \qquad s := \frac{2\rho}{\rho-2} \in [4,6] \quad \text{and} \quad t := \frac{2\rho}{\rho+2} \in \left[\frac{6}{5},\frac{4}{3}\right]. \tag{3.26}$$

These parameters allow us to define the spaces $\mathrm{X} := \mathbf{H}(\mathrm{div}_t;\Omega)$ and $\mathrm{Y} := \mathrm{L}^s(\Omega)$, in addition to the spaces $\mathcal{H} := \mathbb{H}_0(\mathbf{div}_\ell;\Omega)$ and $\mathcal{Q} := \mathbf{L}^\rho(\Omega)$ already introduced in the mixed-primal formulation (cf. (3.6)). Thus, according to the first two equations of (3.6), and proceeding as described above to derive the mixed weak formulation of the CDR equation based on the diffusion vector (cf. (3.24)), the fully-mixed formulation of problem (2.1) reads: Find $(\boldsymbol{\sigma},\mathbf{u}) \in \mathcal{H}\times\mathcal{Q}$ and $(\boldsymbol{\vartheta},\phi) \in \mathrm{X}\times\mathrm{Y}$ such that

$$\begin{array}{rcll} \mathbf{a}(\boldsymbol{\sigma},\boldsymbol{\tau}) + \mathbf{b}(\boldsymbol{\tau},\mathbf{u}) & = & \mathbf{F}(\boldsymbol{\tau}) & \forall\, \boldsymbol{\tau} \in \mathcal{H}\,, \\ \mathbf{b}(\boldsymbol{\sigma},\mathbf{v}) - \mathbf{c}_{\mathbf{u}}(\mathbf{u},\mathbf{v}) & = & \mathbf{G}_\phi(\mathbf{v}) & \forall\, \mathbf{v} \in \mathcal{Q}\,, \\ \widehat{a}(\boldsymbol{\vartheta},\boldsymbol{\psi}) + \widehat{b}(\boldsymbol{\psi},\phi) & = & \widehat{\mathrm{F}}(\boldsymbol{\psi}) & \forall\, \boldsymbol{\psi} \in \mathrm{X}\,, \\ \widehat{b}(\boldsymbol{\vartheta},\xi) - \widehat{c}(\phi,\xi) + d_{\mathbf{u}}(\boldsymbol{\vartheta},\xi) & = & \widehat{\mathrm{G}}(\xi) & \forall\, \xi \in \mathrm{Y}\,, \end{array} \tag{3.27}$$

where the bilinear forms $\mathbf{a} : \mathcal{H}\times\mathcal{H} \to \mathrm{R}$, $\mathbf{b} : \mathcal{H}\times\mathcal{Q} \to \mathrm{R}$ and $\mathbf{c}_{\mathbf{z}} : \mathcal{Q}\times\mathcal{Q} \to \mathrm{R}$, for each $\mathbf{z} \in \mathcal{Q}$, and the linear functionals $\mathbf{F} : \mathcal{H} \to \mathrm{R}$ and $\mathbf{G}_\varphi : \mathcal{Q} \to \mathrm{R}$, for each $\varphi \in \mathrm{Y}$, are already defined in (3.7)–(3.9). In turn, the bilinear forms $\widehat{a} : \mathrm{X}\times\mathrm{X} \to \mathrm{R}$, $\widehat{b} : \mathrm{X}\times\mathrm{Y} \to \mathrm{R}$, $d_{\mathbf{z}} : \mathrm{X}\times\mathrm{Y} \to \mathrm{R}$, for each $\mathbf{z} \in \mathcal{Q}$, $\widehat{c} : \mathrm{Y}\times\mathrm{Y} \to \mathrm{R}$, and the linear functionals $\widehat{\mathrm{F}} : \mathrm{X} \to \mathrm{R}$ and $\widehat{\mathrm{G}} : \mathrm{Y} \to \mathrm{R}$, are defined as

$$\widehat{a}(\boldsymbol{\zeta},\boldsymbol{\psi}) := \int_\Omega \kappa^{-1}\, \boldsymbol{\zeta}\cdot\boldsymbol{\psi}\,, \quad \widehat{b}(\boldsymbol{\psi},\xi) := \int_\Omega \xi\, \mathrm{div}(\boldsymbol{\psi})\,, \quad d_{\mathbf{z}}(\boldsymbol{\zeta},\xi) := -\int_\Omega \kappa^{-1}\,(\mathbf{z}\cdot\boldsymbol{\zeta})\,\xi\,,$$

$$\widehat{c}(\zeta,\xi) := \int_\Omega \eta\,\zeta\,\xi\,, \quad \widehat{\mathrm{F}}(\boldsymbol{\psi}) := \langle \boldsymbol{\psi}\cdot\mathbf{n}, \phi_{\mathrm{D}}\rangle\,, \quad \widehat{\mathrm{G}}(\xi) := -\int_\Omega g\,\xi\,.$$

In order to introduce the Galerkin scheme associated with (3.27), let us define the finite element subspaces

$$\mathbf{H}_h^{\boldsymbol{\vartheta}} := \left\{ \boldsymbol{\psi}_h \in \mathbf{H}(\mathrm{div}_t;\Omega) : \quad \boldsymbol{\psi}_h\big|_K \in \mathbf{RT}_k(K) \quad \forall\, K \in \mathcal{T}_h \right\},$$

$$\widehat{\mathrm{H}}_h^{\phi} := \left\{ \xi_h \in \mathrm{L}^s(\Omega) : \quad \xi_h\big|_K \in \mathrm{P}_k(K) \quad \forall\, K \in \mathcal{T}_h \right\},$$

which we use to approximate the solutions $\boldsymbol{\vartheta}$ and ϕ of the problem (3.27). In turn, $\boldsymbol{\sigma}$ and $\mathbf{u}$ are approximated by functions belonging to the first two spaces in (3.12). As mentioned also in the mixed-primal approach (cf. Section 3.1), in [6] we consider arbitrary finite element spaces to develop the solvability analysis, but we include in [6, Section 4.5] these specific choices that satisfy the suitable hypotheses detailed therein.

Thus, the announced Galerkin scheme reads: Find $(\boldsymbol{\sigma}_h,\mathbf{u}_h) \in \mathbb{H}_h^{\boldsymbol{\sigma}} \times \mathbf{H}_h^{\mathbf{u}}$ and $(\boldsymbol{\vartheta}_h,\phi_h) \in \mathbf{H}_h^{\boldsymbol{\vartheta}} \times \widehat{\mathrm{H}}_h^{\phi}$ such that

$$\begin{array}{rcll} \mathbf{a}(\boldsymbol{\sigma}_h,\boldsymbol{\tau}_h) + \mathbf{b}(\boldsymbol{\tau}_h,\mathbf{u}_h) & = & \mathbf{F}(\boldsymbol{\tau}_h) & \forall\, \boldsymbol{\tau}_h \in \mathbb{H}_h^{\boldsymbol{\sigma}}\,, \\ \mathbf{b}(\boldsymbol{\sigma}_h,\mathbf{v}_h) - \mathbf{c}_{\mathbf{u}_h}(\mathbf{u}_h,\mathbf{v}_h) & = & \mathbf{G}_{\phi_h}(\mathbf{v}_h) & \forall\, \mathbf{v}_h \in \mathbf{H}_h^{\mathbf{u}}\,, \\ \widehat{a}(\boldsymbol{\vartheta}_h,\boldsymbol{\psi}_h) + \widehat{b}(\boldsymbol{\psi}_h,\phi_h) & = & \widehat{\mathrm{F}}(\boldsymbol{\psi}_h) & \forall\, \boldsymbol{\psi}_h \in \mathbf{H}_h^{\boldsymbol{\vartheta}}\,, \\ \widehat{b}(\boldsymbol{\vartheta}_h,\xi_h) - \widehat{c}(\phi_h,\xi_h) + d_{\mathbf{u}_h}(\boldsymbol{\vartheta}_h,\xi_h) & = & \widehat{\mathrm{G}}(\xi_h) & \forall\, \xi_h \in \widehat{\mathrm{H}}_h^{\phi}\,. \end{array} \tag{3.28}$$

In the same way as we introduced the bilinear form $\mathbf{A}_{\mathbf{z}}$ in the mixed-primal approach (cf. (3.21)), we may consider the bilinear form $\widehat{\mathbf{A}} : (\mathrm{X} \times \mathrm{Y}) \times (\mathrm{X} \times \mathrm{Y}) \to \mathrm{R}$ defined by

$$\widehat{\mathbf{A}}\big((\boldsymbol{\varrho}, \zeta), (\boldsymbol{\psi}, \xi)\big) := \widehat{a}(\boldsymbol{\varrho}, \boldsymbol{\psi}) + \widehat{b}(\boldsymbol{\psi}, \zeta) + \widehat{b}(\boldsymbol{\varrho}, \xi) - \widehat{c}(\zeta, \xi)\,, \tag{3.29}$$

for all $\big((\boldsymbol{\varrho}, \zeta), (\boldsymbol{\psi}, \xi)\big) \in \mathrm{X} \times \mathrm{Y}$, which allows us to rewrite the last two rows of (3.27) as

$$\widehat{\mathbf{A}}\big((\boldsymbol{\vartheta}, \phi), (\boldsymbol{\psi}, \xi)\big) + d_{\mathbf{u}}(\boldsymbol{\vartheta}, \xi) = \widehat{\mathrm{F}}(\boldsymbol{\psi}) + \widehat{\mathrm{G}}(\xi) \qquad \forall\, (\boldsymbol{\psi}, \xi) \in \mathrm{X} \times \mathrm{Y}\,.$$

As established in [6, eq. (95)], there exists a positive constant $\alpha_{\widehat{\mathbf{A}}}$, depending only on κ, η, ρ, $C_{\widehat{b}}$ (cf. [6, Lemma 12]) and $|\Omega|$, and thus independent of h, such that

$$\sup_{\mathbf{0} \neq (\boldsymbol{\psi}, \xi) \in \mathrm{X} \times \mathrm{Y}} \frac{\widehat{\mathbf{A}}((\boldsymbol{\varrho}, \zeta), (\boldsymbol{\psi}, \xi)) + d_{\mathbf{z}}(\boldsymbol{\varrho}, \xi)}{\|(\boldsymbol{\psi}, \xi)\|_{\mathrm{X} \times \mathrm{Y}}} \geqslant \frac{\alpha_{\widehat{\mathbf{A}}}}{2} \|(\boldsymbol{\varrho}, \zeta)\|_{\mathrm{X} \times \mathrm{Y}} \qquad \forall\, (\boldsymbol{\varrho}, \zeta) \in \mathrm{X} \times \mathrm{Y}\,, \tag{3.30}$$

for all $\mathbf{z} \in \mathcal{Q}$ such that $\|\mathbf{z}\|_{0,\rho;\,\Omega} \leqslant r$.

Regarding the solvability analysis of (3.27) and (3.28), we let $r \in \big(0, \min\{\widehat{r}_0, \widehat{r}_0^{\mathtt{d}}\}\big]$, where, following [6, eqs. (98) and (112)], $\widehat{r}_0 := \min\{\delta, \widehat{\delta}_0\}$ with $\delta > 0$ and $\widehat{\delta}_0 := \kappa\, \alpha_{\widehat{\mathbf{A}}}/2$, and $\widehat{r}_0^{\mathtt{d}} := \min\{\delta_{\mathtt{d}}, \widehat{\delta}_0^{\mathtt{d}}\}$ with $\delta_{\mathtt{d}} > 0$ and $\widehat{\delta}_0^{\mathtt{d}} := \kappa\, \alpha_{\widehat{\mathbf{A}},\mathtt{d}}/2$. Here $\alpha_{\widehat{\mathbf{A}},\mathtt{d}} > 0$ is the discrete counterpart of the global inf-sup constant of (3.30), as made precise in [6, Lemma 19]. The continuous and discrete balls (3.14) are then defined with this new radius r. The well-posedness of (3.27) and (3.28) was subsequently established in [6, Sections 4.2 and 4.3], respectively, via a fixed-point strategy.

From now on, we shall denote by $(\boldsymbol{\sigma}, \mathbf{u}, \boldsymbol{\vartheta}, \phi) \in \mathcal{H} \times \mathcal{Q} \times \mathrm{X} \times \mathrm{Y}$, with $\mathbf{u} \in \mathbf{W}(r)$, and $(\boldsymbol{\sigma}_h, \mathbf{u}_h, \boldsymbol{\vartheta}_h, \phi_h) \in \mathbb{H}_h^{\boldsymbol{\sigma}} \times \mathbf{H}_h^{\mathbf{u}} \times \mathbf{H}_h^{\boldsymbol{\vartheta}} \times \widehat{\mathrm{H}}_h^{\phi}$, with $\mathbf{u}_h \in \mathbf{W}_h(r)$, the unique solutions of the continuous problem (3.27) and the Galerkin scheme (3.28), respectively. We recall from [6, Theorem 5] that there exist $\mathcal{C}_1 > 0$, depending only on r, ρ, ν_0, ν_1, $\mathtt{D}_1$, $\mathtt{F}_1$, β (cf. [6, eq. (34)]), and $|\Omega|$, and $\mathcal{C}_2 > 0$, depending only on κ, η, ρ, $C_{\widehat{b}}$ (cf. [6, Lemma 12]), and $|\Omega|$, such that the following *a priori* estimates hold:

$$\|(\boldsymbol{\sigma}, \mathbf{u})\|_{\mathcal{H} \times \mathcal{Q}} \leqslant \mathcal{C}_1\, \widehat{\Psi}_1(\mathbf{u}_{\mathrm{D}}, f, \mathbf{g}, g, \phi_{\mathrm{D}}, \phi_{\mathtt{r}})\,, \tag{3.31}$$

$$\text{and} \quad \|(\boldsymbol{\vartheta}, \phi)\|_{\mathrm{X} \times \mathrm{Y}} \leqslant \mathcal{C}_2\, \widehat{\Psi}_2(g, \phi_{\mathrm{D}})\,, \tag{3.32}$$

where $\widehat{\Psi}_1$ and $\widehat{\Psi}_2$ are defined as

$$\widehat{\Psi}_1(\mathbf{u}_{\mathrm{D}}, f, \mathbf{g}, g, \phi_{\mathrm{D}}, \phi_{\mathtt{r}}) := \|\mathbf{u}_{\mathrm{D}}\|_{1/2,\Gamma} + \|f\|_{0,\Omega} + \|\mathbf{g}\|_{0,\Omega} \Big(\|g\|_{0,t;\Omega} + \|\phi_{\mathrm{D}}\|_{1/2,\Gamma} + \|\phi_{\mathtt{r}}\|_{0,s;\,\Omega} \Big)\,,$$
$$\text{and} \quad \widehat{\Psi}_2(g, \phi_{\mathrm{D}}) := \|g\|_{0,t;\Omega} + \|\phi_{\mathrm{D}}\|_{1/2,\Gamma}\,.$$

Moreover, from [6, Theorem 6], there exist $\mathcal{C}_{1,\mathtt{d}} > 0$, depending only on r, ρ, ν_0, ν_1, $\mathtt{D}_1$, $\mathtt{F}_1$, $\beta_{\mathtt{d}}$ (cf. [6, eq. (60)]), and $|\Omega|$, and $\mathcal{C}_{2,\mathtt{d}} > 0$, depending only on κ, η, ρ, $C_{\widehat{b},\mathtt{d}}$ (cf. [6, eq. (108)]) and $|\Omega|$, such that

$$\|(\boldsymbol{\sigma}_h, \mathbf{u}_h)\|_{\mathcal{H} \times \mathcal{Q}} \leqslant \mathcal{C}_{1,\mathtt{d}}\, \widehat{\Psi}_1(\mathbf{u}_{\mathrm{D}}, f, \mathbf{g}, g, \phi_{\mathrm{D}}, \phi_{\mathtt{r}})\,, \tag{3.33}$$

$$\text{and} \quad \|(\boldsymbol{\vartheta}_h, \phi_h)\|_{\mathrm{X} \times \mathrm{Y}} \leqslant \mathcal{C}_{2,\mathtt{d}}\, \widehat{\Psi}_2(g, \phi_{\mathrm{D}})\,. \tag{3.34}$$

Note that the only difference between $\widehat{\Psi}_1$ and $\widehat{\Psi}_2$ and the expressions defined in (3.17) and (3.18) is that g is now measured in the L^t-norm. Furthermore, we emphasize that $\mathcal{C}_i$ and $\mathcal{C}_{i,\mathtt{d}}$, with $i \in \{1, 2\}$, are not the same constants as those appearing in (3.15), (3.16), (3.19) and (3.20). However, as previously noted, they exhibit the same dependence on the physical parameters of the model.

4 A posteriori error analysis for the mixed-primal scheme

The main goal of this section is to propose a residual-based *a posteriori* error estimator for the Galerkin scheme (3.13) and to prove its reliability and efficiency. To this end, throughout this section we employ the notation and auxiliary results presented in Appendices A and B.

Let us introduce the following residual based *a posteriori* error estimator for the mixed-primal Galerkin scheme (3.13):

$$\Theta_{\mathtt{MP}} := \left\{ \sum_{K\in\mathcal{T}_h} \Theta_{1,K}^{\rho} \right\}^{1/\rho} + \left\{ \sum_{K\in\mathcal{T}_h} \left(\Theta_{2,K}^2 + \Theta_{3,K}^2 \right) \right\}^{1/2} + \left\{ \sum_{K\in\mathcal{T}_h} \Theta_{4,K}^{\ell} \right\}^{1/\ell} + \|\phi_{\mathrm{D}} - \phi_h\|_{1/2,\Gamma}\,, \tag{4.1}$$

where, for each $K \in \mathcal{T}_h$, the local error indicators $\Theta_{i,K}$, $i \in \{1,2,3,4\}$, are defined as

$$\Theta_{1,K}^{\rho} := h_K^{\rho} \left\| \frac{1}{\nu}\,\boldsymbol{\sigma}_h^{\mathrm{d}} + \frac{1}{n}\,f\,\mathbb{I} - \nabla \mathbf{u}_h \right\|_{0,\rho;K}^{\rho} + \sum_{e\in\mathcal{E}_h(\Gamma)\cap\mathcal{E}_h(K)} h_e\,\|\mathbf{u}_{\mathrm{D}} - \mathbf{u}_h\|_{0,\rho;\,e}^{\rho}\,, \tag{4.2}$$

$$\begin{aligned} \Theta_{2,K}^2 := h_K^2 & \left\| \underline{\mathbf{curl}} \left(\frac{1}{\nu}\,\boldsymbol{\sigma}_h^{\mathrm{d}} + \frac{1}{n}\,f\,\mathbb{I} \right) \right\|_{0,K}^2 + \sum_{e\in\mathcal{E}_h(\Omega)\cap\mathcal{E}_h(K)} h_e \left\| \left[\!\!\left[\boldsymbol{\delta}_* \left(\frac{1}{\nu}\,\boldsymbol{\sigma}_h^{\mathrm{d}} + \frac{1}{n}\,f\,\mathbb{I} \right) \right]\!\!\right] \right\|_{0,e}^2 \\ & + \sum_{e\in\mathcal{E}_h(\Gamma)\cap\mathcal{E}_h(K)} h_e \left\| \boldsymbol{\delta}_* \left(\frac{1}{\nu}\,\boldsymbol{\sigma}_h^{\mathrm{d}} + \frac{1}{n}\,f\,\mathbb{I} - \nabla \mathbf{u}_{\mathrm{D}} \right) \right\|_{0,e}^2\,, \end{aligned} \tag{4.3}$$

$$\begin{aligned} \Theta_{3,K}^2 := h_K^2 & \left\| g + \kappa\,\Delta\phi_h - \mathbf{u}_h\cdot\nabla\phi_h - \eta\,\phi_h \right\|_{0,K}^2 + \sum_{e\in\mathcal{E}_h(\Omega)\cap\mathcal{E}_h(K)} h_e \left\| \left[\!\!\left[\kappa\,\nabla\phi_h\cdot\mathbf{n} \right]\!\!\right] \right\|_{0,e}^2 \\ & + \sum_{e\in\mathcal{E}_h(\Gamma)\cap\mathcal{E}_h(K)} h_e \left\| \lambda_{\tilde{h}} + \kappa\,\nabla\phi_h\cdot\mathbf{n} \right\|_{0,e}^2\,, \end{aligned} \tag{4.4}$$

and

$$\Theta_{4,K}^{\ell} := \left\| \mathbf{f}(\phi_h) + \mathbf{div}(\boldsymbol{\sigma}_h) - \mathtt{D}\,\mathbf{u}_h - \mathtt{F}\,|\mathbf{u}_h|^{\rho-2}\,\mathbf{u}_h \right\|_{0,\ell;\,K}^{\ell}\,. \tag{4.5}$$

Note that the last term in $\Theta_{2,K}$ requires that $\boldsymbol{\delta}_*(\nabla\mathbf{u}_{\mathrm{D}})|_e \in \mathbf{L}^2(e)$ for all $e \in \mathcal{E}_h(\Gamma)$. A sufficient condition for this property is to assume that $\mathbf{u}_{\mathrm{D}} \in \mathbf{H}^1(\Gamma)$, and for simplicity we will make this assumption throughout the remainder of this work. We emphasize, however, that this requirement can in fact be relaxed. Indeed, it would suffice to require that $\mathbf{u}_{\mathrm{D}}$ admits an extension $\widetilde{\mathbf{u}}_{\mathrm{D}} \in \mathbf{H}^{3/2+\varepsilon}(\Omega)$ for some $\varepsilon > 0$, so that the trace of $\nabla\widetilde{\mathbf{u}}_{\mathrm{D}}$ on Γ belongs to $\mathbb{L}^2(\Gamma)$. On the other hand, the first term in the definition of $\Theta_{2,K}$ requires that the source term f to be sufficiently regular so as to ensure that $\underline{\mathbf{curl}}(f\,\mathbb{I}) \in \mathbb{L}^2(K)$ for all $K \in \mathcal{T}_h$, while the second and third terms in $\Theta_{2,K}$ require that $\boldsymbol{\delta}_*(f\,\mathbb{I}) \in \mathbb{L}^2(e)$ for all $e \in \mathcal{E}_h$. Both requirements are satisfied by assuming that $f|_K \in \mathrm{H}^1(K)$ for all $K \in \mathcal{T}_h$.

The residual character of each term defining $\Theta_{\mathtt{MP}}$ becomes clear by examining the strong problem (2.1) and the regularity of the continuous weak solution. Indeed, if the discrete solutions coincide with the continuous ones, the local error indicators $\Theta_{1,K}$ and $\Theta_{2,K}$ vanish owing to (3.3a) and the Dirichlet boundary condition for the velocity in (3.3d). In turn, $\Theta_{3,K}$ vanishes at the continuous solution due to (3.3c) and the Dirichlet boundary condition for the concentration in (3.3d), while $\Theta_{4,K}$ also vanishes at the continuous solution by virtue of (3.3b). We stress here that the presence of the last term in (4.1) prevents $\Theta_{\mathtt{MP}}$ from being fully local. To overcome this issue, we will show in Section 4.4 that this estimator induces another one that is indeed fully computable, which will allow us to construct an adaptive refinement algorithm.

In what follows, our goal is to establish the efficiency and reliability of the *a posteriori* error estimator (4.1). More precisely, we show that there exist positive constants $C_{\rm rel}$ and $C_{\rm eff}$, independent of the mesh sizes h and $\widetilde{h}$, and of both the continuous and discrete solutions, such that

$$C_{\rm eff}\,\Theta_{\mathtt{MP}} + \mathtt{h.o.t.} \leqslant \|(\boldsymbol{\sigma}-\boldsymbol{\sigma}_h, \mathbf{u}-\mathbf{u}_h)\|_{\mathcal{H}\times\mathcal{Q}} + \|(\phi-\phi_h, \lambda-\lambda_{\widetilde{h}})\|_{\mathrm{H}^1(\Omega)\times\mathrm{H}^{-1/2}(\Gamma)} \leqslant C_{\rm rel}\,\Theta_{\mathtt{MP}}\,, \tag{4.6}$$

where $\mathtt{h.o.t.}$ stands for one or several terms of higher order. To establish the reliability of the estimator (upper bound in (4.6)), we first derive some preliminary results in Section 4.1, and then complete the proof in Section 4.2. The efficiency (lower bound in (4.6)) is then addressed in Section 4.3.

4.1 Preliminaries for the reliability analysis

In this section, we derive some preliminary estimates required for the proof of the reliability. We first define the residual functionals $\mathcal{R}_1 : \mathcal{H} \to \mathrm{R}$ and $\mathcal{R}_2 : \mathcal{Q} \to \mathrm{R}$ by

$$\mathcal{R}_1(\boldsymbol{\tau}) := \mathbf{F}(\boldsymbol{\tau}) - \mathbf{a}(\boldsymbol{\sigma}_h, \boldsymbol{\tau}) - \mathbf{b}(\boldsymbol{\tau}, \mathbf{u}_h) \qquad \forall\, \boldsymbol{\tau} \in \mathcal{H}\,, \tag{4.7}$$

and

$$\mathcal{R}_2(\mathbf{v}) := \mathbf{G}_{\phi_h}(\mathbf{v}) - \mathbf{b}(\boldsymbol{\sigma}_h, \mathbf{v}) - \mathbf{c}_{\mathbf{u}_h}(\mathbf{u}_h, \mathbf{v}) \qquad \forall\, \mathbf{v} \in \mathcal{Q}\,, \tag{4.8}$$

respectively. Notice that, according to the first and second equations of the Galerkin scheme (3.13), there hold

$$\mathcal{R}_1(\boldsymbol{\tau}_h) = 0 \qquad \forall\, \boldsymbol{\tau}_h \in \mathbb{H}_h^{\boldsymbol{\sigma}}\,, \quad \text{and} \quad \mathcal{R}_2(\mathbf{v}_h) = 0 \qquad \forall\, \mathbf{v}_h \in \mathbf{H}_h^{\mathbf{u}}\,.$$

The following result gives us an estimate for the error associated with the continuous and discrete solutions of the Brinkman–Forchheimer part of the systems (3.6) and (3.13).

Lemma 4.1 *There exists a positive constant C_1, depending on r, ρ, ν_0, ν_1, $\mathtt{D}_1$, $\mathtt{F}_1$, $\|i_s\|$, β, $\beta_{\mathtt{d}}$, and $|\Omega|$, but independent of h and $\widetilde{h}$, such that*

$$\begin{aligned} C_1\,\|(\boldsymbol{\sigma}-\boldsymbol{\sigma}_h, \mathbf{u}-\mathbf{u}_h)\|_{\mathcal{H}\times\mathcal{Q}} \leqslant \|\mathcal{R}_1\|_{\mathcal{H}'} + \|\mathcal{R}_2\|_{\mathcal{Q}'} + \|\mathbf{g}\|_{0,\Omega}\,\|\phi-\phi_h\|_{1,\Omega} \\ + \Psi_1(\mathbf{u}_{\mathrm{D}}, f, \mathbf{g}, g, \phi_{\mathrm{D}}, \phi_{\mathtt{r}})\,\|\mathbf{u}-\mathbf{u}_h\|_{0,\rho;\Omega}\,. \end{aligned} \tag{4.9}$$

Proof. By using (3.21), the definition of the residual functionals $\mathcal{R}_1$ and $\mathcal{R}_2$ (cf. (4.7)–(4.8)), and performing some algebraic manipulations, we obtain, for all $(\boldsymbol{\tau}, \mathbf{v}) \in \mathcal{H} \times \mathcal{Q}$,

$$\begin{aligned} \mathbf{A}_{\mathbf{u}}\big((\boldsymbol{\sigma}-\boldsymbol{\sigma}_h, \mathbf{u}-\mathbf{u}_h), (\boldsymbol{\tau}, \mathbf{v})\big) &= \mathbf{R}_{\phi}(\boldsymbol{\tau}, \mathbf{v}) - \mathbf{A}_{\mathbf{u}}\big((\boldsymbol{\sigma}_h, \mathbf{u}_h), (\boldsymbol{\tau}, \mathbf{v})\big) \\ &= \mathcal{R}_1(\boldsymbol{\tau}) + \mathcal{R}_2(\mathbf{v}) + \mathbf{G}_{\phi}(\mathbf{v}) - \mathbf{G}_{\phi_h}(\mathbf{v}) + \mathbf{c}_{\mathbf{u}}(\mathbf{u}_h, \mathbf{v}) - \mathbf{c}_{\mathbf{u}_h}(\mathbf{u}_h, \mathbf{v})\,, \end{aligned}$$

which together with the global inf-sup condition (3.22) with $\mathbf{z} = \mathbf{u}$, $\boldsymbol{\chi} = \boldsymbol{\sigma} - \boldsymbol{\sigma}_h$, and $\mathbf{w} = \mathbf{u} - \mathbf{u}_h$, yields

$$\alpha_{\mathbf{A}}\,\|(\boldsymbol{\sigma}-\boldsymbol{\sigma}_h, \mathbf{u}-\mathbf{u}_h)\|_{\mathcal{H}\times\mathcal{Q}} \leqslant \|\mathcal{R}_1\|_{\mathcal{H}'} + \|\mathcal{R}_2\|_{\mathcal{Q}'} + \|\mathbf{G}_{\phi} - \mathbf{G}_{\phi_h}\|_{\mathcal{Q}'} + \|\mathbf{c}_{\mathbf{u}}(\mathbf{u}_h, \cdot) - \mathbf{c}_{\mathbf{u}_h}(\mathbf{u}_h, \cdot)\|_{\mathcal{Q}'}\,. \tag{4.10}$$

Then, to bound the last two terms, we may proceed as in [6, eqs. (69)–(70)] to establish that

$$\begin{aligned} \|\mathbf{G}_{\phi} - \mathbf{G}_{\phi_h}\|_{\mathcal{Q}'} &\leqslant \|i_s\|\,\|\mathbf{g}\|_{0,\Omega}\,\|\phi-\phi_h\|_{1,\Omega}\,, \quad \text{and} \\ \|\mathbf{c}_{\mathbf{u}}(\mathbf{u}_h, \cdot) - \mathbf{c}_{\mathbf{u}_h}(\mathbf{u}_h, \cdot)\|_{\mathcal{Q}'} &\leqslant L_{\mathbf{c}}\,(2r)^{\rho-3}\,\|\mathbf{u}_h\|_{0,\rho;\Omega}\,\|\mathbf{u}-\mathbf{u}_h\|_{0,\rho;\Omega}\,, \end{aligned}$$

where $L_{\mathbf{c}}$ is a positive constant depending only on ρ, $\mathtt{F}_1$ and $|\Omega|$ (cf. [6, eq. (46)]). Putting these estimates into (4.10), and then using the *a priori* estimate (3.19), we conclude (4.9), as desired. ∎

With the aim of obtaining an estimate analogous to (4.9), but now for the error associated with the CDR system, we introduce the residual functionals $\widetilde{\mathcal{R}}_1 : \mathrm{H}^1(\Omega) \to \mathrm{R}$ and $\widetilde{\mathcal{R}}_2 : \mathrm{H}^{-1/2}(\Gamma) \to \mathrm{R}$ defined by

$$\widetilde{\mathcal{R}}_1(\psi) := \mathrm{F}(\psi) - a_{\mathbf{u}_h}(\phi_h, \psi) - b(\psi, \lambda_{\widetilde{h}}) \qquad \forall\, \psi \in \mathrm{H}^1(\Omega)\,, \tag{4.11}$$

and

$$\widetilde{\mathcal{R}}_2(\xi) := \mathrm{G}(\xi) - b(\phi_h, \xi) \qquad \forall\, \xi \in \mathrm{H}^{-1/2}(\Gamma)\,, \tag{4.12}$$

respectively. From the third and fourth equations of (3.13), it follows that

$$\widetilde{\mathcal{R}}_1(\psi_h) = 0 \qquad \forall\, \psi_h \in \mathrm{H}_h^{\phi} \quad \text{and} \quad \widetilde{\mathcal{R}}_2(\xi_{\widetilde{h}}) = 0 \qquad \forall\, \xi_{\widetilde{h}} \in \mathrm{H}_{\widetilde{h}}^{\lambda}\,. \tag{4.13}$$

Lemma 4.2 *There exists a positive constant C_2 depending on κ, η, ρ, $\|i_s\|$, $\widetilde{\beta}$, $\widetilde{\beta}_{\mathtt{d}}$, and $|\Omega|$, but independent of h and $\widetilde{h}$, such that*

$$C_2\, \|(\phi - \phi_h, \lambda - \lambda_{\widetilde{h}})\|_{\mathrm{H}^1(\Omega)\times\mathrm{H}^{-1/2}(\Gamma)} \leqslant \|\widetilde{\mathcal{R}}_1\|_{(\mathrm{H}^1(\Omega))'} + \|\widetilde{\mathcal{R}}_2\|_{(\mathrm{H}^{-1/2}(\Gamma))'} + \Psi_2(g, \phi_{\mathrm{D}})\, \|\mathbf{u} - \mathbf{u}_h\|_{0,\rho;\Omega}\,. \tag{4.14}$$

Proof. We proceed similarly as in the proof of Lemma 4.1. In fact, using the last two rows of (3.6) and performing some algebraic manipulations, we have that, for all $(\psi, \xi) \in \mathrm{H}^1(\Omega) \times \mathrm{H}^{-1/2}(\Gamma)$,

$$\begin{aligned} a_{\mathbf{u}}(\phi - \phi_h, \psi) + b(\psi, \lambda - \lambda_{\widetilde{h}}) + b(\phi - \phi_h, \xi) &= \mathrm{F}(\psi) - a_{\mathbf{u}}(\phi_h, \psi) - b(\psi, \lambda_{\widetilde{h}}) + \mathrm{G}(\xi) - b(\phi_h, \xi) \\ &= \widetilde{\mathcal{R}}_1(\psi) + \widetilde{\mathcal{R}}_2(\xi) + a_{\mathbf{u}_h}(\phi_h, \psi) - a_{\mathbf{u}}(\phi_h, \psi)\,. \end{aligned}$$

Now, by using the global inf-sup condition (3.23) with $\mathbf{z} = \mathbf{u}$, $\varphi = \phi - \phi_h$, and $\varsigma = \lambda - \lambda_{\widetilde{h}}$, along with the above equation, we find that

$$\alpha_{\mathtt{CDR}}\, \|(\phi - \phi_h, \lambda - \lambda_{\widetilde{h}})\| \leqslant \|\widetilde{\mathcal{R}}_1\|_{(\mathrm{H}^1(\Omega))'} + \|\widetilde{\mathcal{R}}_2\|_{(\mathrm{H}^{-1/2}(\Gamma))'} + \|a_{\mathbf{u}_h}(\phi_h, \cdot) - a_{\mathbf{u}}(\phi_h, \cdot)\|_{(\mathrm{H}^1(\Omega))'}\,. \tag{4.15}$$

To bound the last term, we apply the Hölder inequality and the *a priori* estimate (3.20), so that

$$\|a_{\mathbf{u}_h}(\phi_h, \cdot) - a_{\mathbf{u}}(\phi_h, \cdot)\|_{(\mathrm{H}^1(\Omega))'} \leqslant \|i_s\|\, \|\mathbf{u} - \mathbf{u}_h\|_{0,\rho;\Omega}\, \|\phi_h\|_{1,\Omega} \leqslant \mathcal{C}_{2,\mathtt{d}}\, \|i_s\|\, \Psi_2(g, \phi_{\mathrm{D}})\, \|\mathbf{u} - \mathbf{u}_h\|_{0,\rho;\Omega}\,.$$

Putting this into (4.15), we obtain (4.14), thus concluding the proof. ∎

As a consequence of this lemma, we can bound the concentration error in (4.9), thereby arriving at

$$\begin{aligned} \widetilde{C}_1\, \|(\boldsymbol{\sigma} - \boldsymbol{\sigma}_h, \mathbf{u} - \mathbf{u}_h)\|_{\mathcal{H}\times\mathcal{Q}} \leqslant\, & \|\mathcal{R}_1\|_{\mathcal{H}'} + \|\mathcal{R}_2\|_{\mathcal{Q}'} + \|\widetilde{\mathcal{R}}_1\|_{(\mathrm{H}^1(\Omega))'} + \|\widetilde{\mathcal{R}}_2\|_{(\mathrm{H}^{-1/2}(\Gamma))'} \\ & + \Big\{\Psi_1(\mathbf{u}_{\mathrm{D}}, f, \mathbf{g}, g, \phi_{\mathrm{D}}, \phi_{\mathtt{r}}) + \Psi_2(g, \phi_{\mathrm{D}})\Big\}\|\mathbf{u} - \mathbf{u}_h\|_{0,\rho;\Omega}\,, \end{aligned} \tag{4.16}$$

where $\widetilde{C}_1 = C_1 C_2 / \max\{C_2, \|\mathbf{g}\|_{0,\Omega}\}$. As a result, and employing once again the previous lemma, we can establish the following preliminary upper bound for the total error.

Theorem 4.3 *Assume that the data satisfy*

$$\Psi_1(\mathbf{u}_{\mathrm{D}}, f, \mathbf{g}, g, \phi_{\mathrm{D}}, \phi_{\mathtt{r}}) + \Psi_2(g, \phi_{\mathrm{D}}) \leqslant \frac{\widetilde{C}_1}{2}\,. \tag{4.17}$$

Then, there exists a positive constant C_3, depending on r, ρ, ν_0, ν_1, $\mathtt{D}_1$, $\mathtt{F}_1$, $\|i_s\|$, β, $\beta_{\mathtt{d}}$, $\|\mathbf{g}\|_{0,\Omega}$, κ, η, $\widetilde{\beta}$, $\widetilde{\beta}_{\mathtt{d}}$, and $|\Omega|$, but independent of h and $\widetilde{h}$, such that

$$\begin{aligned} &\|(\boldsymbol{\sigma} - \boldsymbol{\sigma}_h, \mathbf{u} - \mathbf{u}_h)\|_{\mathcal{H}\times\mathcal{Q}} + \|(\phi - \phi_h, \lambda - \lambda_{\widetilde{h}})\|_{\mathrm{H}^1(\Omega)\times\mathrm{H}^{-1/2}(\Gamma)} \\ &\qquad \leqslant C_3 \Big\{\|\mathcal{R}_1\|_{\mathcal{H}'} + \|\mathcal{R}_2\|_{\mathcal{Q}'} + \|\widetilde{\mathcal{R}}_1\|_{(\mathrm{H}^1(\Omega))'} + \|\widetilde{\mathcal{R}}_2\|_{(\mathrm{H}^{-1/2}(\Gamma))'}\Big\}\,. \end{aligned} \tag{4.18}$$

Proof. Substituting the assumption (4.17) into (4.16) yields

$$\frac{\widetilde{C}_1}{2}\,\|(\boldsymbol{\sigma}-\boldsymbol{\sigma}_h,\mathbf{u}-\mathbf{u}_h)\|_{\mathcal{H}\times\mathcal{Q}} \leqslant \|\mathcal{R}_1\|_{\mathcal{H}'}+\|\mathcal{R}_2\|_{\mathcal{Q}'}+\|\widetilde{\mathcal{R}}_1\|_{(\mathrm{H}^1(\Omega))'}+\|\widetilde{\mathcal{R}}_2\|_{(\mathrm{H}^{-1/2}(\Gamma))'}\,. \tag{4.19}$$

Replacing this into (4.14) to control the last term, invoking $\Psi_2(g,\phi_{\mathrm{D}}) \leqslant \widetilde{C}_1/2$ from (4.17), and adding the resulting inequality to (4.19), we obtain (4.18) with $C_3 := 2\,\max\{1/\widetilde{C}_1, 1/C_2\}$. ▫

It follows from (4.18) that, in order to establish the reliability of the *a posteriori* error estimator (cf. (4.6)), it is necessary to derive suitable bounds for the residual functionals. This will be the main objective of the following section.

4.2 Reliability

We start our analysis by establishing estimates for $\|\mathcal{R}_1\|_{\mathcal{H}'}$ and $\|\mathcal{R}_2\|_{\mathcal{Q}'}$. For the sake of brevity, we do not reproduce the proof of the first estimate here and instead refer the reader to [11, Lemma 3.4], where an analogous result is given for the convective Brinkman–Forchheimer equations. Nevertheless, the argument follows a standard strategy based on a Helmholtz decomposition, which will be illustrated later in the proof of Lemma 5.5.

Lemma 4.4 *There exists a positive constant C, independent of h and $\widetilde{h}$, such that*

$$\|\mathcal{R}_1\|_{\mathcal{H}'} \leqslant C\,\left(\left\{\sum_{K\in\mathcal{T}_h}\Theta_{1,K}^{\rho}\right\}^{1/\rho}+\left\{\sum_{K\in\mathcal{T}_h}\Theta_{2,K}^{2}\right\}^{1/2}\right),$$

where $\Theta_{1,K}$ and $\Theta_{2,K}$ are defined in (4.2) and (4.3), respectively.

Proof. The proof follows by a slight modification of that of [11, Lemma 3.4], where the local error indicator additionally accounts for a convective term and the L^4-norm is employed instead of the L^{ρ}-norm, which explains the presence of the exponent ρ in our case. ▫

Lemma 4.5 *Let $\Theta_{4,K}$ be defined as in (4.5). Then, there holds*

$$\|\mathcal{R}_2\|_{\mathcal{Q}'} \leqslant \left\{\sum_{K\in\mathcal{T}_h}\Theta_{4,K}^{\ell}\right\}^{1/\ell}.$$

Proof. It follows directly from the definition of $\mathcal{R}_2$ (cf. (4.8)) and the Hölder inequality. ▫

We continue the reliability analysis by deriving suitable bounds for the norms of the residual functionals $\widetilde{\mathcal{R}}_1$ and $\widetilde{\mathcal{R}}_2$ (cf. (4.11) and (4.12)).

Lemma 4.6 *There exists a positive constant C, independent of h and $\widetilde{h}$, such that*

$$\|\widetilde{\mathcal{R}}_1\|_{(\mathrm{H}^1(\Omega))'} \leqslant C\,\left\{\sum_{K\in\mathcal{T}_h}\Theta_{3,K}^{2}\right\}^{1/2} \quad \textit{and} \quad \|\widetilde{\mathcal{R}}_2\|_{(\mathrm{H}^{-1/2}(\Gamma))} \leqslant \|\phi_{\mathrm{D}}-\phi_h\|_{1/2,\Gamma}\,, \tag{4.20}$$

where $\Theta_{3,K}$ is defined in (4.4).

Proof. We proceed as in [22, Lemma 3.12]. In fact, to prove the first estimate in (4.20), we fix $\psi \in \mathrm{H}^1(\Omega)$ and define $\widehat{\psi} := \psi - \mathcal{I}_h(\psi)$, so that employing the first relation in (4.13) we find that $\widetilde{\mathcal{R}}_1(\psi) = \widetilde{\mathcal{R}}_1(\widehat{\psi})$. Then, by using the definition of $\widetilde{\mathcal{R}}_1$ (cf. (4.11)) and performing local integration by parts, we get

$$\widetilde{\mathcal{R}}_1(\psi) = \sum_{K \in \mathcal{T}_h} \left\{ \int_K g\, \widehat{\psi} + \kappa \int_K \Delta \phi_h\, \widehat{\psi} - \int_K (\mathbf{u}_h \cdot \nabla \phi_h)\, \widehat{\psi} - \eta \int_K \phi_h\, \widehat{\psi} \right\}$$
$$- \sum_{e \in \mathcal{E}_h(\Omega)} \kappa \int_e [\![\nabla \phi_h \cdot \mathbf{n}]\!]\, \widehat{\psi} - \sum_{e \in \mathcal{E}_h(\Gamma)} \int_e (\lambda_{\widetilde{h}} + \kappa\, \nabla \phi_h \cdot \mathbf{n})\, \widehat{\psi}\,.$$

Hence, by using the Cauchy–Schwarz inequality and the approximation properties (A.5) and (A.6), we conclude the first estimate in (4.20). The second estimate follows directly from the definitions of $\widetilde{\mathcal{R}}_2$ (cf. (4.12)) and of the dual norm. This completes the proof. ▫

The main result of this section, which is the reliability of the *a posteriori* error estimator $\Theta_{\mathtt{MP}}$ (cf. (4.1)), is stated below.

Theorem 4.7 *Let $(\boldsymbol{\sigma}, \mathbf{u}, \phi, \lambda) \in \mathcal{H} \times \mathcal{Q} \times \mathrm{H}^1(\Omega) \times \mathrm{H}^{-1/2}(\Gamma)$ and $(\boldsymbol{\sigma}_h, \mathbf{u}_h, \phi_h, \lambda_{\widetilde{h}}) \in \mathbb{H}_h^{\boldsymbol{\sigma}} \times \mathbf{H}_h^{\mathbf{u}} \times \mathrm{H}_h^{\phi} \times \mathrm{H}_{\widetilde{h}}^{\lambda}$ be the solutions to (3.6) and (3.13), respectively. Assume that the data satisfy the assumption of Theorem 4.3. Then, $\Theta_{\mathtt{MP}}$ is a reliable estimator, i.e. there exists a positive constant C_{rel}, depending on r, ρ, ν_0, ν_1, $\mathtt{D}_1$, $\mathtt{F}_1$, $\|i_s\|$, β, $\beta_{\mathtt{d}}$, $\|\mathbf{g}\|_{0,\Omega}$, κ, η, $\widetilde{\beta}$, $\widetilde{\beta}_{\mathtt{d}}$, and $|\Omega|$, but independent of h and $\widetilde{h}$, such that*

$$\|(\boldsymbol{\sigma} - \boldsymbol{\sigma}_h, \mathbf{u} - \mathbf{u}_h)\|_{\mathcal{H} \times \mathcal{Q}} + \|(\phi - \phi_h, \lambda - \lambda_{\widetilde{h}})\|_{\mathrm{H}^1(\Omega) \times \mathrm{H}^{-1/2}(\Gamma)} \leqslant C_{\mathrm{rel}}\, \Theta_{\mathtt{MP}}\,.$$

Proof. It follows from the estimate (4.18), together with a straightforward application of Lemmas 4.4, 4.5 and 4.6. ▫

4.3 Efficiency

Having established the reliability of the *a posteriori* error estimator (4.1) (cf. Theorem 4.7), it remains to prove its efficiency, that is, the upper bound in (4.6). In this regard, we observe that the resulting arguments closely follow those available in the literature (see, for instance, [7, 11, 13, 30, 31]), which rely on classical inverse and discrete trace inequalities, together with the localization technique based on bubble functions. For convenience, these auxiliary results are recalled in Appendix B, and we adopt the notation introduced therein.

Throughout this section, we assume that $\mathbf{u}_{\mathrm{D}}$, f, g, and $\frac{1}{\nu}$ are piecewise polynomials. Otherwise, if the data are sufficiently smooth, one can proceed as in [15, Section 6.2], in which case additional higher-order terms, arising from suitable polynomial approximations of these functions, appear in the lower bound of (4.6). This accounts for the possible presence of the `h.o.t.` term in that inequality.

The following result provides estimates for the terms involved in $\Theta_{1,K}$ (cf. (4.2)).

Lemma 4.8 *There exists a positive constant C_1, depending on ν_0, but independent of h and $\widetilde{h}$, such that*

$$h_K^{\rho} \left\| \frac{1}{\nu}\, \boldsymbol{\sigma}_h^{\mathrm{d}} + \frac{1}{n}\, f\, \mathbb{I} - \nabla \mathbf{u}_h \right\|_{0,\rho;K}^{\rho} \leqslant C_1 \left\{ h_K^{\varrho}\, \|\boldsymbol{\sigma} - \boldsymbol{\sigma}_h\|_{0,K}^{\rho} + \|\mathbf{u} - \mathbf{u}_h\|_{0,\rho;K}^{\rho} \right\}, \tag{4.21}$$

for all $K \in \mathcal{T}_h$, where $\varrho = 2$ when $n = 2$, and $\varrho = 3 - \rho/2$ when $n = 3$.

Proof. We proceed as in [11, Lemma 3.7]. We fix $K \in \mathcal{T}_h$ and define $\boldsymbol{\chi}_K := \frac{1}{\nu}\,\boldsymbol{\sigma}_h^{\mathrm{d}} + \frac{1}{n}\,f\,\mathbb{I} - \nabla \mathbf{u}_h$ in K. By assumption, both $\frac{1}{\nu}$ and f are piecewise polynomials, which, together with the fact that $\boldsymbol{\sigma}_h|_K \in \mathbb{RT}_k(K) \subset \mathbb{P}_{k+1}(K)$ and $\nabla \mathbf{u}_h|_K \in \mathbb{P}_{k-1}(K)$, implies that $\boldsymbol{\chi}_K \in \mathbb{P}_{\bar{k}}(K)$ for some positive integer $\bar{k}$ depending on k and the polynomial degrees of $\frac{1}{\nu}$ and f. Hence, by (B.2) in Lemma B.1, there holds

$$c_1\,\|\boldsymbol{\chi}_K\|_{0,\rho;\,K} \leqslant \sup_{\mathbf{0}\neq\boldsymbol{\tau}\in\mathbb{P}_{\bar{k}}(K)} \frac{\displaystyle\int_K \boldsymbol{\chi}_K : (\psi_K\,\boldsymbol{\tau})}{\|\boldsymbol{\tau}\|_{0,\ell;K}}\,. \tag{4.22}$$

Moreover, since $\boldsymbol{\sigma}$ and $\mathbf{u}$ satisfy (3.3a) in the sense of distributions, it follows that

$$\int_K \left(\frac{1}{\nu}\,\boldsymbol{\sigma}^{\mathrm{d}} + \frac{1}{n}\,f\,\mathbb{I} - \nabla \mathbf{u}\right) : (\psi_K\,\boldsymbol{\tau}) = 0\,. \tag{4.23}$$

Hence, combining this with an integration by parts and the fact that $\psi_K = 0$ on ∂K (cf. (B.1)), we obtain

$$\begin{aligned}\int_K \boldsymbol{\chi}_K : (\psi_K\,\boldsymbol{\tau}) &= \int_K \left(\frac{1}{\nu}\,(\boldsymbol{\sigma}_h - \boldsymbol{\sigma})^{\mathrm{d}} - \nabla(\mathbf{u}_h - \mathbf{u})\right) : (\psi_K\,\boldsymbol{\tau}) \\ &= \int_K \frac{1}{\nu}\,(\boldsymbol{\sigma}_h - \boldsymbol{\sigma})^{\mathrm{d}} : (\psi_K\,\boldsymbol{\tau}) + \int_K (\mathbf{u}_h - \mathbf{u}) \cdot \mathbf{div}(\psi_K\,\boldsymbol{\tau})\,.\end{aligned}$$

Thus, employing the Cauchy–Schwarz and Hölder inequalities, the boundedness of ν (cf. (2.2)), the fact that $\|\mathbf{div}(\psi_K\,\boldsymbol{\tau})\|_{0,\ell;K} \leqslant \|\nabla(\psi_K\,\boldsymbol{\tau})\|_{0,\ell;K}$, the estimate (B.3), and (B.1), we arrive at

$$\begin{aligned}\int_K \boldsymbol{\chi}_K : (\psi_K\,\boldsymbol{\tau}) &\leqslant \frac{1}{\nu_0}\,\|\boldsymbol{\sigma} - \boldsymbol{\sigma}_h\|_{0,K}\,\|\psi_K\,\boldsymbol{\tau}\|_{0,K} + \|\mathbf{u} - \mathbf{u}_h\|_{0,\rho;\,K}\,\|\nabla(\psi_K\,\boldsymbol{\tau})\|_{0,\ell;K} \\ &\leqslant \frac{1}{\nu_0}\,\|\boldsymbol{\sigma} - \boldsymbol{\sigma}_h\|_{0,K}\,\|\boldsymbol{\tau}\|_{0,K} + c_3\,h_K^{-1}\|\mathbf{u} - \mathbf{u}_h\|_{0,\rho;\,K}\|\boldsymbol{\tau}\|_{0,\ell;K}\,,\end{aligned}$$

which, together with the inverse inequality (B.4) with $l = m = 0$, $\mathrm{p} = 2$ and $\mathrm{q} = \ell$, gives

$$\int_K \boldsymbol{\chi}_K : (\psi_K\,\boldsymbol{\tau}) \leqslant \left(\frac{1}{\nu_0}\,h_K^{n(1/2-1/\ell)}\,\|\boldsymbol{\sigma} - \boldsymbol{\sigma}_h\|_{0,K} + c_3\,h_K^{-1}\|\mathbf{u} - \mathbf{u}_h\|_{0,\rho;\,K}\right)\|\boldsymbol{\tau}\|_{0,\ell;K}\,.$$

Hence, returning to (4.22), recalling that $1/\ell = 1 - 1/\rho$ and the definition of $\boldsymbol{\chi}_K$, we get

$$c_1\left\|\frac{1}{\nu}\,\boldsymbol{\sigma}_h^{\mathrm{d}} + \frac{1}{n}\,f\,\mathbb{I} - \nabla \mathbf{u}_h\right\|_{0,\rho;K} \leqslant \frac{1}{\nu_0}\,h_K^{n(1/\rho-1/2)}\,\|\boldsymbol{\sigma} - \boldsymbol{\sigma}_h\|_{0,K} + c_3\,h_K^{-1}\|\mathbf{u} - \mathbf{u}_h\|_{0,\rho;\,K}\,,$$

whence, upon multiplying by h_K and raising the resulting expression to the power ρ, we arrive at (4.21). □

Lemma 4.9 *There exists a positive constant C_2 depending on ν_0, but independent of h and $\widetilde{h}$, such that*

$$h_e\,\|\mathbf{u}_{\mathrm{D}} - \mathbf{u}_h\|_{0,\rho;\,e}^{\rho} \leqslant C_2\,\left\{h_{K_e}^{\varrho}\,\|\boldsymbol{\sigma} - \boldsymbol{\sigma}_h\|_{0,K_e}^{\rho} + \|\mathbf{u} - \mathbf{u}_h\|_{0,\rho;\,K_e}^{\rho}\right\}\,, \tag{4.24}$$

for all $e \in \mathcal{E}_h(\Gamma)$, where K_e is the triangle/tetrahedron of $\mathcal{T}_h$ having e as an edge/face, and ϱ is defined as in Lemma 4.8.

Proof. We proceed as in [11, Lemma 3.8]. Indeed, fixing $e \in \mathcal{E}_h(\Gamma)$, we first note that since $\mathbf{u}_{\mathrm{D}}$ is piecewise polynomial, we are able to use the local inverse inequality (B.4) in the $(n-1)$-dimensional element e, with $l = m = 0$, $\mathrm{p} = \rho$, $\mathrm{q} = \rho/2$, to obtain

$$\|\mathbf{u}_{\mathrm{D}} - \mathbf{u}_h\|_{0,\rho;\, e} \leqslant c\, h_e^{(1-n)/\rho}\, \|\mathbf{u}_{\mathrm{D}} - \mathbf{u}_h\|_{0,\rho/2;\, e} = c\, h_e^{(1-n)/\rho}\, \|\mathbf{u} - \mathbf{u}_h\|_{0,\rho/2;\, e}\,,$$

where in the last equality we used that $\mathbf{u} = \mathbf{u}_{\mathrm{D}}$ weakly on Γ, according to (3.3d). Then, multiplying by $h_e^{(n-1)/\rho}$, and then applying the discrete trace inequality (B.5), we arrive at

$$h_e^{(n-1)/\rho}\, \|\mathbf{u}_{\mathrm{D}} - \mathbf{u}_h\|_{0,\rho;\, e} \leqslant C\, \left\{ h_{K_e}^{-1} \|\mathbf{u} - \mathbf{u}_h\|_{0,\rho/2;K_e}^{\rho/2} + h_{K_e}^{\rho/2-1}\, \|\nabla(\mathbf{u} - \mathbf{u}_h)\|_{0,\rho/2;K_e}^{\rho/2} \right\}^{2/\rho}.$$

In turn, applying the subadditivity inequality with $2/\rho < 1$, the above estimate implies that

$$h_e^{(n-1)/\rho}\, \|\mathbf{u}_{\mathrm{D}} - \mathbf{u}_h\|_{0,\rho;\, e} \leqslant C\, \left\{ h_{K_e}^{-2/\rho} \|\mathbf{u} - \mathbf{u}_h\|_{0,\rho/2;K_e} + h_{K_e}^{1-2/\rho}\, \|\nabla(\mathbf{u} - \mathbf{u}_h)\|_{0,\rho/2;K_e} \right\}, \tag{4.25}$$

where C is certainly different to the constant in the previous estimate, but still independent of h and $\widetilde{h}$.

Similarly to (4.23), from (3.3a) it follows that $\nabla \mathbf{u} = \frac{1}{\nu}\, \boldsymbol{\sigma}^{\mathrm{d}} + \frac{1}{n}\, f\, \mathbb{I}$ weakly in K_e, so substituting this into (4.25), adding and subtracting $\frac{1}{\nu}\, \boldsymbol{\sigma}_h^{\mathrm{d}}$, applying the triangle inequality, and performing some algebraic manipulations, we obtain

$$\begin{aligned} h_e^{(n-1)/\rho}\, \|\mathbf{u}_{\mathrm{D}} - \mathbf{u}_h\|_{0,\rho;\, e} \leqslant C\, \Bigg\{ & h_{K_e}^{-2/\rho}\, \|\mathbf{u} - \mathbf{u}_h\|_{0,\rho/2;K_e} + \frac{h_{K_e}^{1-2/\rho}}{\nu_0}\, \|\boldsymbol{\sigma} - \boldsymbol{\sigma}_h\|_{0,\rho/2;K_e} \\ & + h_{K_e}^{1-2/\rho} \left\| \frac{1}{\nu}\, \boldsymbol{\sigma}_h^{\mathrm{d}} + \frac{1}{n}\, f\, \mathbb{I} - \nabla \mathbf{u}_h \right\|_{0,\rho/2;K_e} \Bigg\}. \end{aligned} \tag{4.26}$$

Next, we apply the continuous embedding $\boldsymbol{i}_{\rho,\rho/2}(K_e)$, in its vector- and tensor-valued forms, to the first and third terms on the right-hand side of the above estimate, and the continuous embedding $\boldsymbol{i}_{2,\rho/2}(K_e)$, in its tensor-valued form, to the second term. Moreover, recalling from (1.1) that

$$\|\boldsymbol{i}_{\rho,\rho/2}(K_e)\| \leqslant |K_e|^{1/\rho} \quad \text{and} \quad \|\boldsymbol{i}_{2,\rho/2}(K_e)\| \leqslant |K_e|^{(4-\rho)/(2\rho)}\,,$$

and using the fact that $|K_e| \cong h_{K_e}^n$, the estimate (4.26) becomes

$$\begin{aligned} h_e^{(n-1)/\rho}\, \|\mathbf{u}_{\mathrm{D}} - \mathbf{u}_h\|_{0,\rho;\, e} \leqslant C(\nu_0)\, \Bigg\{ & h_{K_e}^{(n-2)/\rho}\, \|\mathbf{u} - \mathbf{u}_h\|_{0,\rho;K_e} + h_{K_e}^{1-2/\rho+n(4-\rho)/(2\rho)}\, \|\boldsymbol{\sigma} - \boldsymbol{\sigma}_h\|_{0,K_e} \\ & + h_{K_e}^{1+(n-2)/\rho} \left\| \frac{1}{\nu}\, \boldsymbol{\sigma}_h^{\mathrm{d}} + \frac{1}{n}\, f\, \mathbb{I} - \nabla \mathbf{u}_h \right\|_{0,\rho;K_e} \Bigg\}, \end{aligned}$$

where $C(\nu_0) > 0$ depends on ν_0. By raising to the power ρ, using (4.21) to bound the last term, dividing by h_e^{n-2}, and performing some algebraic manipulations, we obtain

$$h_e\, \|\mathbf{u}_{\mathrm{D}} - \mathbf{u}_h\|_{0,\rho;\, e}^{\rho} \leqslant C(\nu_0) \left\{ \left(\frac{h_{K_e}}{h_e} \right)^{n-2} \|\mathbf{u} - \mathbf{u}_h\|_{0,\rho;K_e}^{\rho} + \left(\frac{h_{K_e}}{h_e} \right)^{n-2} h_{K_e}^{n+\rho(1-n/2)}\, \|\boldsymbol{\sigma} - \boldsymbol{\sigma}_h\|_{0,K_e}^{\rho} \right\},$$

whence, by using the uniform bound $h_{K_e} \leqslant c\, h_e$, with a constant $c > 0$ depending only on the shape-regularity parameter of the mesh, we get the desired estimate (4.24). ▫

The corresponding bounds for the terms defining $\Theta_{2,K}$ (cf. (4.3)) are given in the following lemma.

Lemma 4.10 *There exist positive constants C_3 and C_4, depending on ν_0, but independent of h and $\widetilde{h}$, such that*

$$h_K^2 \left\| \underline{\mathbf{curl}} \left(\frac{1}{\nu} \boldsymbol{\sigma}_h^{\mathrm{d}} + \frac{1}{n} f \mathbb{I} \right) \right\|_{0,K}^2 \leqslant C_3 \, \|\boldsymbol{\sigma} - \boldsymbol{\sigma}_h\|_{0,K}^2 \qquad \forall \, K \in \mathcal{T}_h \, , \tag{4.27}$$

and

$$h_e \left\| \left[\left[\boldsymbol{\delta}_* \left(\frac{1}{\nu} \boldsymbol{\sigma}_h^{\mathrm{d}} + \frac{1}{n} f \mathbb{I} \right) \right] \right] \right\|_{0,e}^2 \leqslant C_4 \, \|\boldsymbol{\sigma} - \boldsymbol{\sigma}_h\|_{0,\omega_e}^2 \qquad \forall \, e \in \mathcal{E}_h(\Omega) \, , \tag{4.28}$$

where ω_e denotes the union of the two elements of $\mathcal{T}_h$ sharing the edge/face e. Additionally, there exists a positive constant C_5, depending on ν_0, but independent of h and $\widetilde{h}$, such that

$$h_e \left\| \boldsymbol{\delta}_* \left(\frac{1}{\nu} \boldsymbol{\sigma}_h^{\mathrm{d}} + \frac{1}{n} f \mathbb{I} - \nabla \mathbf{u}_{\mathrm{D}} \right) \right\|_{0,e}^2 \leqslant C_5 \, \|\boldsymbol{\sigma} - \boldsymbol{\sigma}_h\|_{0,K_e}^2 \qquad \forall \, e \in \mathcal{E}_h(\Gamma) \, , \tag{4.29}$$

where K_e is the element to which the boundary edge/face e belongs.

Proof. Noting from (3.3a) that $\nabla \mathbf{u} = \frac{1}{\nu} \boldsymbol{\sigma}^{\mathrm{d}} + \frac{1}{n} f \mathbb{I}$ and $\underline{\mathbf{curl}}(\frac{1}{\nu} \boldsymbol{\sigma}^{\mathrm{d}} + \frac{1}{n} f \mathbb{I}) = \mathbf{0}$ weakly in Ω, the estimates (4.27) and (4.28) follow from slight adaptations of [31, Lemma 4.11] when $n = 2$, and of [28, Lemma 4.10] when $n = 3$. In turn, for the proof of (4.29), we refer the reader to [31, Lemma 4.15] for $n = 2$, and to [28, Lemma 4.12] for $n = 3$. ▫

The following result provides an estimate for $\Theta_{4,K}$ (cf. (4.5)).

Lemma 4.11 *There exists a positive constant C_6, depending on $\mathtt{D}_1$ and $\mathtt{F}_1$, but independent of h and $\widetilde{h}$, such that*

$$\begin{aligned} &\left\| \mathbf{f}(\phi_h) + \mathbf{div}(\boldsymbol{\sigma}_h) - \mathtt{D} \, \mathbf{u}_h - \mathtt{F} \, |\mathbf{u}_h|^{\rho-2} \mathbf{u}_h \right\|_{0,\ell;\, K}^{\ell} \\ &\quad \leqslant C_6 \left\{ \|\mathbf{div}(\boldsymbol{\sigma} - \boldsymbol{\sigma}_h)\|_{0,\ell;K}^{\ell} + \|\mathbf{u} - \mathbf{u}_h\|_{0,\ell;\, K}^{\ell} + \left\| |\mathbf{u}|^{\rho-2} \mathbf{u} - |\mathbf{u}_h|^{\rho-2} \mathbf{u}_h \right\|_{0,\ell;\, K}^{\ell} + \|\phi - \phi_h\|_{1,K}^{\ell} \right\} , \end{aligned} \tag{4.30}$$

for all $K \in \mathcal{T}_h$.

Proof. According to the second row in (3.6), we have that $\mathtt{D} \, \mathbf{u} + \mathtt{F} \, |\mathbf{u}|^{\rho-2} \, \mathbf{u} - \mathbf{div}(\boldsymbol{\sigma}) = \mathbf{f}(\phi)$ in $\mathbf{L}^{\ell}(\Omega)$. Using this identity together with the triangle inequality, gives us

$$\begin{aligned} \left\| \mathbf{f}(\phi_h) + \mathbf{div}(\boldsymbol{\sigma}_h) - \mathtt{D} \, \mathbf{u}_h - \mathtt{F} \, |\mathbf{u}_h|^{\rho-2} \mathbf{u}_h \right\|_{0,\ell;\, K} &\leqslant \|\mathbf{f}(\phi) - \mathbf{f}(\phi_h)\|_{0,\ell;\, K} + \|\mathbf{div}(\boldsymbol{\sigma} - \boldsymbol{\sigma}_h)\|_{0,\ell;\, K} \\ &\quad + \|\mathtt{D} \, (\mathbf{u} - \mathbf{u}_h)\|_{0,\ell;\, K} + \left\| \mathtt{F} \, (|\mathbf{u}|^{\rho-2} \mathbf{u} - |\mathbf{u}_h|^{\rho-2} \mathbf{u}_h) \right\|_{0,\ell;\, K} . \end{aligned} \tag{4.31}$$

We continue by bounding the first term on the right-hand side. Indeed, from relation (2.3), we apply the Hölder inequality and the continuous embedding $i_s(K) : \mathrm{H}^1(K) \to \mathrm{L}^s(K)$ to obtain

$$\|\mathbf{f}(\phi) - \mathbf{f}(\phi_h)\|_{0,\ell;\, K} = \|(\phi - \phi_h) \, \mathbf{g}\|_{0,\ell;\, K} \leqslant \|\mathbf{g}\|_{0,K} \, \|\phi - \phi_h\|_{0,s;\, K} \leqslant \|i_s(K)\| \, \|\mathbf{g}\|_{0,K} \, \|\phi - \phi_h\|_{0,s;\, K} \, .$$

Here, we note that the constant arising from the continuous embedding depends on $|K|$, which, in turn, is bounded by another constant depending on $|\Omega|$. Using this and substituting the result into (4.31), bounding the third and fourth terms according to (2.2), and raising to the power ℓ, we arrive at (4.30). This completes the proof. ▫

Next, we establish bounds for each term defining $\Theta_{3,K}$ (cf. (4.4)).

Lemma 4.12 *There exists a positive constant C_7, depending on κ, η, r, ρ and $\Psi_2(g,\phi_{\rm D})$, but independent of h and $\widetilde{h}$, such that*

$$\begin{aligned} h_K^2\,\|g+\kappa\,\Delta\phi_h-\mathbf{u}_h\cdot\nabla\phi_h-\eta\,\phi_h\|_{0,K}^2 \\ \leqslant C_7\,\Big\{(1+h_K^2+h_K^{\tilde{\varrho}})\,\|\phi-\phi_h\|_{1,K}^2+h_K^{\tilde{\varrho}}\,\|\mathbf{u}-\mathbf{u}_h\|_{0,\rho;K}^2\Big\}\,, \end{aligned} \tag{4.32}$$

where $\tilde{\varrho}=8/\rho$ when $n=2$, and $\tilde{\varrho}=12/\rho-1$ when $n=3$.

Proof. Similarly as in the proof of Lemma 4.8, we fix $K\in\mathcal{T}_h$ and define $\chi_K:=g+\kappa\,\Delta\phi_h-\mathbf{u}_h\cdot\nabla\phi_h-\eta\,\phi_h$ in K, which, thanks to the assumption that g is piecewise polynomial, belongs to $\mathrm{P}_{\bar{k}}(K)$ for some non-negative integer $\bar{k}$ depending on k and the polynomial degree of g. Then, using (B.2) in Lemma B.1,

$$c_1\,\|\chi_K\|_{0,K}\leqslant\sup_{0\neq v\in\mathrm{P}_{\bar{k}}(K)}\frac{\displaystyle\int_K\chi_K\,\psi_K\,v}{\|v\|_{0,K}}\,. \tag{4.33}$$

In turn, from the third row in (3.6), we have that $g+\kappa\,\Delta\phi-\mathbf{u}\cdot\nabla\phi-\eta\,\phi=0$ weakly in K. Then, combining this with integration by parts, and the fact that $\psi_K=0$ on ∂K, gives

$$\begin{aligned} \int_K\chi_K\,\psi_K\,v&=\int_K\Big\{\kappa\,\Delta(\phi_h-\phi)-\mathbf{u}_h\cdot\nabla\phi_h+\mathbf{u}\cdot\nabla\phi-\eta\,(\phi_h-\phi)\Big\}\,\psi_K\,v \\ &=-\kappa\int_K\nabla(\phi-\phi_h)\cdot\nabla(\psi_K\,v)+\int_K\Big\{\mathbf{u}_h\cdot\nabla(\phi-\phi_h)+(\mathbf{u}-\mathbf{u}_h)\cdot\nabla\phi-\eta\,(\phi_h-\phi)\Big\}\,\psi_K\,v\,. \end{aligned}$$

for all $v\in\mathrm{P}_{\bar{k}}(K)$. Thus, by applying the Hölder and Cauchy–Schwarz inequalities, we find that

$$\begin{aligned} \int_K\chi_K\,\psi_K v&\leqslant\kappa\,\|\phi-\phi_h\|_{1,K}\,\|\nabla(\psi_K\,v)\|_{0,K}+\|\mathbf{u}_h\|_{0,\rho;K}\,\|\phi-\phi_h\|_{1,K}\,\|\psi_K\,v\|_{0,s;K} \\ &\quad+\|\mathbf{u}-\mathbf{u}_h\|_{0,\rho;K}\,\|\phi\|_{1,K}\,\|\psi_K\,v\|_{0,s;K}+\eta\,\|\phi-\phi_h\|_{0,K}\,\|\psi_K\,v\|_{0,K}\,. \end{aligned} \tag{4.34}$$

To bound the terms on the right-hand side, we use that $0\leqslant\psi_K\leqslant 1$ in K, the continuous embedding from $\mathrm{L}^s(K)$ to $\mathrm{L}^2(K)$, the fact that $|K|\cong h_K^n$ and the definition of s in terms of ρ (cf. (3.26)). This yields

$$\|\psi_K\,v\|_{0,s;K}\leqslant\|v\|_{0,s;K}\leqslant|K|^{(s-2)/(2s)}\,\|v\|_{0,K}\leqslant c\,h_K^{n(4-\rho)/(2\rho)}\,\|v\|_{0,K}\qquad\forall\,v\in\mathrm{P}_{\bar{k}}(K)\,.$$

For the term $\|\nabla(\psi_K\,v)\|_{0,K}$ we in turn employ the estimate (B.3). Moreover, by recalling that $\mathbf{u}_h\in\mathbf{W}_h(r)$, we have $\|\mathbf{u}_h\|_{0,\rho;\,K}\leqslant r$, while to bound $\|\phi\|_{1,K}$ we use the *a priori* estimate (3.16). Therefore, by putting these bounds into (4.34) and using the fact that $\|\phi-\phi_h\|_{0,K}\leqslant\|\phi-\phi_h\|_{1,K}$, we arrive at

$$\begin{aligned} \int_K\chi_K\,\psi_K v&\leqslant\Big(c_3\,\kappa\,h_K^{-1}+c\,r\,h_K^{n(4-\rho)/(2\rho)}+\eta\Big)\,\|\phi-\phi_h\|_{1,K}\,\|v\|_{0,K} \\ &\quad+\mathcal{C}_2\,\Psi_2(g,\phi_{\rm D})\,c\,h_K^{n(4-\rho)/(2\rho)}\,\|\mathbf{u}-\mathbf{u}_h\|_{0,\rho;K}\,\|v\|_{0,K}\qquad\forall\,v\in\mathrm{P}_{\bar{k}}(K)\,. \end{aligned} \tag{4.35}$$

Thus, substituting (4.35) into (4.33), and then multiplying by h_K and squaring, we obtain (4.32), as desired. ▫

Lemma 4.13 *There exists a positive constant C_8, depending on κ, η, r, ρ and $\Psi_2(g,\phi_{\rm D})$, but independent of h and $\widetilde{h}$, such that*

$$h_e\,\|\,[\![\kappa\,\nabla\phi_h\cdot\mathbf{n}]\!]\,\|_{0,e}^2\leqslant C_8\sum_{K_e\in\omega_e}\Big\{\Big(1+h_{K_e}^2+h_{K_e}^{\tilde{\varrho}}\Big)\,\|\phi-\phi_h\|_{1,K_e}^2+h_{K_e}^{\tilde{\varrho}}\,\|\mathbf{u}-\mathbf{u}_h\|_{0,\rho;K_e}^2\Big\}\,, \tag{4.36}$$

where ω_e is the set conformed by the two elements in $\mathcal{T}_h$ having e as an edge/face, and $\tilde{\varrho}$ is defined as in Lemma 4.12.

Proof. It follows from a slight adaptation of [29, Lemma 4.21] (see also [22, Lemma 3.19]). We omit further details for brevity. ▫

Lemma 4.14 *Assume that the partition on* Γ *inherited from* $\mathcal{T}_h$ *is quasi-uniform, and that each edge/face of* $\mathcal{E}_h(\Gamma)$ *is contained in one of the elements of the independent partition of* Γ *defining* $\mathrm{H}^{\lambda}_{\widetilde{h}}$. *Then, there exists a positive constant* C_9, *depending on* κ, η, r, ρ *and* $\Psi_2(g,\phi_{\mathrm{D}})$, *but independent of* h *and* $\widetilde{h}$, *such that*

$$\sum_{e\in\mathcal{E}_h(\Gamma)} h_e \,\|\lambda_{\widetilde{h}} + \kappa\,\nabla\phi_h\cdot\mathbf{n}\|^2_{0,e} \leqslant C_9\left\{\|\phi-\phi_h\|^2_{1,\Omega} + \|\mathbf{u}-\mathbf{u}_h\|^2_{0,\rho;\Omega} + \|\lambda-\lambda_{\widetilde{h}}\|_{-1/2,\Gamma}\right\}.$$

Proof. The result is proved by repeating the argument of [22, Lemma 3.20] in our setting. Details are omitted. ▫

Our final step to prove the efficiency of the *a posteriori* error estimator is to bound the non-linear term appearing at the right-hand side in (4.30). To this end, we recall that $\mathbf{u}\in\mathbf{W}(r)$ and $\mathbf{u}_h\in\mathbf{W}_h(r)$, and proceed as in [11, eqs. (3.37)–(3.38)] to find that

$$\sum_{K\in\mathcal{T}_h} \left\||\mathbf{u}|^{\rho-2}\mathbf{u} - |\mathbf{u}_h|^{\rho-2}\mathbf{u}_h\right\|^{\ell}_{0,\ell;\,K} \leqslant C\,\|\mathbf{u}-\mathbf{u}_h\|^{\ell}_{0,\rho;\Omega}\,, \tag{4.37}$$

where C is a positive constant depending on ρ, r and other constants. Thus, we have arrived at the main result of this section.

Theorem 4.15 *Let* $(\boldsymbol{\sigma},\mathbf{u},\phi,\lambda)\in\mathcal{H}\times\mathcal{Q}\times\mathrm{H}^1(\Omega)\times\mathrm{H}^{-1/2}(\Gamma)$ *and* $(\boldsymbol{\sigma}_h,\mathbf{u}_h,\phi_h,\lambda_{\widetilde{h}})\in\mathbb{H}^{\boldsymbol{\sigma}}_h\times\mathbf{H}^{\mathbf{u}}_h\times\mathrm{H}^{\phi}_h\times\mathrm{H}^{\lambda}_{\widetilde{h}}$ *be the solutions to* (3.6) *and* (3.13), *respectively. Assume that the partition on* Γ *inherited from* $\mathcal{T}_h$ *is quasi-uniform, and that each edge/face of* $\mathcal{E}_h(\Gamma)$ *is contained in one of the elements of the independent partition of* Γ *defining* $\mathrm{H}^{\lambda}_{\widetilde{h}}$. *Then,* $\Theta_{\mathtt{MP}}$ *is an efficient estimator, i.e. there exists a positive constant* C_{eff}, *depending on* ν_0, $\mathtt{D}_1$, $\mathtt{F}_1$, κ, η, ρ, r, $\Psi_2(g,\phi_{\mathrm{D}})$, *but independent of* h *and* $\widetilde{h}$, *such that*

$$C_{\mathrm{eff}}\,\Theta_{\mathtt{MP}} + \mathtt{h.o.t.} \leqslant \|(\boldsymbol{\sigma}-\boldsymbol{\sigma}_h,\mathbf{u}-\mathbf{u}_h)\|_{\mathcal{H}\times\mathcal{Q}} + \|(\phi-\phi_h,\lambda-\lambda_{\widetilde{h}})\|_{\mathrm{H}^1(\Omega)\times\mathrm{H}^{-1/2}(\Gamma)}\,. \tag{4.38}$$

Proof. Assuming that $\mathbf{u}_{\mathrm{D}}$, f, g, and $\frac{1}{\nu}$ are piecewise polynomials, the result is a direct consequence of Lemmas 4.8–4.14 together with (4.37). Otherwise, as mentioned at the beginning of this section, one proceeds as in [15, Section 6.2] by employing suitable polynomial approximations of the data, which results in additional higher-order terms appearing on the left-hand side of the estimate (4.38). ▫

4.4 A fully local estimator

As discussed at the beginning of Section 4, the estimator $\Theta_{\mathtt{MP}}$ (cf. (4.1)) has the disavantage of not being fully local and computable. However, it is possible to construct another estimator that is induced by $\Theta_{\mathtt{MP}}$, with the aforementioned properties. In fact, let $\widetilde{\Theta}_{\mathtt{MP}}$ be defined as

$$\widetilde{\Theta}_{\mathtt{MP}} := \left\{\sum_{K\in\mathcal{T}_h}\Theta^{\rho}_{1,K}\right\}^{1/\rho} + \left\{\sum_{K\in\mathcal{T}_h}\left(\Theta^2_{2,K}+\Theta^2_{3,K}+\Theta^2_{5,K}\right)\right\}^{1/2} + \left\{\sum_{K\in\mathcal{T}_h}\Theta^{\ell}_{4,K}\right\}^{1/\ell}, \tag{4.39}$$

where $\Theta_{i,K}$, $i\in\{1,2,3,4\}$, are given in (4.2)–(4.5), and $\Theta_{5,K}$ is defined by

$$\Theta_{5,K} := \sum_{e\in\mathcal{E}_h(K)\cap\mathcal{E}_h(\Gamma)} \|\phi_{\mathrm{D}}-\phi_h\|^2_{1,e}\,. \tag{4.40}$$

Notice that the only difference between $\widetilde{\Theta}_{\mathtt{MP}}$ and $\Theta_{\mathtt{MP}}$ is the local error indicator $\Theta_{5,K}$ instead of the non-local term $\|\phi_{\mathrm{D}} - \phi_h\|_{1/2,\Gamma}$. Observe also that, in view of the definition of $\Theta_{5,K}$, we now require $\phi_{\mathrm{D}} \in \mathrm{H}^1(\Gamma)$.

Certainly, as in [4, Theorem 4.3] (see also [21, Section 4]), an interpolation argument shows

$$\|\phi_{\mathrm{D}} - \phi_h\|^2_{1/2,\Gamma} \leqslant C \, \|\phi_{\mathrm{D}} - \phi_h\|^2_{1,\Gamma} = C \sum_{e \in \mathcal{E}_h(\Gamma)} \|\phi_{\mathrm{D}} - \phi_h\|^2_{1,e} \, ,$$

for some $C > 0$, which says, in particular, that $\widetilde{\Theta}_{\mathtt{MP}}$ is induced by $\Theta_{\mathtt{MP}}$ (cf. (4.1)). Moreover, by proceeding as in Section 4.2, one deduces that $\widetilde{\Theta}_{\mathtt{MP}}$ is reliable and satisfies the estimate given in Theorem 4.7 with the same constant C_{rel} up to another h- and $\widetilde{h}$-independent multiplicative constant C. In turn, up to the term $\Theta_{5,K}$ in (4.39), we also have that $\widetilde{\Theta}_{\mathtt{MP}}$ is efficient. Nevertheless, we will see in the numerical examples (cf. Section 6) that, in practice, this estimator actually satisfies both properties.

5 A posteriori error analysis for the fully-mixed scheme

We now turn our attention to the derivation of an *a posteriori* error estimator for the fully-mixed Galerkin scheme (3.28), following the same approach as in Section 4 but applied to the diffusion-based mixed formulation for the CDR equation instead of its primal formulation. Since the first two equations of the fully-mixed continuous and discrete systems (cf. (3.27) and (3.28)) coincide with those of the mixed-primal formulation (cf. (3.6) and (3.13)), the resulting estimator shares all the terms associated with the Brinkman–Forchheimer part of the system. Accordingly, we define $\Theta_{\mathtt{FM}}$ by

$$\begin{aligned} \Theta_{\mathtt{FM}} := \left\{ \sum_{K \in \mathcal{T}_h} \Theta^{\rho}_{1,K} \right\}^{1/\rho} + \left\{ \sum_{K \in \mathcal{T}_h} (\Theta^2_{2,K} + \widehat{\Theta}^2_{1,K}) \right\}^{1/2} + \left\{ \sum_{K \in \mathcal{T}_h} \Theta^{\ell}_{4,K} \right\}^{1/\ell} \\ + \left\{ \sum_{K \in \mathcal{T}_h} \widehat{\Theta}^{s}_{2,K} \right\}^{1/s} + \left\{ \sum_{K \in \mathcal{T}_h} \widehat{\Theta}^{t}_{3,K} \right\}^{1/t} , \end{aligned} \tag{5.1}$$

where $\Theta_{1,K}$, $\Theta_{2,K}$ and $\Theta_{4,K}$ are defined in (4.2), (4.3) and (4.5), respectively, whereas the remaining local error indicators are given by

$$\begin{aligned} \widehat{\Theta}^2_{1,K} := h_K^2 \, \|\underline{\mathrm{curl}}(\kappa^{-1} \, \boldsymbol{\vartheta}_h)\|^2_{0,K} + \sum_{e \in \mathcal{E}_h(\Omega) \cap \mathcal{E}_h(K)} h_e \, \| \, [\![\boldsymbol{\delta}_*(\kappa^{-1} \, \boldsymbol{\vartheta}_h)]\!] \, \|^2_{0,e} \\ + \sum_{e \in \mathcal{E}_h(\Gamma) \cap \mathcal{E}_h(K)} h_e \, \|\boldsymbol{\delta}_*\big(\nabla \phi_{\mathrm{D}} - \kappa^{-1} \boldsymbol{\vartheta}_h\big)\|^2_{0,e} \, , \end{aligned} \tag{5.2}$$

$$\widehat{\Theta}^s_{2,K} := h_K^s \, \|\nabla \phi_h - \kappa^{-1} \, \boldsymbol{\vartheta}_h\|^s_{0,s;K} + \sum_{e \in \mathcal{E}_h(\Gamma) \cap \mathcal{E}_h(K)} h_e \, \|\phi_{\mathrm{D}} - \phi_h\|^s_{0,s;\, e} \, , \tag{5.3}$$

$$\widehat{\Theta}^t_{3,K} := \|g + \mathrm{div}(\boldsymbol{\vartheta}_h) - \eta \, \phi_h - \kappa^{-1} \, \mathbf{u}_h \cdot \boldsymbol{\vartheta}_h\|^t_{0,t;K} \, . \tag{5.4}$$

Notice that these terms are associated with the CDR system in its mixed formulation, and therefore replace the terms $\Theta_{3,K}$ and $\|\phi_{\mathrm{D}} - \phi_h\|_{1/2,\Gamma}$ in the definition of $\Theta_{\mathtt{MP}}$ (cf. (4.1)). Observe also that the third term in the definition of $\widehat{\Theta}_{1,K}$ requires $\boldsymbol{\delta}_*(\nabla \phi_{\mathrm{D}})$ to belong to $\mathbf{L}^2(e)$. This requirement is satisfied by simply assuming that $\phi_{\mathrm{D}} \in \mathrm{H}^1(\Gamma)$. As explained for $\mathbf{u}_{\mathrm{D}}$ at the beginning of Section 4, we emphasize that this additional assumption on ϕ_{D} can also be relaxed by the same reasoning.

It is worth noting the residual character of these error estimators. Indeed, if the discrete solutions coincide with the continuous ones, we readily observe that $\widehat{\Theta}_{1,K}$ and $\widehat{\Theta}_{2,K}$ vanish thanks to (3.25a) and the Dirichlet condition (3.25c). In turn, $\widehat{\Theta}_{3,K}$ also vanishes owing to (3.25b). This, together with the residual character of the remaining local error indicators in (5.1), already defined and analyzed in Section 4, confirms that $\Theta_{\mathtt{FM}}$ is a residual-based *a posteriori* error estimator. Moreover, examining the definition of each local error indicator, we observe that, in contrast to $\Theta_{\mathtt{MP}}$ (cf. (4.1)), $\Theta_{\mathtt{FM}}$ is fully local and computable.

5.1 Preliminaries for the reliability analysis

Following the same outline as in Section 4, we now derive some preliminary estimates that are required for the proof of the reliability. In particular, the following result provides an estimate analogous to that of Lemma 4.1, the only difference being that the associated constant now depends on the *a priori* estimates of the fully-mixed scheme (cf. (3.31)–(3.34)). Since the proof is entirely analogous to the one already presented, it is omitted.

Lemma 5.1 *There exists a positive constant $\widehat{C}_1$, depending on r, ρ, ν_0, ν_1, $\mathtt{D}_1$, $\mathtt{F}_1$, β, $\beta_{\mathtt{d}}$, and $|\Omega|$, but independent of h, such that*

$$\begin{aligned}\widehat{C}_1 \, \|(\boldsymbol{\sigma} - \boldsymbol{\sigma}_h, \mathbf{u} - \mathbf{u}_h)\|_{\mathcal{H}\times\mathcal{Q}} \leqslant \|\mathcal{R}_1\|_{\mathcal{H}'} + \|\mathcal{R}_2\|_{\mathcal{Q}'} + \|\mathbf{g}\|_{0,\Omega} \, \|\phi - \phi_h\|_{0,s;\Omega} \\ + \widehat{\Psi}_1(\mathbf{u}_{\mathrm{D}}, f, \mathbf{g}, g, \phi_{\mathrm{D}}, \phi_{\mathtt{r}}) \, \|\mathbf{u} - \mathbf{u}_h\|_{0,\rho;\Omega} \, ,\end{aligned} \tag{5.5}$$

where $\mathcal{R}_1$ and $\mathcal{R}_2$ are defined in (4.7) and (4.8), respectively.

We now turn our attention to the CDR system. Let $\widehat{\mathcal{R}}_1 : \mathrm{X} \to \mathrm{R}$ and $\widehat{\mathcal{R}}_2 : \mathrm{Y} \to \mathrm{R}$ be the residual functionals defined by

$$\widehat{\mathcal{R}}_1(\boldsymbol{\psi}) := \widehat{\mathrm{F}}(\boldsymbol{\psi}) - \widehat{a}(\boldsymbol{\vartheta}_h, \boldsymbol{\psi}) - \widehat{b}(\boldsymbol{\psi}, \phi_h) \qquad \forall \, \boldsymbol{\psi} \in \mathrm{X} \, , \tag{5.6}$$

and

$$\widehat{\mathcal{R}}_2(\xi) := \widehat{\mathrm{G}}(\xi) - \widehat{b}(\boldsymbol{\vartheta}_h, \xi) + \widehat{c}(\phi_h, \xi) - d_{\mathbf{u}_h}(\boldsymbol{\vartheta}_h, \xi) \qquad \forall \, \xi \in \mathrm{Y} \, ,$$

respectively. According to the third and fourth rows of the Galerkin scheme (3.28), it follows that

$$\widehat{\mathcal{R}}_1(\boldsymbol{\psi}_h) = 0 \qquad \forall \, \boldsymbol{\psi}_h \in \mathbf{H}_h^{\boldsymbol{\vartheta}} \, , \quad \text{and} \quad \widehat{\mathcal{R}}_2(\xi_h) = 0 \qquad \forall \, \xi_h \in \widehat{\mathrm{H}}_h^{\phi} \, . \tag{5.7}$$

Similarly as in Lemma 4.2, the following result provides an estimate for the error associated with the continuous and discrete solutions of the CDR part of the systems (3.27) and (3.28).

Lemma 5.2 *There exists a positive constant $\widehat{C}_2$ depending on κ, η, ρ, $C_{\widehat{b}}$, $C_{\widehat{b},\mathtt{d}}$, and $|\Omega|$, but independent of h, such that*

$$\widehat{C}_2 \, \|(\boldsymbol{\vartheta} - \boldsymbol{\vartheta}_h, \phi - \phi_h)\|_{\mathrm{X}\times\mathrm{Y}} \leqslant \|\widehat{\mathcal{R}}_1\|_{\mathrm{X}'} + \|\widehat{\mathcal{R}}_2\|_{\mathrm{Y}'} + \widehat{\Psi}_2(g, \phi_{\mathrm{D}}) \, \|\mathbf{u} - \mathbf{u}_h\|_{0,\rho;\Omega} \, . \tag{5.8}$$

Proof. Similarly as in the proof of Lemma 4.2, we use the definition of $\widehat{\mathbf{A}}$ (cf. (3.29)), the last two rows of (3.27), and perform some algebraic manipulations to obtain

$$\begin{aligned}\widehat{\mathbf{A}}\big((\boldsymbol{\vartheta} - \boldsymbol{\vartheta}_h, \phi - \phi_h), (\boldsymbol{\psi}, \xi)\big) + d_{\mathbf{u}}(\boldsymbol{\vartheta} - \boldsymbol{\vartheta}_h, \xi) &= \widehat{\mathrm{F}}(\boldsymbol{\psi}) + \widehat{\mathrm{G}}(\xi) - \widehat{\mathbf{A}}\big((\boldsymbol{\vartheta}_h, \phi_h), (\boldsymbol{\psi}, \xi)\big) - d_{\mathbf{u}}(\boldsymbol{\vartheta}_h, \xi) \\ &= \widehat{\mathcal{R}}_1(\boldsymbol{\psi}) + \widehat{\mathcal{R}}_2(\xi) + d_{\mathbf{u}_h}(\boldsymbol{\vartheta}_h, \xi) - d_{\mathbf{u}}(\boldsymbol{\vartheta}_h, \xi) \, ,\end{aligned}$$

for all $(\boldsymbol{\psi},\xi)\in \mathrm{X}\times\mathrm{Y}$. Using this into the global inf-sup condition (3.30) with $\mathbf{z}=\mathbf{u}$, $\boldsymbol{\varrho}=\boldsymbol{\vartheta}-\boldsymbol{\vartheta}_h$, and $\zeta=\phi-\phi_h$, we obtain

$$\frac{\alpha_{\widehat{\mathbf{A}}}}{2}\,\|(\boldsymbol{\vartheta}-\boldsymbol{\vartheta}_h,\phi-\phi_h)\|_{\mathrm{X}\times\mathrm{Y}}\leqslant \|\widehat{\mathcal{R}}_1\|_{\mathrm{X}'}+\|\widehat{\mathcal{R}}_2\|_{\mathrm{Y}'}+\|d_{\mathbf{u}}(\boldsymbol{\vartheta}_h,\cdot)-d_{\mathbf{u}_h}(\boldsymbol{\vartheta}_h,\cdot)\|_{\mathrm{X}'}\,. \tag{5.9}$$

In order to estimate the last term in the above inequality, we use the Hölder inequality and the *a priori* estimate (3.34) yielding

$$\|d_{\mathbf{u}}(\boldsymbol{\vartheta}_h,\cdot)-d_{\mathbf{u}_h}(\boldsymbol{\vartheta}_h,\cdot)\|_{\mathrm{X}'}=\kappa^{-1}\,\|\boldsymbol{\vartheta}_h\|_{\mathrm{div}_t;\Omega}\,\|\mathbf{u}-\mathbf{u}_h\|_{0,\rho;\Omega}\leqslant\kappa^{-1}\,\mathcal{C}_{2,\mathtt{d}}\,\widehat{\Psi}_2(g,\phi_{\mathrm{D}})\,\|\mathbf{u}-\mathbf{u}_h\|_{0,\rho;\Omega}\,.$$

Putting this into (5.9), we arrive at (5.8), as desired. ▫

By reasoning as in (4.16), we now combine (5.8) with the estimate (5.5) to deduce

$$\begin{aligned}\bar{C}_1\,\|(\boldsymbol{\sigma}-\boldsymbol{\sigma}_h,\mathbf{u}-\mathbf{u}_h)\|_{\mathcal{H}\times\mathcal{Q}}&\leqslant\|\mathcal{R}_1\|_{\mathcal{H}'}+\|\mathcal{R}_2\|_{\mathcal{Q}'}+\|\widehat{\mathcal{R}}_1\|_{\mathrm{X}'}+\|\widehat{\mathcal{R}}_2\|_{\mathrm{Y}'}\\&\quad+\Big\{\widehat{\Psi}_1(\mathbf{u}_{\mathrm{D}},f,\mathbf{g},g,\phi_{\mathrm{D}},\phi_{\mathtt{r}})+\widehat{\Psi}_2(g,\phi_{\mathrm{D}})\Big\}\,\|\mathbf{u}-\mathbf{u}_h\|_{0,\rho;\Omega}\,,\end{aligned}$$

where $\bar{C}_1=\widehat{C}_1\widehat{C}_2/\max\{\widehat{C}_2,\|\mathbf{g}\|_{0,\Omega}\}$. Then, using again Lemma 5.2 together with this estimate, we readily obtain the following theorem, which constitutes the fully-mixed counterpart of Theorem 4.3.

Theorem 5.3 *Assume that the data satisfy*

$$\widehat{\Psi}_1(\mathbf{u}_{\mathrm{D}},f,\mathbf{g},g,\phi_{\mathrm{D}},\phi_{\mathtt{r}})+\widehat{\Psi}_2(g,\phi_{\mathrm{D}})\leqslant\frac{\bar{C}_1}{2}\,.$$

Then, there exists a positive constant $\widehat{C}_3$, depending on r, ρ, ν_0, ν_1, $\mathtt{D}_1$, $\mathtt{F}_1$, β, $\beta_{\mathtt{d}}$, κ, η, $C_{\widehat{b}}$, $C_{\widehat{b},\mathtt{d}}$, and $|\Omega|$, but independent of h, such that

$$\begin{aligned}&\|(\boldsymbol{\sigma}-\boldsymbol{\sigma}_h,\mathbf{u}-\mathbf{u}_h)\|_{\mathcal{H}\times\mathcal{Q}}+\|(\boldsymbol{\vartheta}-\boldsymbol{\vartheta}_h,\phi-\phi_h)\|_{\mathrm{X}\times\mathrm{Y}}\\&\qquad\leqslant\widehat{C}_3\,\Big\{\|\mathcal{R}_1\|_{\mathcal{H}'}+\|\mathcal{R}_2\|_{\mathcal{Q}'}+\|\widehat{\mathcal{R}}_1\|_{\mathrm{X}'}+\|\widehat{\mathcal{R}}_2\|_{\mathrm{Y}'}\Big\}\,.\end{aligned}\tag{5.10}$$

5.2 Reliability

In view of Theorem 5.3, it only remains to establish suitable bounds for the residual functionals appearing on the right-hand side of (5.10). We recall that the terms $\mathcal{R}_1$ and $\mathcal{R}_2$ have already been bounded in Lemmas 4.4 and 4.5, respectively, so it suffices to derive corresponding estimates for the residual functionals associated with the CDR system. We begin with a bound for $\|\widehat{\mathcal{R}}_2\|_{\mathrm{Y}'}$.

Lemma 5.4 *Let $\widehat{\Theta}_{3,K}$ be defined as in (5.4). Then, there holds*

$$\|\widehat{\mathcal{R}}_2\|_{\mathrm{Y}'}\leqslant\left\{\sum_{K\in\mathcal{T}_h}\widehat{\Theta}_{3,K}^{\,t}\right\}^{1/t}\,.$$

Proof. It follows from a straightforward application of the Hölder inequality in the definition of $\widehat{\mathcal{R}}_2$. We omit further details. ▫

We now turn our attention to $\widehat{\mathcal{R}}_1$. We note that the definition of the curl operator (cf. Appendix A) differs in the cases $n=2$ and $n=3$, and, in particular, that the Helmholtz decomposition stated in Lemma A.2 depends on the spatial dimension. For the sake of simplicity and clarity, we restrict

ourselves to the case $n = 2$ for the proof of the following lemma, while emphasizing that the analysis remains valid for $n = 3$. Accordingly, we fix $\boldsymbol{\psi} \in \mathrm{X}$ and use Lemma A.2 to deduce the existence of $\boldsymbol{\zeta} \in \mathbf{W}^{1,t}(\Omega)$ and $w \in \mathrm{H}^1(\Omega)$ such that

$$\boldsymbol{\psi} = \boldsymbol{\zeta} + \mathrm{curl}(w) \quad \text{and} \quad \|\boldsymbol{\zeta}\|_{1,t;\,\Omega} + \|w\|_{1,\Omega} \leqslant C_t \, \|\boldsymbol{\psi}\|_{\mathrm{div}_t;\Omega} \, , \tag{5.11}$$

where C_t is a positive constant depending on t (cf. (3.26)), but independent of h. Then, we may define

$$\boldsymbol{\psi}_h := \boldsymbol{\Pi}_h^k(\boldsymbol{\zeta}) + \mathrm{curl}(\mathcal{I}_h(w)) \in \mathbf{H}_h^{\boldsymbol{\vartheta}} \, .$$

Now, by using the first identity in (5.7), we find that

$$\widehat{\mathcal{R}}_1(\boldsymbol{\psi}) = \widehat{\mathcal{R}}_1(\boldsymbol{\psi} - \boldsymbol{\psi}_h) = \widehat{\mathcal{R}}_1(\widehat{\boldsymbol{\zeta}}) + \widehat{\mathcal{R}}_1(\mathrm{curl}(\widehat{w})) \, , \tag{5.12}$$

where $\widehat{\boldsymbol{\zeta}} := \boldsymbol{\zeta} - \boldsymbol{\Pi}_h^k(\boldsymbol{\zeta})$ and $\widehat{w} := w - \mathcal{I}_h(w)$. The following result provides an estimate for $\|\widehat{\mathcal{R}}_1\|_{\mathrm{X}'}$, whose proof is based on bounding each term in the above decomposition.

Lemma 5.5 *There exists a positive constant C, independent of h, such that*

$$\|\widehat{\mathcal{R}}_1\|_{\mathrm{X}'} \leqslant C \left\{ \left(\sum_{K \in \mathcal{T}_h} \widehat{\Theta}_{1,K}^2 \right)^{1/2} + \left(\sum_{K \in \mathcal{T}_h} \widehat{\Theta}_{2,K}^s \right)^{1/s} \right\} , \tag{5.13}$$

where $\widehat{\Theta}_{1,K}$ and $\widehat{\Theta}_{2,K}$ are defined in (5.2) and (5.3), respectively.

Proof. According to the previous discussion, given $\boldsymbol{\psi} \in \mathrm{X}$, we focus on derive estimates for each term in the right-hand side of (5.12). To that end, we use the definition of $\widehat{\mathcal{R}}_1$ (cf. (5.6)) and integrate by parts locally to find that

$$\begin{aligned} \widehat{\mathcal{R}}_1(\widehat{\boldsymbol{\zeta}}) &= \langle \widehat{\boldsymbol{\zeta}} \cdot \mathbf{n}, \phi_{\mathrm{D}} \rangle_{\Gamma} - \int_{\Omega} \kappa^{-1} \, \boldsymbol{\vartheta}_h \cdot \widehat{\boldsymbol{\zeta}} - \int_{\Omega} \phi_h \, \mathrm{div}(\widehat{\boldsymbol{\zeta}}) \\ &= \sum_{e \in \mathcal{E}_h(\Gamma)} \int_e \widehat{\boldsymbol{\zeta}} \cdot \mathbf{n} \, \phi_{\mathrm{D}} - \sum_{K \in \mathcal{T}_h} \int_K \kappa^{-1} \, \boldsymbol{\vartheta}_h \cdot \widehat{\boldsymbol{\zeta}} + \sum_{K \in \mathcal{T}_h} \left(\int_K \nabla \phi_h \cdot \widehat{\boldsymbol{\zeta}} - \int_{\partial K} \widehat{\boldsymbol{\zeta}} \cdot \mathbf{n} \, \phi_h \right) . \end{aligned}$$

In turn, by recalling the identity (A.1), we observe that the last term in the above equality vanishes. Moreover, the same identity allows us to introduce an artificial term into the first one, thereby obtaining

$$\widehat{\mathcal{R}}_1(\widehat{\boldsymbol{\zeta}}) = \sum_{e \in \mathcal{E}_h(\Gamma)} \int_e \widehat{\boldsymbol{\zeta}} \cdot \mathbf{n} \, (\phi_{\mathrm{D}} - \phi_h) + \sum_{K \in \mathcal{T}_h} \int_K \left(\nabla \phi_h - \kappa^{-1} \, \boldsymbol{\vartheta}_h \right) \cdot \widehat{\boldsymbol{\zeta}} \, ,$$

which, by applying the Hölder inequality and the approximation properties (A.4) and (A.3), implies

$$\widehat{\mathcal{R}}_1(\widehat{\boldsymbol{\zeta}}) \leqslant \sum_{e \in \mathcal{E}_h(\Gamma)} c_2 \, h_e^{1/s} \, \|\phi_{\mathrm{D}} - \phi_h\|_{0,s;\,e} \, |\boldsymbol{\zeta}|_{1,t;\,K_e} + \sum_{K \in \mathcal{T}_h} c_1 \, h_K \, \|\nabla \phi_h - \kappa^{-1} \, \boldsymbol{\vartheta}_h\|_{0,s;\,K} \, |\boldsymbol{\zeta}|_{1,t;\,K} \, ,$$

where K_e denotes the element of $\mathcal{T}_h$ that has e as one of its edges/faces. Then, we use the Hölder inequality, the estimate given in (5.11) and perform some algebraic manipulations to deduce the existence of $c > 0$, independent of all physical parameters and h, such that

$$\widehat{\mathcal{R}}_1(\widehat{\boldsymbol{\zeta}}) \leqslant c \left\{ \sum_{K \in \mathcal{T}_h} \widehat{\Theta}_{2,K}^s \right\}^{1/s} \|\boldsymbol{\psi}\|_{\mathrm{div}_t;\,\Omega} \, . \tag{5.14}$$

We now focus on the last term in (5.12). Using the definition of $\widehat{\mathcal{R}}_1$ (see (5.6)) and the fact that $\mathrm{curl}(\widehat{w})$ is divergence-free, we obtain

$$\widehat{\mathcal{R}}_1(\mathrm{curl}(\widehat{w})) = \langle \mathrm{curl}(\widehat{w}) \cdot \mathbf{n}, \phi_{\mathrm{D}} \rangle_{\Gamma} - \int_{\Omega} \kappa^{-1}\, \boldsymbol{\vartheta}_h \cdot \mathrm{curl}(\widehat{w})\,. \tag{5.15}$$

Recalling that $\phi_{\mathrm{D}} \in \mathrm{H}^1(\Gamma)$, we invoke [24, Lemma 3.5] to perform integration by parts on the boundary thus obtaining

$$\langle \mathrm{curl}(\widehat{w}) \cdot \mathbf{n}, \phi_{\mathrm{D}} \rangle_{\Gamma} = -\langle \boldsymbol{\delta}_*(\nabla \phi_{\mathrm{D}}), \widehat{w} \rangle_{\Gamma} = -\sum_{e \in \mathcal{E}_h(\Gamma)} \int_e \boldsymbol{\delta}_*(\nabla \phi_{\mathrm{D}})\, \widehat{w}\,,$$

which, combined with a local integration by parts of the second term on the right-hand side of (5.15), gives

$$\widehat{\mathcal{R}}_1(\mathrm{curl}(\widehat{w})) = -\sum_{e \in \mathcal{E}_h(\Gamma)} \int_e \boldsymbol{\delta}_*(\nabla \phi_{\mathrm{D}})\, \widehat{w} - \sum_{K \in \mathcal{T}_h} \int_K \underline{\mathrm{curl}}(\kappa^{-1}\, \boldsymbol{\vartheta}_h)\, \widehat{w} + \sum_{K \in \mathcal{T}_h} \int_{\partial K} \boldsymbol{\delta}_*(\kappa^{-1}\, \boldsymbol{\vartheta}_h)\, \widehat{w}\,.$$

Splitting the last term into boundary and interior skeleton contributions, we arrive at

$$\begin{aligned}\widehat{\mathcal{R}}_1(\mathrm{curl}(\widehat{w})) = &-\sum_{e \in \mathcal{E}_h(\Gamma)} \int_e \boldsymbol{\delta}_*(\nabla \phi_{\mathrm{D}} - \kappa^{-1}\, \boldsymbol{\vartheta}_h)\, \widehat{w} - \sum_{K \in \mathcal{T}_h} \int_K \underline{\mathrm{curl}}(\kappa^{-1}\, \boldsymbol{\vartheta}_h)\, \widehat{w} \\ &+ \sum_{e \in \mathcal{E}_h(\Omega)} \int_e \big[\!\big[\boldsymbol{\delta}_*(\kappa^{-1}\, \boldsymbol{\vartheta}_h) \big]\!\big]\, \widehat{w}\,.\end{aligned}$$

Now, by applying the Cauchy–Schwarz inequality and the approximation properties (A.6) and (A.5), we obtain

$$\begin{aligned}\widehat{\mathcal{R}}_1(\mathrm{curl}(\widehat{w})) \leqslant &\sum_{e \in \mathcal{E}_h(\Gamma)} \big\| \boldsymbol{\delta}_*(\nabla \phi_{\mathrm{D}} - \kappa^{-1}\, \boldsymbol{\vartheta}_h) \big\|_{0,e}\, c_2\, h_e^{1/2}\, \|w\|_{1,\Delta(e)} + \sum_{K \in \mathcal{T}_h} \big\| \underline{\mathrm{curl}}(\kappa^{-1}\, \boldsymbol{\vartheta}_h) \big\|_{0,K}\, c_1\, h_K\, \|w\|_{1,\Delta(K)} \\ &+ \sum_{e \in \mathcal{E}_h(\Omega)} \big\| \big[\!\big[\boldsymbol{\delta}_*(\kappa^{-1}\, \boldsymbol{\vartheta}_h) \big]\!\big] \big\|_{0,e}\, c_2\, h_e^{1/2}\, \|w\|_{1,\Delta(e)}\,.\end{aligned}$$

Hence, by employing once again the Cauchy–Schwarz inequality in each term, bearing in mind the shape-regularity of the mesh, and using the estimate (5.11), we conclude that

$$\widehat{\mathcal{R}}_1(\mathrm{curl}(\widehat{w})) \leqslant \widetilde{c} \left\{ \sum_{K \in \mathcal{T}_h} \widehat{\Theta}_{1,K}^2 \right\}^{1/2} \|\boldsymbol{\psi}\|_{\mathrm{div}_t;\,\Omega}\,, \tag{5.16}$$

for some positive constant $\widetilde{c}$ independent of all physical parameters and h. Therefore, putting the estimates (5.14) and (5.16) into the decomposition (5.12), we deduce (5.13), as desired. ▫

The main result of this section is stated below. Its proof follows immediately from combining Lemmas 4.4, 4.5, 5.4, and 5.5 with the estimate provided by Theorem 5.3.

Theorem 5.6 *Let* $(\boldsymbol{\sigma}, \mathbf{u}, \boldsymbol{\vartheta}, \phi) \in \mathcal{H} \times \mathcal{Q} \times \mathrm{X} \times \mathrm{Y}$ *and* $(\boldsymbol{\sigma}_h, \mathbf{u}_h, \boldsymbol{\vartheta}_h, \phi_h) \in \mathbb{H}_h^{\boldsymbol{\sigma}} \times \mathbf{H}_h^{\mathbf{u}} \times \mathbf{H}_h^{\boldsymbol{\vartheta}} \times \widehat{\mathrm{H}}_h^{\phi}$ *be the solutions to* (3.27) *and* (3.28)*, respectively. Assume that the data satisfies the assumption of Theorem 5.3. Then,* $\Theta_{\mathtt{FM}}$ *is a reliable estimator, i.e. there exists a positive constant* C_{rel}*, depending on* r*,* ρ*,* ν_0*,* ν_1*,* $\mathtt{D}_1$*,* $\mathtt{F}_1$*,* β*,* $\beta_{\mathtt{d}}$*,* κ*,* η*,* $C_{\widehat{b}}$*,* $C_{\widehat{b},\mathtt{d}}$*, and* $|\Omega|$*, but independent of* h*, such that*

$$\|(\boldsymbol{\sigma} - \boldsymbol{\sigma}_h, \mathbf{u} - \mathbf{u}_h)\|_{\mathcal{H} \times \mathcal{Q}} + \|(\boldsymbol{\vartheta} - \boldsymbol{\vartheta}_h, \phi - \phi_h)\|_{\mathrm{X} \times \mathrm{Y}} \leqslant C_{\mathrm{rel}}\, \Theta_{\mathtt{FM}}\,.$$

5.3 Efficiency

We now aim to establish the efficiency of the *a posteriori* error estimator $\Theta_{\mathtt{FM}}$ (cf. (5.1)). To this end, we note that the local error indicators associated with the Brinkman–Forchheimer system, namely $\Theta_{1,K}$, $\Theta_{2,K}$, and $\Theta_{4,K}$, appearing in the definition of $\Theta_{\mathtt{FM}}$, have already been analyzed in Lemmas 4.8–4.11. Consequently, it only remains to derive suitable bounds for the local error indicators defined in (5.2), (5.3), and (5.4). Furthermore, throughout this section, and following the same approach as in Section 4.3, we assume for simplicity that ϕ_{D}, $\mathbf{u}_{\mathrm{D}}$, f, and $\frac{1}{\nu}$ are piecewise polynomials.

The following three results provide estimates for each term defining $\widehat{\Theta}_{1,K}$, $\widehat{\Theta}_{2,K}$, and $\widehat{\Theta}_{3,K}$, respectively.

Lemma 5.7 *There exist positive constants $\widehat{C}_1$ and $\widehat{C}_2$, depending on κ, but independent of h, such that*

$$h_K^2 \, \|\underline{\mathrm{curl}}(\kappa^{-1}\,\boldsymbol{\vartheta}_h)\|_{0,K}^2 \leqslant \widehat{C}_1 \, \|\boldsymbol{\vartheta} - \boldsymbol{\vartheta}_h\|_{0,K}^2 \qquad \forall\, K \in \mathcal{T}_h \,,$$

and

$$h_e \, \|[\![\boldsymbol{\delta}_*(\kappa^{-1}\,\boldsymbol{\vartheta}_h)]\!]\|_{0,e}^2 \leqslant \widehat{C}_2 \, \|\boldsymbol{\vartheta} - \boldsymbol{\vartheta}_h\|_{0,\omega_e}^2 \qquad \forall\, e \in \mathcal{E}_h(\Omega) \,,$$

where ω_e denotes the union of the two elements of $\mathcal{T}_h$ sharing the edge/face e. Additionally, there exists a positive constant $\widehat{C}_3$, depending on κ, but independent of h, such that

$$h_e \, \|\boldsymbol{\delta}_*(\nabla\phi_{\mathrm{D}} - \kappa^{-1}\,\boldsymbol{\vartheta}_h)\|_{0,e}^2 \leqslant \widehat{C}_3 \, \|\boldsymbol{\vartheta} - \boldsymbol{\vartheta}_h\|_{0,K_e}^2 \qquad \forall\, e \in \mathcal{E}_h(\Gamma) \,,$$

where K_e is the element to which the boundary edge/face e belongs.

Proof. We follow the same strategy as in [16, Lemma 5.13]. More precisely, by a straightforward adaptation of [28, Lemmas 4.9 and 4.10] to the vector-valued setting, we deduce that for each $\boldsymbol{\psi}_h \in \mathbf{L}^2(\Omega)$, piecewise polynomial of degree $k \geqslant 0$ on every $K \in \mathcal{T}_h$, and for all $\boldsymbol{\psi} \in \mathbf{L}^2(\Omega)$ satisfying $\underline{\mathrm{curl}}(\boldsymbol{\psi}) = 0$ on each $K \in \mathcal{T}_h$, there exist positive constants c_1 and c_2, independent of h, such that

$$\|\underline{\mathrm{curl}}(\boldsymbol{\psi}_h)\|_{0,K} \leqslant c_1 \, h_K^{-1} \, \|\boldsymbol{\psi} - \boldsymbol{\psi}_h\|_{0,K} \quad \text{and} \quad \|\,[\![\boldsymbol{\delta}_*(\boldsymbol{\psi}_h)]\!]\,\|_{0,e} \leqslant c_2 \, h_e^{-1/2} \, \|\boldsymbol{\psi} - \boldsymbol{\psi}_h\|_{0,\omega_e} \,. \tag{5.17}$$

Next, observe that $\kappa^{-1}\,\boldsymbol{\vartheta} = \nabla\phi$ in Ω (see (3.25a)), which immediately implies $\underline{\mathrm{curl}}(\kappa^{-1}\,\boldsymbol{\vartheta}) = 0$. Therefore, the first two estimates follow by applying (5.17) with $\boldsymbol{\psi} = \kappa^{-1}\,\boldsymbol{\vartheta}$ and $\boldsymbol{\psi}_h = \kappa^{-1}\,\boldsymbol{\vartheta}_h$.

Finally, the last estimate is obtained by adapting [31, Lemma 4.15] to the vector-valued case. We omit the details for brevity. ▫

Lemma 5.8 *There exist positive constants $\widehat{C}_4$ and $\widehat{C}_5$, depending on κ, but independent of h, such that*

$$h_K^s \, \|\nabla\phi_h - \kappa^{-1}\,\boldsymbol{\vartheta}_h\|_{0,s;K}^s \leqslant \widehat{C}_4 \left\{ h_K^\sigma \, \|\boldsymbol{\vartheta} - \boldsymbol{\vartheta}_h\|_{0,K}^s + \|\phi - \phi_h\|_{0,s;K}^s \right\} \qquad \forall\, K \in \mathcal{T}_h \tag{5.18}$$

and

$$h_e \, \|\phi_{\mathrm{D}} - \phi_h\|_{0,s;e}^s \leqslant \widehat{C}_5 \left\{ h_{K_e}^\sigma \, \|\boldsymbol{\vartheta} - \boldsymbol{\vartheta}_h\|_{0,K_e}^s + \|\phi - \phi_h\|_{0,s;K_e}^s \right\} \qquad \forall\, e \in \mathcal{E}_h(\Gamma) \,, \tag{5.19}$$

where K_e is the triangle/tetrahedron of $\mathcal{T}_h$ having e as an edge/face, while $\sigma = 2$ when $n = 2$, and $\sigma = 3 - s/2$ when $n = 3$.

Proof. The estimates (5.18) and (5.19) follow from straightforward adaptations of [16, Lemmas 5.11 and 5.12], respectively, by replacing the L^4-norm used therein with the L^s-norm and omitting the

nonlinear terms considered there. Alternatively, the proof follows the same strategy as in Lemmas 4.8 and 4.9. We omit the details. ▫

As a preliminary step before proving an estimate for $\widehat{\Theta}_{3,K}$, we note that, by applying the triangle and Hölder inequalities, we obtain

$$\begin{aligned}\|\mathbf{u}\cdot\boldsymbol{\vartheta}-\mathbf{u}_h\cdot\boldsymbol{\vartheta}_h\|_{0,t;K} &\leqslant \|\mathbf{u}\cdot(\boldsymbol{\vartheta}-\boldsymbol{\vartheta}_h)\|_{0,t;K}+\|(\mathbf{u}-\mathbf{u}_h)\cdot\boldsymbol{\vartheta}_h\|_{0,t;K}\\ &\leqslant \|\mathbf{u}\|_{0,\rho;K}\,\|\boldsymbol{\vartheta}-\boldsymbol{\vartheta}_h\|_{0,K}+\|\mathbf{u}-\mathbf{u}_h\|_{0,\rho;K}\,\|\boldsymbol{\vartheta}_h\|_{0,\Omega}\,,\end{aligned}$$

which, together with the fact that $\mathbf{u}\in\mathbf{W}(r)$ and the *a priori* estimate (3.34), becomes

$$\|\mathbf{u}\cdot\boldsymbol{\vartheta}-\mathbf{u}_h\cdot\boldsymbol{\vartheta}_h\|_{0,t;K}\leqslant C\left\{\|\boldsymbol{\vartheta}-\boldsymbol{\vartheta}_h\|_{\mathrm{div}_t;K}+\|\mathbf{u}-\mathbf{u}_h\|_{0,\rho;K}\right\}, \tag{5.20}$$

where C is a positive constant depending only on κ, η, ρ, $C_{\widehat{b},\mathtt{d}}$, $|\Omega|$, r, and $\widehat{\Psi}_2(g,\phi_{\mathrm{D}})$.

Lemma 5.9 *There exists a positive constant $\widehat{C}_6$, depending on κ, η, ρ, $C_{\widehat{b},\mathtt{d}}$, $|\Omega|$, r, and $\widehat{\Psi}_2(g,\phi_{\mathrm{D}})$, but independent of h, such that*

$$\|g+\mathrm{div}(\boldsymbol{\vartheta}_h)-\eta\,\phi_h-\kappa^{-1}\,\mathbf{u}_h\cdot\boldsymbol{\vartheta}_h\|^t_{0,t;K}\leqslant\widehat{C}_6\left\{\|\boldsymbol{\vartheta}-\boldsymbol{\vartheta}_h\|^t_{\mathrm{div}_t;K}+\|\phi-\phi_h\|^t_{0,s;K}+\|\mathbf{u}-\mathbf{u}_h\|^t_{0,\rho;K}\right\}, \tag{5.21}$$

for all $K\in\mathcal{T}_h$.

Proof. We first observe that the fourth row of the system (3.27) implies $\mathrm{div}(\boldsymbol{\vartheta})-\eta\,\phi-\kappa^{-1}\,\mathbf{u}\cdot\boldsymbol{\vartheta}=-g$ in $\mathrm{L}^t(\Omega)$. Then, by applying the triangle inequality together with the estimate (5.20), we readily obtain (5.21). Further details are omitted. ▫

We are now in a position to establish the main result of this section, namely, the efficiency of the *a posteriori* error estimator $\Theta_{\mathtt{FM}}$.

Theorem 5.10 *Let $(\boldsymbol{\sigma},\mathbf{u},\boldsymbol{\vartheta},\phi)\in\mathcal{H}\times\mathcal{Q}\times\mathrm{X}\times\mathrm{Y}$ and $(\boldsymbol{\sigma}_h,\mathbf{u}_h,\boldsymbol{\vartheta}_h,\phi_h)\in\mathbb{H}^{\boldsymbol{\sigma}}_h\times\mathbf{H}^{\mathbf{u}}_h\times\mathbf{H}^{\boldsymbol{\vartheta}}_h\times\widehat{\mathrm{H}}^{\phi}_h$ be the solutions to (3.27) and (3.28), respectively. Then, $\Theta_{\mathtt{FM}}$ is an efficient estimator, i.e. there exists a positive constant C_{eff}, depending on ν_0, $\mathtt{D}_1$, $\mathtt{F}_1$, κ, η, ρ, $C_{\widehat{b},\mathtt{d}}$, r, $\widehat{\Psi}_2(g,\phi_{\mathrm{D}})$, but independent of h, such that*

$$C_{\mathrm{eff}}\,\Theta_{\mathtt{FM}}+\mathtt{h.o.t.}\leqslant\|(\boldsymbol{\sigma}-\boldsymbol{\sigma}_h,\mathbf{u}-\mathbf{u}_h)\|_{\mathcal{H}\times\mathcal{Q}}+\|(\boldsymbol{\vartheta}-\boldsymbol{\vartheta}_h,\phi-\phi_h)\|_{\mathrm{X}\times\mathrm{Y}}\,.$$

Proof. Assuming that ϕ_{D}, $\mathbf{u}_{\mathrm{D}}$, f, and $\frac{1}{\nu}$ are piecewise polynomial, the result follows directly from Lemmas 4.8–4.11 together with Lemmas 5.7–5.8 and the bound (4.37). Further details are omitted. ▫

6 Numerical results

In this section, we assess the performance and accuracy of the mixed schemes (3.13) and (3.28), and illustrate the reliability and efficiency of the *a posteriori* error estimators $\widetilde{\Theta}_{\mathtt{MP}}$ and $\Theta_{\mathtt{FM}}$ (cf. (4.39) and (5.1)) derived in Sections 4 and 5. We emphasize here that the implementation of $\widetilde{\Theta}_{\mathtt{MP}}$ is preferred over $\Theta_{\mathtt{MP}}$ for the reasons detailed in Section 4.4. The corresponding finite element subspaces generated by $k\in\{0,1\}$ are denoted by $\mathbb{RT}_k-\mathbf{P}_k-\mathrm{P}_{k+1}-\mathrm{P}_k$ for the mixed-primal scheme and $\mathbb{RT}_k-\mathbf{P}_k-\mathbf{RT}_k-\mathrm{P}_k$ for the fully-mixed case. The computational results were obtained using `FreeFEM` [32], where the resulting nonlinear systems (3.13) and (3.28) are solved via a Newton–Raphson algorithm with a fixed

tolerance of $\mathtt{tol} = 1\mathrm{E}-06$. The iterative process terminates when the relative error between two successive iterates of the full coefficient vector $\mathbf{coeff}^m$ and $\mathbf{coeff}^{m+1}$ satisfies

$$\frac{\|\mathbf{coeff}^{m+1} - \mathbf{coeff}^m\|_{\mathtt{DoF}}}{\|\mathbf{coeff}^{m+1}\|_{\mathtt{DoF}}} \leqslant \mathtt{tol}\,,$$

where $\|\cdot\|_{\mathtt{DoF}}$ denotes the standard Euclidean norm in $\mathrm{R}^{\mathtt{DoF}}$, and $\mathtt{DoF}$ represents the total number of degrees of freedom associated with the finite element subspaces involved.

The global errors for the mixed-primal and fully-mixed formulations are defined, respectively, by

$$\mathsf{e}_{\mathtt{MP}} := \mathsf{e}(\boldsymbol{\sigma}) + \mathsf{e}(\mathbf{u}) + \mathsf{e}(\phi) + \mathsf{e}(\lambda) \quad \text{and} \quad \mathsf{e}_{\mathtt{FM}} := \mathsf{e}(\boldsymbol{\sigma}) + \mathsf{e}(\mathbf{u}) + \mathsf{e}(\boldsymbol{\vartheta}) + \widehat{\mathsf{e}}(\phi)\,,$$

where

$$\mathsf{e}(\boldsymbol{\sigma}) := \|\boldsymbol{\sigma} - \boldsymbol{\sigma}_h\|_{\mathbf{div}_\ell;\Omega}\,, \quad \mathsf{e}(\mathbf{u}) := \|\mathbf{u} - \mathbf{u}_h\|_{0,\rho;\Omega}\,, \quad \mathsf{e}(\phi) := \|\phi - \phi_h\|_{1,\Omega}\,,$$

$$\mathsf{e}(\lambda) := \|\lambda - \lambda_{\widetilde{h}}\|_{0,\Gamma}\,, \quad \mathsf{e}(\boldsymbol{\vartheta}) := \|\boldsymbol{\vartheta} - \boldsymbol{\vartheta}_h\|_{\mathrm{div}_t;\Omega}\,, \quad \text{and} \quad \widehat{\mathsf{e}}(\phi) := \|\phi - \phi_h\|_{0,s;\Omega}\,,$$

and ℓ, t and s are described in (3.26) in terms of $\rho \in [3,4]$, and will be specified in the examples below. Furthermore, the effectivity index associated to the global estimators $\widetilde{\Theta}_{\mathtt{MP}}$ and $\Theta_{\mathtt{FM}}$ (cf. (4.39) and (5.1)) are denoted, respectively, by

$$\mathrm{eff}(\widetilde{\Theta}_{\mathtt{MP}}) := \frac{\mathsf{e}_{\mathtt{MP}}}{\widetilde{\Theta}_{\mathtt{MP}}} \quad \text{and} \quad \mathrm{eff}(\Theta_{\mathtt{FM}}) := \frac{\mathsf{e}_{\mathtt{FM}}}{\Theta_{\mathtt{FM}}}\,.$$

The uniform boundedness of this index provides computational evidence for the reliability and efficiency of the corresponding estimator. As anticipated in Section 4.4, we will see in the following examples that $\mathrm{eff}(\widetilde{\Theta}_{\mathtt{MP}})$ is indeed uniformly bounded.

Next, by using that $\mathtt{DoF}^{-1/n} \cong h$, we compute the corresponding experimental convergence rates as

$$\mathsf{r}(\diamond) := -n\,\frac{\log(\mathsf{e}(\diamond)/\mathsf{e}'(\diamond))}{\log(\mathtt{DoF}/\mathtt{DoF}')} \qquad \text{for } \diamond \in \{\boldsymbol{\sigma}, \mathbf{u}, \boldsymbol{\vartheta}, \phi, \lambda\}\,,$$

where $\mathtt{DoF}$ and $\mathtt{DoF}'$ denote the total degrees of freedom associated to two consecutive triangulations with errors e and e', respectively. The experimental rates of convergence associated with ϕ in the fully-mixed approach, denoted by $\widehat{\mathsf{r}}(\phi)$, is computed by replacing $\mathsf{e}(\phi)$ by $\widehat{\mathsf{e}}(\phi)$ in the above formula. We also denote by $\mathsf{r}_{\mathtt{MP}}$ and $\mathsf{r}_{\mathtt{FM}}$ the convergence rates associated with the total errors for the mixed-primal and fully-mixed formulations, respectively, which are computed as in the above formula by replacing the individual errors by the global errors.

As noted in [6, Section 5], additional physically relevant variables, including the pressure, velocity gradient, vorticity, and shear stress tensor, can be recovered via suitable postprocessing formulae. Here, we restrict attention to the pressure field, which is approximated by means of (3.2) as

$$p_h = -\frac{1}{n}\mathrm{tr}(\boldsymbol{\sigma}_h) + \frac{\nu}{n}\,f \quad \text{in} \quad \Omega\,.$$

Regarding the construction of the boundary mesh in the mixed-primal approach, the partition $\{\Gamma_1, \ldots, \Gamma_m\}$ is defined such that each segment Γ_i consists of exactly two edges of $\mathcal{E}_h(\Gamma)$. Consequently, the assumptions of Theorem 4.15 are satisfied, and the mesh constraint $h \leqslant C_0\,\widetilde{h}$ (cf. [6, Section 3.5]) is fulfilled with $C_0 = 1/2$.

The examples considered in this section are described below. For all subsequent tests, the potential gravitational acceleration is taken as $\mathbf{g} = -\mathbf{e}_n$, where $\mathbf{e}_n$ denotes the n-th canonical vector in R^n.

In the first three tests, for the sake of simplicity, we set $\kappa = 1$, $\eta = 1$, and $\phi_{\mathtt{r}} = 0$, and choose the Brinkman, Darcy, and Forchheimer coefficients as follows:

$$\nu(\mathbf{x}) = \exp\left(-\prod_{i=1}^{n} x_i\right), \quad \mathtt{D}(\mathbf{x}) = \exp\left(-\sum_{i=1}^{n} x_i\right), \quad \text{and} \quad \mathtt{F}(\mathbf{x}) = \exp\left(\sum_{i=1}^{n} x_i\right),$$

respectively. Notice that ν, $\mathtt{D}$ and $\mathtt{F}$ satisfy (2.2). In addition, the mean value of $\mathrm{tr}(\boldsymbol{\sigma}_h)$ over Ω is fixed via a Lagrange multiplier strategy, which means adding one row and one column to the matrix system that solves (3.13) and (3.28) for $(\boldsymbol{\sigma}_h, \mathbf{u}_h)$.

Example 1 is devoted to validating the reliability and efficiency of the *a posteriori* error estimators $\widetilde{\Theta}_{\mathtt{MP}}$ and $\Theta_{\mathtt{FM}}$. Examples 2, 3, and 4 are then employed to illustrate the performance of the associated adaptive algorithm on two- and three-dimensional domains, both with and without manufactured solutions, following the adaptive procedure proposed in [39]:

(1) Start with a coarse mesh $\mathcal{T}_h$.

(2) Solve the Newton iterative method associated to (3.13) (resp. (3.28)) for the current mesh $\mathcal{T}_h$.

(3) Compute the local indicator $\widetilde{\Theta}_{\mathtt{MP},K}$ in the mixed-primal case for each $K \in \mathcal{T}_h$, where

$$\widetilde{\Theta}_{\mathtt{MP},K} = \Theta_{1,K} + \left(\Theta_{2,K}^2 + \Theta_{3,K}^2 + \Theta_{5,K}^2\right)^{1/2} + \Theta_{4,K},$$

with each local error indicator defined respectively in (4.2), (4.3), (4.4), (4.40), and (4.5), whereas in the fully-mixed case,

$$\Theta_{\mathtt{FM},K} = \Theta_{1,K} + \left(\Theta_{2,K}^2 + \widehat{\Theta}_{1,K}^2\right)^{1/2} + \Theta_{4,K} + \widehat{\Theta}_{2,K} + \widehat{\Theta}_{3,K},$$

with each local error indicator given in (4.2), (4.3), (5.2), (4.5), (5.3), and (5.4), respectively.

(4) Check the stopping criterion and decide whether to finish or go to the next step.

(5) Use the automatic meshing algorithm adaptmesh from [33, Section 9.1.9] to refine each $K' \in \mathcal{T}_h$ satisfying

$$\Theta_{K'} \geqslant C_{\mathrm{adm}} \frac{1}{\#K} \sum_{K \in \mathcal{T}_h} \Theta_K, \quad \text{for some } C_{\mathrm{adm}} \in (0,1),$$

where $\#K$ denotes the number of triangles of the mesh $\mathcal{T}_h$, and Θ_K stands for $\widetilde{\Theta}_{\mathtt{MP},K}$ or $\Theta_{\mathtt{FM},K}$.

(6) Define the resulting mesh as the current mesh $\mathcal{T}_h$, and go to step (2).

In particular, in Examples 2, 3 and 4, we set C_{adm} as 0.83, 0.9, and 0.85, respectively.

Example 1: Accuracy assessment with a smooth solution in the unit square

In this test, we focus on the accuracy of the mixed methods (3.13) and (3.28), and examine the performance of the effectivity index for both schemes. The domain is the square $\Omega = (0,1)^2$. We choose the inertial power $\rho = 3$, from which the remaining parameters follow as $\ell = 3/2$, $s = 6$, and $t = 6/5$ (cf. (3.26)). We then adjust the data $\mathbf{f}(\phi)$ (cf. (2.3)), f, and g in (2.1) so that the exact solutions are given by

$$\mathbf{u}(\mathbf{x}) = \begin{pmatrix} \cos(\pi x_1)\, \sin(\pi x_2) \\ \sin(\pi x_1)\, \exp(x_2) \end{pmatrix}, \quad p(\mathbf{x}) = \cos(\pi x_1)\, \sin(\pi x_2), \quad \text{and} \quad \phi(\mathbf{x}) = 0.1 + 0.3\, \exp(x_1 x_2).$$

Additionally, the model problem is complemented with the appropriate Dirichlet boundary conditions.

The errors and the corresponding convergence rates are reported in Tables 6.1 and 6.2, and are consistent with the theoretical bounds established in [6, Theorems 4 and 8]. In addition, we compute the global *a posteriori* error indicators $\widetilde{\Theta}_{\texttt{MP}}$ and $\Theta_{\texttt{FM}}$ (cf. (4.39) and (5.1)) and assess their reliability and efficiency through the effectivity index. We observe that this index remains uniformly bounded. In all cases, and for both discrete schemes, the Newton iteration converges in four steps.

Mixed-primal $\mathbb{RT}_k - \mathbf{P}_k - \mathrm{P}_{k+1} - \mathrm{P}_k$ scheme with $k = 0$											
DoF	$\mathsf{e}(\boldsymbol{\sigma})$	$\mathsf{r}(\boldsymbol{\sigma})$	$\mathsf{e}(\mathbf{u})$	$\mathsf{r}(\mathbf{u})$	$\mathsf{e}(\phi)$	$\mathsf{r}(\phi)$	$\mathsf{e}(\lambda)$	$\mathsf{r}(\lambda)$	$\mathsf{e}_{\texttt{MP}}$	$\mathsf{r}_{\texttt{MP}}$	$\mathrm{eff}(\widetilde{\Theta}_{\texttt{MP}})$
914	1.58E+00	–	1.54E-01	–	3.25E-02	–	1.07E-01	–	1.88E+00	–	0.409
1988	1.04E+00	1.094	9.97E-02	1.114	2.20E-02	0.999	7.07E-02	1.071	1.23E+00	1.093	0.393
5313	6.28E-01	1.019	6.16E-02	0.979	1.29E-02	1.081	4.06E-02	1.131	7.43E-01	1.023	0.394
17342	3.42E-01	1.029	3.34E-02	1.037	6.96E-03	1.050	2.22E-02	1.023	4.04E-01	1.029	0.394
60969	1.81E-01	1.010	1.76E-02	1.013	3.71E-03	1.000	1.16E-02	1.034	2.14E-01	1.012	0.392
227170	9.41E-02	0.995	9.13E-03	1.003	1.95E-03	0.981	5.92E-03	1.018	1.11E-01	0.997	0.393

Fully-mixed $\mathbb{RT}_k - \mathbf{P}_k - \mathbf{RT}_k - \mathrm{P}_k$ scheme with $k = 0$											
DoF	$\mathsf{e}(\boldsymbol{\sigma})$	$\mathsf{r}(\boldsymbol{\sigma})$	$\mathsf{e}(\mathbf{u})$	$\mathsf{r}(\mathbf{u})$	$\mathsf{e}(\boldsymbol{\vartheta})$	$\mathsf{r}(\boldsymbol{\vartheta})$	$\widehat{\mathsf{e}}(\phi)$	$\widehat{\mathsf{r}}(\phi)$	$\mathsf{e}_{\texttt{FM}}$	$\mathsf{r}_{\texttt{FM}}$	$\mathrm{eff}(\Theta_{\texttt{FM}})$
1188	1.58E+00	–	1.54E-01	–	5.80E-02	–	1.81E-02	–	1.81E+00	–	0.386
2622	1.04E+00	1.074	9.97E-02	1.094	3.95E-02	0.969	1.41E-02	0.619	1.19E+00	1.067	0.371
7095	6.28E-01	1.006	6.16E-02	0.967	2.36E-02	1.039	8.25E-03	1.082	7.21E-01	1.005	0.374
23376	3.42E-01	1.020	3.34E-02	1.029	1.25E-02	1.065	4.59E-03	0.983	3.92E-01	1.022	0.374
82623	1.81E-01	1.006	1.76E-02	1.009	6.73E-03	0.981	2.61E-03	0.893	2.08E-01	1.004	0.372
308772	9.41E-02	0.993	9.13E-03	1.001	3.46E-03	1.007	1.34E-03	1.013	1.08E-01	0.994	0.373

Table 6.1: [Example 1, $k = 0$] Number of degrees of freedom, errors, rates of convergence, and effectivity index for the mixed approximations.

Mixed-primal $\mathbb{RT}_k - \mathbf{P}_k - \mathrm{P}_{k+1} - \mathrm{P}_k$ scheme with $k = 1$											
DoF	$\mathsf{e}(\boldsymbol{\sigma})$	$\mathsf{r}(\boldsymbol{\sigma})$	$\mathsf{e}(\mathbf{u})$	$\mathsf{r}(\mathbf{u})$	$\mathsf{e}(\phi)$	$\mathsf{r}(\phi)$	$\mathsf{e}(\lambda)$	$\mathsf{r}(\lambda)$	$\mathsf{e}_{\texttt{MP}}$	$\mathsf{r}_{\texttt{MP}}$	$\mathrm{eff}(\widetilde{\Theta}_{\texttt{MP}})$
2891	9.28E-02	–	7.22E-03	–	1.14E-03	–	4.84E-03	–	1.06E-01	–	0.284
6427	3.99E-02	2.114	3.16E-03	2.066	4.79E-04	2.178	2.14E-03	2.043	4.57E-02	2.108	0.274
17531	1.45E-02	2.016	1.21E-03	1.918	1.62E-04	2.163	7.61E-04	2.061	1.66E-02	2.013	0.273
56983	4.43E-03	2.014	3.71E-04	2.005	4.51E-05	2.166	2.34E-04	2.001	5.08E-03	2.014	0.275
198563	1.26E-03	2.011	1.04E-04	2.034	1.25E-05	2.055	6.54E-05	2.041	1.44E-03	2.014	0.277
743263	3.39E-04	1.993	2.77E-05	2.008	3.26E-06	2.037	1.73E-05	2.012	3.87E-04	1.995	0.276

Fully-mixed $\mathbb{RT}_k - \mathbf{P}_k - \mathbf{RT}_k - \mathrm{P}_k$ scheme with $k = 1$											
DoF	$\mathsf{e}(\boldsymbol{\sigma})$	$\mathsf{r}(\boldsymbol{\sigma})$	$\mathsf{e}(\mathbf{u})$	$\mathsf{r}(\mathbf{u})$	$\mathsf{e}(\boldsymbol{\vartheta})$	$\mathsf{r}(\boldsymbol{\vartheta})$	$\widehat{\mathsf{e}}(\phi)$	$\widehat{\mathsf{r}}(\phi)$	$\mathsf{e}_{\texttt{FM}}$	$\mathsf{r}_{\texttt{FM}}$	$\mathrm{eff}(\Theta_{\texttt{FM}})$
3744	9.28E-02	–	7.22E-03	–	1.61E-03	–	5.31E-04	–	1.02E-01	–	0.268
8400	3.99E-02	2.090	3.16E-03	2.043	7.53E-04	1.883	2.81E-04	1.570	4.41E-02	2.080	0.258
23088	1.45E-02	2.001	1.21E-03	1.904	2.69E-04	2.034	1.14E-04	1.785	1.61E-02	1.993	0.258
75456	4.43E-03	2.005	3.71E-04	1.996	8.02E-05	2.046	3.26E-05	2.115	4.91E-03	2.005	0.260
263760	1.26E-03	2.006	1.04E-04	2.029	2.30E-05	1.993	1.05E-05	1.812	1.40E-03	2.006	0.262
989088	3.39E-04	1.990	2.77E-05	2.005	6.21E-06	1.985	2.73E-06	2.038	3.76E-04	1.991	0.261

Table 6.2: [Example 1, $k = 1$] Number of degrees of freedom, errors, rates of convergence, and effectivity index for the mixed approximations.

Example 2: Adaptivity in a 2D nonconvex horseshoe-shaped domain

The second numerical example is aimed at testing the performance of the adaptive mesh refinement based on the *a posteriori* error estimators $\widetilde{\Theta}_{\texttt{MP}}$ and $\Theta_{\texttt{FM}}$ (cf. (4.39) and (5.1)). To this end, we consider a 2D horseshoe-shaped domain defined as $\Omega = (-1,1)\times(-0.25,1.25)\backslash(-0.75,0.75)\times(0.25,1.25)$, and the inertial power given by $\rho = 7/2$, thus leaving the other parameters as $\ell = 7/5$, $s = 14/3$, and $t = 14/11$ (cf. (3.26)). The data $\mathbf{f}(\phi)$, f and g are defined so that the exact solutions are given by

$$\mathbf{u}(\mathbf{x}) = \begin{pmatrix} \dfrac{x_2-0.26}{r_2(\mathbf{x})} + \dfrac{x_2-0.26}{r_1(\mathbf{x})} \\ -\dfrac{x_1+0.74}{r_2(\mathbf{x})} - \dfrac{x_1-0.74}{r_1(\mathbf{x})} \end{pmatrix}, \quad p(\mathbf{x}) = \sin(\pi x_1)\,\cos(\pi x_2)\,,$$

$$\text{and} \quad \phi(\mathbf{x}) = 0.5 + 0.2\,\tanh(25\,\alpha(\mathbf{x}))\,,$$

where

$$r_1(\mathbf{x}) = \sqrt{(x_1-0.74)^2+(x_2-0.26)^2}\,, \quad r_2(\mathbf{x}) = \sqrt{(x_1+0.74)^2+(x_2-0.26)^2}\,,$$
$$\text{and} \quad \alpha(\mathbf{x}) = x_2 - (0.3 + 0.4\,x_1^2)\,.$$

Note that $\mathbf{u}$ exhibits two singularities near the points $(\pm 0.25, 0.75)$ placed in the boundary of the domain Ω, and ϕ has large gradients along the curve $\alpha(\mathbf{x}) = 0$.

The refinement histories for the mixed-primal formulation with $k = 0$ and $k = 1$ are reported in Tables 6.3 and 6.4, respectively, to assess the accuracy of the *a posteriori* error estimator $\widetilde{\Theta}_{\texttt{MP}}$ and the asymptotic convergence rates for both the quasi-uniform refinement and the adaptive refinement. We remark that in all the experiments the Newton iteration finished in the fourth step. As the fully-mixed formulation exhibits the same behavior, we restrict the tabulated results to the mixed-primal case and present the remaining comparisons between quasi-uniform and adaptive refinements in Figure 6.1. Notice how the quasi-uniform refinement presents disturbed convergence and how optimal convergence rates are attained at the presence of adaptive refinement guided by the *a posteriori* error estimators. Moreover, from Figure 6.1, we observe that in all cases, adaptive refinement leads to more accurate results at a cheaper computational cost. Finally, the initial mesh, some refinements, and some computed solutions, are illustrated in Figure 6.2. The computed solutions were obtained with the mixed-primal formulation with $k = 1$, in the nine step of the adaptive process, and with 1,133,942 `DoF`.

Example 3: Adaptivity in a 3D L-shaped domain

In this third test, we consider the L-shaped 3D domain $\Omega = (-0.5,0.5)\times(0,0.5)\times(-0.5,0.5)\backslash(0,0.5)^3$ and set the inertial power to $\rho = 4$, which leads to the indices $\ell = 4/3$, $s = 4$, and $t = 4/3$ (cf. (3.26)). The manufactured solutions are defined by

$$\mathbf{u}(\mathbf{x}) = \begin{pmatrix} \sin(\pi x_1)\,\sin(\pi x_2)\,\sin(\pi x_3) \\ -\cos(\pi x_1)\,\cos(\pi x_2)\,\cos(\pi x_3) \\ \cos(\pi x_1)\,\cos(\pi x_2)\,\sin(\pi x_3) \end{pmatrix}, \quad p(\mathbf{x}) = \frac{10\,x_3}{(x_1-0.05)^2+(x_3-0.05)^2} + p_0\,,$$

$$\text{and} \quad \phi(\mathbf{x}) = 0.1 + 0.3\,\exp(x_1\,x_2\,x_3)\,,$$

where $p_0 \in \mathrm{R}$ is prescribed such that $\int_\Omega p = 0$. The source terms $\mathbf{f}(\phi)$, f, and g, as well as the Dirichlet boundary conditions, are then computed according to these exact solutions.

Mixed-primal $\mathbb{RT}_k - \mathbf{P}_k - \mathrm{P}_{k+1} - \mathrm{P}_k$ scheme with $k = 0$											
Quasi-uniform refinement											
DoF	$\mathsf{e}(\boldsymbol{\sigma})$	$\mathsf{r}(\boldsymbol{\sigma})$	$\mathsf{e}(\mathbf{u})$	$\mathsf{r}(\mathbf{u})$	$\mathsf{e}(\phi)$	$\mathsf{r}(\phi)$	$\mathsf{e}(\lambda)$	$\mathsf{r}(\lambda)$	$\mathsf{e}_{\mathtt{MP}}$	$\mathsf{r}_{\mathtt{MP}}$	$\mathrm{eff}(\widetilde{\Theta}_{\mathtt{MP}})$
1354	5.56E+01	–	2.25E-01	–	7.05E-01	–	1.48E+00	–	5.80E+01	–	0.932
5328	4.54E+01	0.298	1.37E-01	0.724	4.22E-01	0.751	1.29E+00	0.197	4.72E+01	0.301	0.943
21053	3.04E+01	0.583	8.72E-02	0.655	2.21E-01	0.938	6.73E-01	0.951	3.14E+01	0.595	0.907
77858	1.91E+01	0.708	4.71E-02	0.942	1.25E-01	0.877	3.47E-01	1.011	1.96E+01	0.716	0.885
311764	1.02E+01	0.905	2.49E-02	0.917	6.07E-02	1.039	1.59E-01	1.131	1.04E+01	0.910	0.862
1242181	5.41E+00	0.917	1.18E-02	1.080	3.11E-02	0.966	7.77E-02	1.032	5.53E+00	0.919	0.860
Adaptive refinement											
1354	5.56E+01	–	2.25E-01	–	7.05E-01	–	1.48E+00	–	5.80E+01	–	0.932
2155	3.67E+01	1.793	1.27E-01	2.461	4.62E-01	1.826	1.21E+00	0.869	3.85E+01	1.770	0.917
3148	1.91E+01	3.446	1.05E-01	1.022	4.55E-01	0.078	1.26E+00	-0.202	2.09E+01	3.219	0.882
4827	1.03E+01	2.884	9.68E-02	0.358	3.79E-01	0.858	1.21E+00	0.177	1.20E+01	2.600	0.848
7546	7.90E+00	1.187	8.05E-02	0.825	2.81E-01	1.332	8.06E-01	1.820	9.07E+00	1.249	0.829
11276	6.57E+00	0.921	6.04E-02	1.434	2.24E-01	1.120	5.96E-01	1.503	7.45E+00	0.981	0.822
16258	5.40E+00	1.071	5.25E-02	0.766	1.84E-01	1.081	4.53E-01	1.503	6.09E+00	1.102	0.815
23390	4.54E+00	0.947	4.20E-02	1.225	1.47E-01	1.230	4.50E-01	0.038	5.18E+00	0.885	0.827
33001	3.84E+00	0.980	3.55E-02	0.976	1.24E-01	0.998	2.93E-01	2.491	4.29E+00	1.097	0.812
46773	3.22E+00	1.008	2.92E-02	1.120	1.01E-01	1.172	2.54E-01	0.815	3.60E+00	1.000	0.817
66324	2.72E+00	0.957	2.42E-02	1.086	8.16E-02	1.230	2.12E-01	1.040	3.04E+00	0.972	0.816
92927	2.30E+00	1.005	2.01E-02	1.079	7.22E-02	0.726	1.73E-01	1.215	2.56E+00	1.012	0.813

Table 6.3: [Example 2, $k = 0$] Number of degrees of freedom, errors, rates of convergence, and effectivity index for the mixed-primal approximations.

Mixed-primal $\mathbb{RT}_k - \mathbf{P}_k - \mathrm{P}_{k+1} - \mathrm{P}_k$ scheme with $k = 1$											
Quasi-uniform refinement											
DoF	$\mathsf{e}(\boldsymbol{\sigma})$	$\mathsf{r}(\boldsymbol{\sigma})$	$\mathsf{e}(\mathbf{u})$	$\mathsf{r}(\mathbf{u})$	$\mathsf{e}(\phi)$	$\mathsf{r}(\phi)$	$\mathsf{e}(\lambda)$	$\mathsf{r}(\lambda)$	$\mathsf{e}_{\mathtt{MP}}$	$\mathsf{r}_{\mathtt{MP}}$	$\mathrm{eff}(\widetilde{\Theta}_{\mathtt{MP}})$
4191	3.48E+01	–	7.40E-02	–	4.74E-01	–	1.18E+00	–	3.65E+01	–	0.783
16955	2.61E+01	0.410	4.60E-02	0.680	1.36E-01	1.784	4.96E-01	1.243	2.68E+01	0.442	0.820
67935	1.52E+01	0.782	2.04E-02	1.172	3.92E-02	1.794	2.18E-01	1.187	1.54E+01	0.793	0.819
252875	6.34E+00	1.327	7.04E-03	1.618	1.23E-02	1.770	5.22E-02	2.173	6.42E+00	1.337	0.762
1016451	1.91E+00	1.724	2.11E-03	1.733	2.96E-03	2.044	1.29E-02	2.013	1.93E+00	1.727	0.724
Adaptive refinement											
4191	3.48E+01	–	7.40E-02	–	4.74E-01	–	1.18E+00	–	3.65E+01	–	0.783
6977	1.86E+01	2.447	2.98E-02	3.568	1.66E-01	4.118	7.31E-01	1.886	1.96E+01	2.447	0.841
10271	5.07E+00	6.735	7.21E-03	7.344	1.35E-01	1.067	5.12E-01	1.845	5.72E+00	6.359	0.793
17461	1.30E+00	5.132	5.41E-03	1.083	5.31E-02	3.513	3.18E-01	1.790	1.68E+00	4.629	0.731
33986	6.52E-01	2.070	2.63E-03	2.159	3.74E-02	1.053	2.13E-01	1.207	9.05E-01	1.850	0.759
64341	3.49E-01	1.954	1.54E-03	1.683	1.44E-02	2.985	7.94E-02	3.092	4.45E-01	2.226	0.732
130177	1.73E-01	1.987	6.76E-04	2.337	8.45E-03	1.521	3.37E-02	2.431	2.16E-01	2.045	0.714
259210	8.74E-02	1.991	3.62E-04	1.814	3.53E-03	2.537	2.05E-02	1.447	1.12E-01	1.918	0.739
557851	4.07E-02	1.996	1.48E-04	2.341	2.05E-03	1.417	7.55E-03	2.605	5.04E-02	2.078	0.716
1133942	2.11E-02	1.848	8.08E-05	1.698	7.76E-04	2.738	4.25E-03	1.619	2.62E-02	1.843	0.736

Table 6.4: [Example 2, $k = 1$] Number of degrees of freedom, errors, rates of convergence, and effectivity index for the mixed-primal approximations.

Table 6.5 reports the convergence history, once again showing that adaptive refinement yields accurate approximations at a significantly lower computational cost. This effect is particularly evident when compared with the quasi-uniform refinement, where the convergence of the pseudostress tensor approximation is noticeably slower, a behavior that can be attributed to the singularity present in the pressure field. Figure 6.3 displays several refinement iterations, illustrating how the adaptive strategy

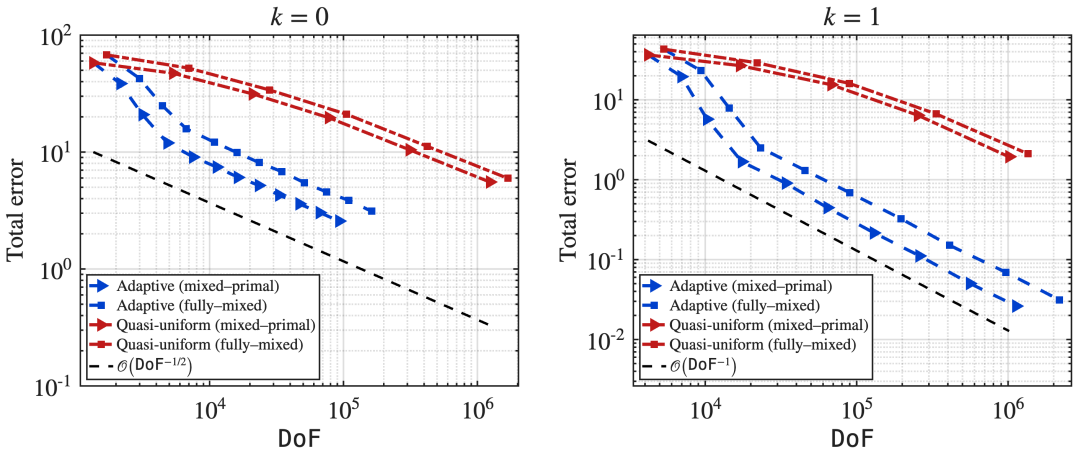

Figure 6.1: [Example 2] Log-log plots of the total error vs. degrees of freedom for $k \in \{0, 1\}$ and for each formulation.

effectively localizes the sources of error in the vicinity of the pressure singularity. The solutions shown were obtained using 543,308 DoF.

Fully-mixed $\mathbb{RT}_k - \mathbf{P}_k - \mathbf{RT}_k - \mathrm{P}_k$ scheme with $k = 0$											
Quasi-uniform refinement											
DoF	$\mathtt{e}(\boldsymbol{\sigma})$	$\mathtt{r}(\boldsymbol{\sigma})$	$\mathtt{e}(\mathbf{u})$	$\mathtt{r}(\mathbf{u})$	$\mathtt{e}(\vartheta)$	$\mathtt{r}(\vartheta)$	$\widehat{\mathtt{e}}(\phi)$	$\widehat{\mathtt{r}}(\phi)$	$\mathtt{e}_{\mathtt{FM}}$	$\mathtt{r}_{\mathtt{FM}}$	$\mathrm{eff}(\Theta_{\mathtt{FM}})$
1952	7.04E+01	–	7.16E-01	–	9.59E-03	–	2.38E-03	–	7.11E+01	–	0.978
14720	5.45E+01	0.379	4.20E-01	0.792	4.77E-03	1.036	1.18E-03	1.041	5.49E+01	0.383	1.013
114176	3.27E+01	0.749	1.81E-01	1.231	2.27E-03	1.090	5.88E-04	1.019	3.29E+01	0.752	1.026
381312	2.29E+01	0.882	1.03E-01	1.397	1.46E-03	1.090	3.92E-04	1.010	2.30E+01	0.884	1.032
1077392	1.67E+01	0.919	5.96E-02	1.588	1.01E-03	1.072	2.76E-04	1.007	1.67E+01	0.922	1.039
Adaptive refinement											
1952	7.04E+01	–	7.16E-01	–	9.59E-03	–	2.38E-03	–	7.11E+01	–	0.978
6148	4.81E+01	0.995	2.89E-01	2.370	8.30E-03	0.377	2.04E-03	0.393	4.84E+01	1.005	0.997
17080	3.31E+01	1.101	1.55E-01	1.839	5.69E-03	1.106	1.51E-03	0.883	3.32E+01	1.104	1.025
56760	2.06E+01	1.177	7.37E-02	1.851	3.91E-03	0.936	1.07E-03	0.869	2.07E+01	1.180	1.035
171208	1.42E+01	1.024	4.46E-02	1.363	2.60E-03	1.108	7.13E-04	1.101	1.42E+01	1.025	1.042
543308	9.74E+00	0.972	2.82E-02	1.190	1.76E-03	1.018	4.88E-04	0.983	9.77E+00	0.973	1.043

Table 6.5: [Example 3, $k = 0$] Number of degrees of freedom, errors, rates of convergence, and effectivity index for the mixed approximations.

Example 4: Flow across a highly heterogeneous porous matrix

In this final example, we evaluate the performance of the proposed adaptive scheme in a domain featuring non-convex geometry and coefficients that vary in space. The setup simulates a fluid passing through a heterogeneous porous matrix into a free-flow regime, validating the robustness of the estimator under complex coupling conditions. For simplicity, in this test we only employ the fully-mixed method (cf. (3.28)). We consider the non-convex domain $\Omega = (0, 4) \times (0, 1) \setminus \Omega_{\mathrm{obs}}$, where $\Omega_{\mathrm{obs}} := [1, 1.8] \times [0.45, 0.55] \cup [1.8, 2.4] \times [0.3, 0.7]$.

Let us define the following functions to regularize the transition between the free-flow and porous

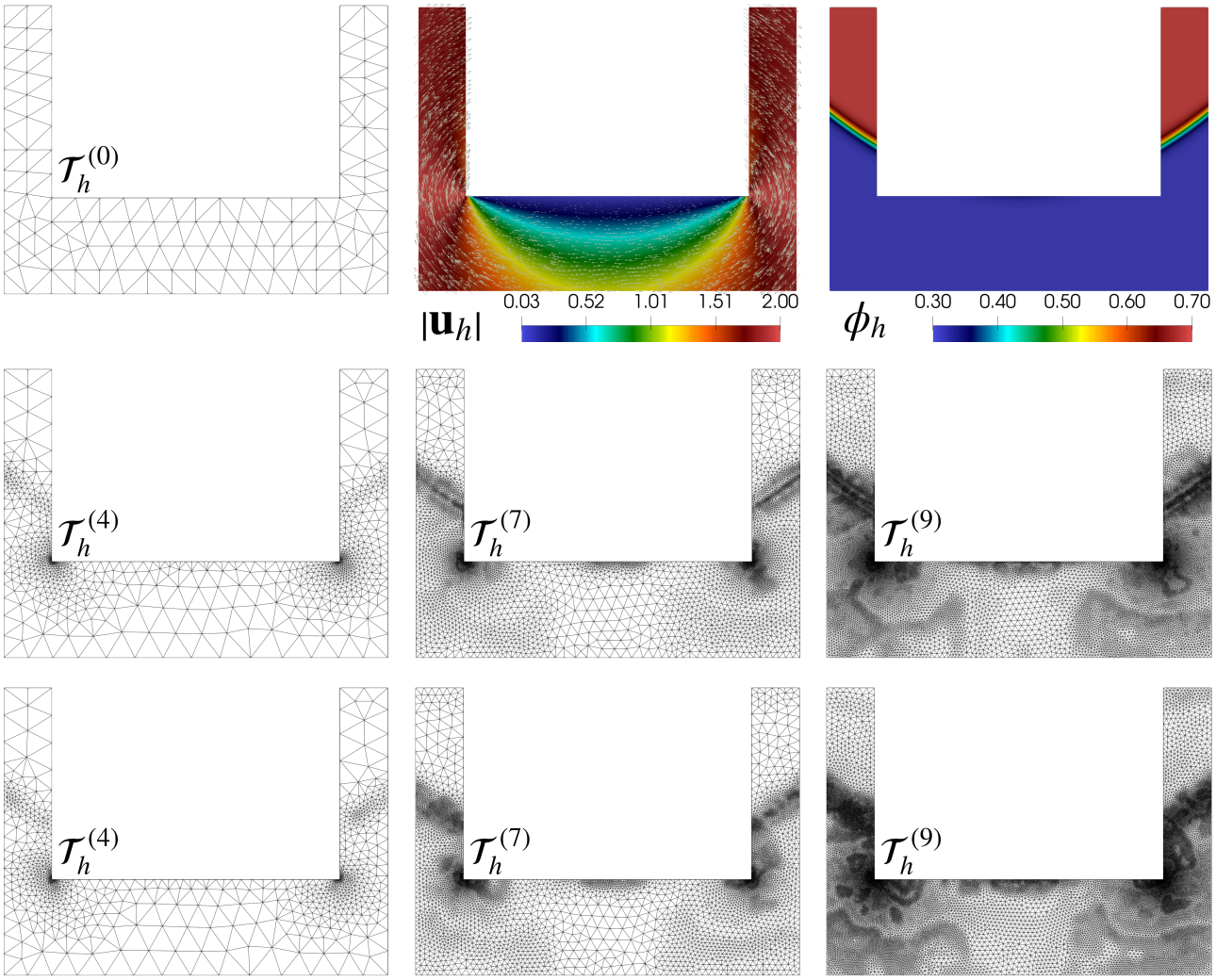

Figure 6.2: [Example 2] Initial mesh (top left), computed velocity and concentration fields (top center and right), three successive adaptive mesh refinements for the mixed-primal scheme (middle row) and for the fully mixed scheme (bottom row).

regions:

$$\delta_1(\mathbf{x}) := \frac{1}{2}\left[1 + \tanh\left(\frac{x_1 - 2.4}{\epsilon_1}\right)\right] \quad \text{and} \quad \delta_2(\mathbf{x}) := \frac{1}{2}\left[1 + \tanh\left(\frac{P(\mathbf{x}) - 0.4}{\epsilon_2}\right)\right] \quad \text{in} \quad \Omega\,,$$

where $\epsilon_1 = 0.1$ and $\epsilon_2 = 0.15$ are small positive parameters that control the thickness of the transition interfaces, and P is the pattern function defined by

$$P(\mathbf{x}) := \sin(2\pi x_1)\cos(3\pi x_2) + 0.5\cos(4\pi x_1)\sin(5\pi x_2) + 0.25\sin(7\pi x_1)\cos(2\pi x_2) \quad \text{in} \quad \Omega\,.$$

Notice that δ_1 is close to 1 in the region where $x_1 > 2.4$ and decays smoothly to 0 as x_1 decreases, while δ_2 is close to 1 in the region where $P(\mathbf{x}) > 0.4$ and decays smoothly to 0 as $P(\mathbf{x})$ decreases. The region governed by free flow is now described by the global indicator function χ_f, constructed from the algebraic union of both transitions:

$$\chi_f(\mathbf{x}) := \delta_1(\mathbf{x}) + \delta_2(\mathbf{x}) - \delta_1(\mathbf{x})\,\delta_2(\mathbf{x}) \quad \text{in} \quad \Omega\,.$$

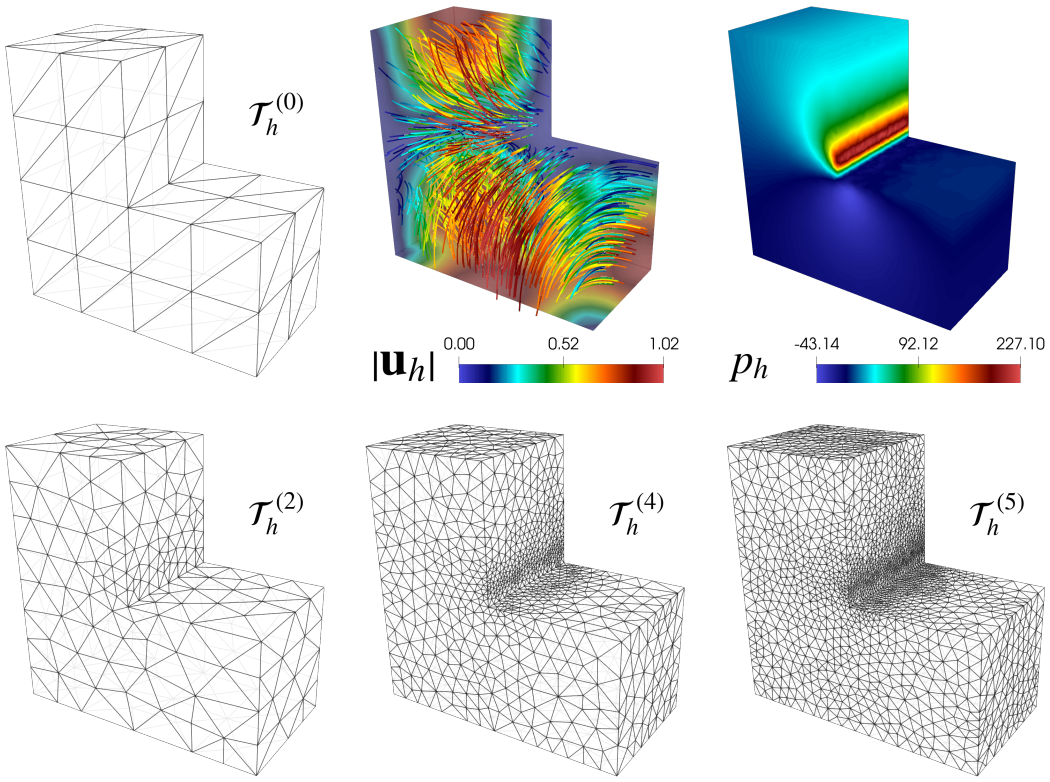

Figure 6.3: [Example 3] Initial mesh, velocity streamlines and pressure field (top), and three adaptive mesh refinement iterations (bottom).

This function takes values close to 1 in the free-flow region and decays smoothly to 0 in the pure rock matrix. Using $\chi_f(\mathbf{x})$, the Darcy and Forchheimer coefficients are extended continuously across the entire domain Ω:

$$\mathtt{D}(\mathbf{x}) := 250\,\theta(\mathbf{x})\big(1-\chi_f(\mathbf{x})\big) \quad \text{and} \quad \mathtt{F}(\mathbf{x}) := \big(2-\theta(\mathbf{x})\big)\big(1-\chi_f(\mathbf{x})\big) \quad \text{in} \quad \Omega\,,$$

where θ is used to model the heterogeneity of the porous medium, highlighting areas of greater compaction, and is defined by

$$\theta(\mathbf{x}) := 1 + 0.4\,\sin\big(4\pi(x_1+0.2x_2)\big) + 0.1\cos(10\pi x_2) \quad \text{in} \quad \Omega\,.$$

Observe that the first equation in the model (2.1) becomes the Stokes equation where $\mathtt{D} = \mathtt{F} = 0$. We stress here that this case is also valid for the continuous and discrete analysis, as noted in [6, Section 3.2]. We also emphasize that $\mathtt{D}$ and $\mathtt{F}$ have steep gradients in the interface between the porous and free-flow regions. Both coefficients are displayed in Figure 6.4.

As in Example 3, we set the inertial power $\rho = 4$. Furthermore, the Brinkman coefficient, as well as the remaining data and coefficients of the model, are given by

$$\nu(\mathbf{x}) = 0.1 + 0.02x_2\,, \quad f = g = 0 \quad \text{in} \quad \Omega\,, \quad \kappa = 5\cdot 10^{-4} \quad \text{and} \quad \eta = 5\cdot 10^{-2}\,.$$

The boundary is partitioned into three disjoint parts, namely, $\Gamma = \Gamma_{\text{in}} \cup \Gamma_{\text{walls}} \cup \Gamma_{\text{out}}$. The inlet Γ_{in} consists in the left side of the channel, the outlet Γ_{out} is the right side of the channel, and Γ_{walls}

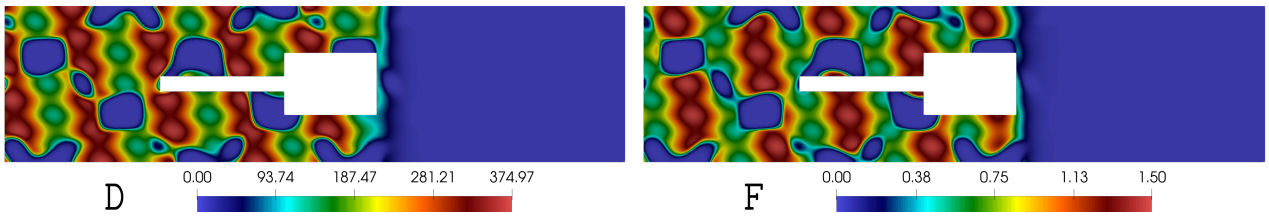

Figure 6.4: [Example 4] Darcy and Forchheimer coefficients.

consists of the ceiling and floor of the channel along with the boundary of the obstacle Ω_{obs}. Under this geometrical setting, the system is complemented with the following mixed boundary conditions:

$$\mathbf{u} = \big(u_{\text{in}}, 0\big)^{\text{t}} \quad \text{on} \quad \Gamma_{\text{in}}\,, \quad \mathbf{u} = \mathbf{0} \quad \text{on} \quad \Gamma_{\text{walls}}\,, \quad \boldsymbol{\sigma}\,\mathbf{n} = \mathbf{0} \quad \text{on} \quad \Gamma_{\text{out}}\,,$$
$$\phi = \phi_{\text{in}} \quad \text{on} \quad \Gamma_{\text{in}}\,, \quad \text{and} \quad \boldsymbol{\vartheta}\cdot\mathbf{n} = 0 \quad \text{on} \quad \Gamma_{\text{walls}} \cup \Gamma_{\text{out}}\,,$$

where

$$u_{\text{in}} = 4\,x_2(1-x_2) \quad \text{and} \quad \phi_{\text{in}} = \begin{cases} 1 - \dfrac{(x_2-0.9)^2}{0.08^2} & \text{if } |x_2 - 0.9| < 0.08\,, \\ 1 - \dfrac{(x_2-0.5)^2}{0.08^2} & \text{if } |x_2 - 0.5| < 0.08\,, \\ 0 & \text{otherwise}\,. \end{cases}$$

As remarked in Example 3 of [6, Section 5], the analysis of the continuous and discrete problems can be slightly adapted to accommodate these particular mixed boundary conditions. Moreover, the *a posteriori* error estimator (5.1) remains unchanged, except that the boundary norms are replaced with norms restricted to the Dirichlet part, since the boundary conditions on the Neumann part are homogeneous. Specifically, we replace Γ with Γ_{in} for the concentration (third term in (5.2) and second term in (5.3)) and with $\Gamma_{\text{in}} \cup \Gamma_{\text{walls}}$ for the velocity (second term in (4.2) and third term in (4.3)). We refer the reader to [18], where this type of boundary conditions is considered.

The proposed setting entails substantial numerical challenges, mainly arising from the sharp transitions of the physical coefficients $\mathtt{D}$ and $\mathtt{F}$ across the porous-fluid interface at $x_1 = 2.4$, as well as from the presence of non-convex corners in Ω_{obs}. These difficulties, together with the heterogeneous structure of the porous matrix and the nonlinear coupling between the Brinkman–Forchheimer and CDR equations, constitute a stringent test for the efficiency and robustness of the adaptive refinement strategy in accurately capturing both localized singularities and complex flow patterns.

Table 6.6 reports the refinement history using the adaptive refinement strategy and the fully-mixed scheme with $k = 1$. We certainly observe a systematic decrease of the error estimator and optimal convergence rates, as expected. Furthermore, Figure 6.5 illustrates how the adaptive refinement successfully detects the steep gradients in $\mathtt{D}$ and $\mathtt{F}$, as well as the corners of the obstacle, while the refinement in the free-flow region remains significantly milder than in the porous region. Figure 6.6 displays the computed velocity, pressure, and concentration profiles. Notably, the fluid exhibits preferential flow paths primarily governed by the heterogeneous porous matrix, which is modeled through the Darcy coefficient. Moreover, the fluid accelerates through narrow constrictions and stabilizes into a parabolic profile upon entering the free-flow region. Regarding the concentration, we observe distinct patterns dictated by the porous matrix and influenced by the localized inlet boundary conditions, which correspond to two separate solute injections that do not initially mix. These behaviors

are in strong agreement with physical expectations, demonstrating that the proposed mixed scheme accurately captures the underlying physics of the coupled model.

Adaptive fully-mixed $\mathbb{RT}_k - \mathbf{P}_k - \mathbf{RT}_k - \mathrm{P}_k$ scheme with $k = 1$									
i	0	1	2	3	4	5	6	7	8
DoF	5169	9882	24255	57405	124974	262299	544056	1130667	2368620
it	8	4	4	4	4	4	4	4	4
$\Theta_{\mathtt{FM}}$	2.93E+02	1.82E+02	9.03E+01	4.88E+01	2.65E+01	1.55E+01	9.54E+00	5.74E+00	3.46E+00
$\mathsf{r}_{\mathtt{FM}}$	–	3.81E+00	1.90E+00	1.76E+00	2.12E+00	1.85E+00	2.15E+00	1.90E+00	2.07E+00

Table 6.6: [Example 4] Number of degrees of freedom, Newton iteration count, global estimator, and experimental rate of convergence of the global estimator for each mesh refinement i.

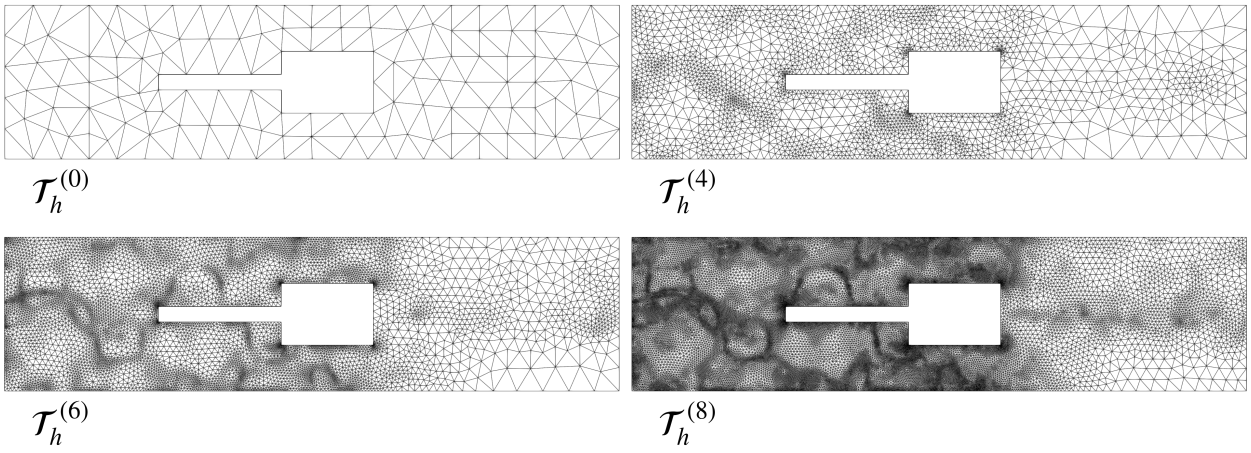

Figure 6.5: [Example 4] Four adaptive mesh refinement iterations.

A Preliminaries for reliability

We start by introducing a few useful notations for describing local information on elements and edges. First, given $K \in \mathcal{T}_h$, we let $\mathcal{E}(K)$ be the set of edges of K, and denote by $\mathcal{E}_h$ the set of all edges of $\mathcal{T}_h$, with corresponding diameters denoted by h_e. Then, we set $\mathcal{E}_h = \mathcal{E}_h(\Omega) \cup \mathcal{E}_h(\Gamma)$, where $\mathcal{E}_h(\Omega) := \{e \in \mathcal{E}_h \ : \ e \subset \Omega\}$ and $\mathcal{E}_h(\Gamma) := \{e \in \mathcal{E}_h \ : \ e \subset \Gamma\}$. Moreover, for each $e \in \mathcal{E}_h$, we fix a unit normal vector to e, denoted by $\mathbf{n}_e$. In the two-dimensional case ($n = 2$), if $\mathbf{n}_e = (n_1, n_2)$, the corresponding unit tangential vector to e is defined as $\mathbf{s}_e := (-n_2, n_1)^{\mathrm{t}}$. When no confusion arises, we will simply write $\mathbf{n}$ and $\mathbf{s}$ instead of $\mathbf{n}_e$ and $\mathbf{s}_e$, respectively. In addition, the usual jump operator $[\![\cdot]\!]$ across an internal edge $e \in \mathcal{E}_h(\Omega)$ is defined for piecewise continuous tensor, vector, or scalar-valued functions ζ as simply $[\![\zeta]\!] := \zeta|_K - \zeta|_{K'}$, where K and K' are the triangles (tetrahedra) of $\mathcal{T}_h$ having e as a common edge (face). Furthermore, for sufficiently smooth scalar w, vector $\mathbf{v} := (v_1, \ldots, v_n)^{\mathrm{t}}$, and tensor fields $\boldsymbol{\tau} := (\tau_{ij})_{i,j=1}^n$, we let

$$\mathrm{curl}(w) := \begin{pmatrix} \dfrac{\partial w}{\partial x_2} \\ -\dfrac{\partial w}{\partial x_1} \end{pmatrix}, \qquad \underline{\mathrm{curl}}(\mathbf{v}) := \begin{cases} \dfrac{\partial v_2}{\partial x_1} - \dfrac{\partial v_1}{\partial x_2} & \text{for } n = 2\,, \\ \nabla \times \mathbf{v} & \text{for } n = 3\,, \end{cases}$$

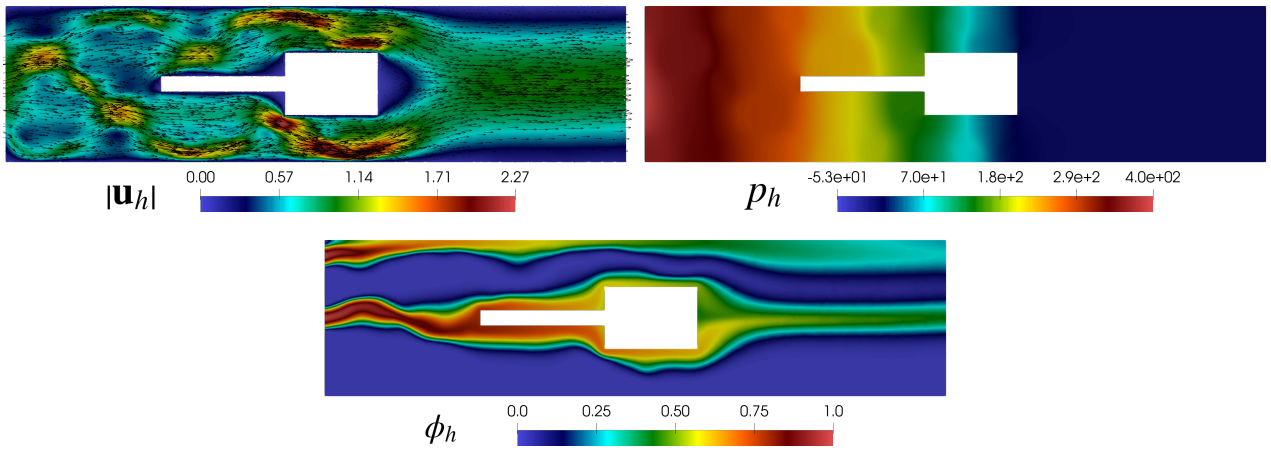

Figure 6.6: [Example 4] Computed velocity, pressure and concentration fields.

$$\mathbf{curl}(\mathbf{v}) := \begin{pmatrix} \dfrac{\partial v_1}{\partial x_2} & -\dfrac{\partial v_1}{\partial x_1} \\ \dfrac{\partial v_2}{\partial x_2} & -\dfrac{\partial v_2}{\partial x_1} \end{pmatrix} \quad \text{for } n = 2\,, \qquad \underline{\mathbf{curl}}(\boldsymbol{\tau}) := \begin{cases} \begin{pmatrix} \underline{\mathrm{curl}}(\boldsymbol{\tau}_1^{\mathrm{t}}) \\ \underline{\mathrm{curl}}(\boldsymbol{\tau}_2^{\mathrm{t}}) \end{pmatrix} & \text{for } n = 2\,, \\ \begin{pmatrix} \underline{\mathrm{curl}}(\boldsymbol{\tau}_1^{\mathrm{t}})^{\mathrm{t}} \\ \underline{\mathrm{curl}}(\boldsymbol{\tau}_2^{\mathrm{t}})^{\mathrm{t}} \\ \underline{\mathrm{curl}}(\boldsymbol{\tau}_3^{\mathrm{t}})^{\mathrm{t}} \end{pmatrix} & \text{for } n = 3\,, \end{cases}$$

$$\boldsymbol{\delta}_*(\mathbf{v}) := \begin{cases} \mathbf{v} \cdot \mathbf{s} & \text{for } n = 2\,, \\ \mathbf{v} \times \mathbf{n} & \text{for } n = 3\,, \end{cases} \qquad \boldsymbol{\delta}_*(\boldsymbol{\tau}) := \begin{cases} \boldsymbol{\tau}\,\mathbf{s} & \text{for } n = 2\,, \\ \begin{pmatrix} (\boldsymbol{\tau}_1^{\mathrm{t}} \times \mathbf{n})^{\mathrm{t}} \\ (\boldsymbol{\tau}_2^{\mathrm{t}} \times \mathbf{n})^{\mathrm{t}} \\ (\boldsymbol{\tau}_3^{\mathrm{t}} \times \mathbf{n})^{\mathrm{t}} \end{pmatrix} & \text{for } n = 3\,, \end{cases}$$

where $\boldsymbol{\tau}_i$ is the i-th row of $\boldsymbol{\tau}$ and the derivatives involved are taken in the distributional sense.

Let us now recall the main properties of the Raviart–Thomas and Clment interpolation operators (cf. [20, 26, 27]). For each $\mathrm{p} \geqslant 2n/(n+2)$, we consider the spaces

$$\mathbf{Z}_{\mathrm{p}} := \Big\{ \boldsymbol{\tau} \in \mathbf{H}(\mathrm{div}_{\mathrm{p}}; \Omega) \ : \quad \boldsymbol{\tau}|_K \in \mathbf{W}^{1,\mathrm{p}}(K) \quad \forall\, K \in \mathcal{T}_h \Big\}\,,$$

and

$$\mathbf{X}_h := \Big\{ \boldsymbol{\tau} \in \mathbf{H}(\mathrm{div}_{\mathrm{p}}; \Omega) \ : \quad \boldsymbol{\tau}|_K \in \mathbf{RT}_k(K) \quad \forall\, K \in \mathcal{T}_h \Big\}\,.$$

In addition, we let $\boldsymbol{\Pi}_h^k : \mathbf{Z}_{\mathrm{p}} \to \mathbf{X}_h$ be the Raviart–Thomas interpolation operator, which is characterized for each $\boldsymbol{\tau} \in \mathbf{Z}_{\mathrm{p}}$ by the identities

$$\int_e \big(\boldsymbol{\Pi}_h^k(\boldsymbol{\tau}) \cdot \mathbf{n}\big)\, \xi = \int_e (\boldsymbol{\tau} \cdot \mathbf{n})\, \xi \qquad \forall\, \xi \in \mathrm{P}_k(e)\,, \quad \forall\, e \in \mathcal{E}_h\,, \tag{A.1}$$

when $k \geqslant 0$, and

$$\int_K \boldsymbol{\Pi}_h^k(\boldsymbol{\tau}) \cdot \boldsymbol{\psi} = \int_K \boldsymbol{\tau} \cdot \boldsymbol{\psi} \qquad \forall\, \boldsymbol{\psi} \in \mathbf{P}_{k-1}(K)\,, \quad \forall\, K \in \mathcal{T}_h\,, \tag{A.2}$$

when $k \geqslant 1$. We now collect some approximation properties of $\boldsymbol{\Pi}_h^k$.

Lemma A.1 *Given* $\mathrm{p} > 1$, *there exist positive constants* c_1 *and* c_2, *independent of* h, *such that for all* $0 \leqslant l \leqslant k$ *and for each* $K \in \mathcal{T}_h$, *there hold*

$$\|\boldsymbol{\tau} - \boldsymbol{\Pi}_h^k(\boldsymbol{\tau})\|_{0,\mathrm{p};K} \leqslant c_1\, h_K^{l+1}\, |\boldsymbol{\tau}|_{l+1,\mathrm{p};K} \qquad \forall\, \boldsymbol{\tau} \in \mathbf{W}^{l+1,\mathrm{p}}(K)\,, \tag{A.3}$$

and

$$\|\boldsymbol{\tau}\cdot\mathbf{n} - \boldsymbol{\Pi}_h^k(\boldsymbol{\tau})\cdot\mathbf{n}\|_{0,\mathrm{p};e} \leqslant c_2\, h_e^{1-1/\mathrm{p}}\, |\boldsymbol{\tau}|_{1,\mathrm{p};K} \qquad \forall\, \boldsymbol{\tau} \in \mathbf{W}^{1,\mathrm{p}}(K)\,, \quad \forall\, e \in \mathcal{E}(K)\,. \tag{A.4}$$

Proof. For the first estimate, we refer to [30, Lemma 3.1], whereas for the second estimate, we refer to [7, Lemma 4.2]. ▫

The following result provides a stable Helmholtz decomposition in $\mathbf{H}(\mathbf{div}_{\mathrm{p}};\Omega)$. Its proof, in the tensor-valued version, can be found in [7, Lemma 4.4].

Lemma A.2 *Let* $1 < \mathrm{p} \leqslant 2$ *when* $n = 2$ *and* $6/5 \leqslant \mathrm{p} \leqslant 2$ *when* $n = 3$. *Then, for each* $\boldsymbol{\psi} \in \mathbf{H}(\mathrm{div}_{\mathrm{p}};\Omega)$, *there exist*

1. $\boldsymbol{\zeta} \in \mathbf{W}^{1,\mathrm{p}}(\Omega)$ *and* $w \in \mathrm{H}^1(\Omega)$ *such that* $\boldsymbol{\psi} = \boldsymbol{\zeta} + \mathrm{curl}(w)$ *in* Ω, *when* $n = 2$,
2. $\boldsymbol{\zeta} \in \mathbf{W}^{1,\mathrm{p}}(\Omega)$ *and* $\mathbf{w} \in \mathbf{H}^1(\Omega)$ *such that* $\boldsymbol{\psi} = \boldsymbol{\zeta} + \underline{\mathrm{curl}}(\mathbf{w})$ *in* Ω, *when* $n = 3$.

Moreover, there hold

$$\|\boldsymbol{\zeta}\|_{1,\mathrm{p};\Omega} + \|w\|_{1,\Omega} \leqslant C_{\mathrm{p}}\, \|\boldsymbol{\psi}\|_{\mathrm{div}_{\mathrm{p}};\Omega} \quad \textit{and} \quad \|\boldsymbol{\zeta}\|_{1,\mathrm{p};\Omega} + \|\mathbf{w}\|_{1,\Omega} \leqslant C_{\mathrm{p}}\, \|\boldsymbol{\psi}\|_{\mathrm{div}_{\mathrm{p}};\Omega}\,,$$

for $n = 2$ *and* $n = 3$, *respectively, where* C_{p} *is a positive constant independent of all the foregoing variables.*

On the other hand, defining $\mathrm{M}_h := \big\{v_h \in C(\overline{\Omega}) \ : \ \ v_h|_K \in \mathrm{P}_1(K) \quad \forall\, K \in \mathcal{T}_h\big\}$ and denoting by $\mathbf{M}_h$ its vector version, we let $\mathcal{I}_h : \mathrm{H}^1(\Omega) \to \mathrm{M}_h$ and $\boldsymbol{\mathcal{I}}_h : \mathbf{H}^1(\Omega) \to \mathbf{M}_h$ be the usual Clment interpolation operator and its vector version, respectively. Some local properties of $\mathcal{I}_h$, and, hence, of $\boldsymbol{\mathcal{I}}_h$, are established in the following lemma.

Lemma A.3 *There exist positive constants* c_1 *and* c_2, *such that*

$$\|v - \mathcal{I}_h(v)\|_{0,K} \leqslant c_1\, h_K\, \|v\|_{1,\Delta(K)} \qquad \forall\, K \in \mathcal{T}_h\,, \tag{A.5}$$

and

$$\|v - \mathcal{I}_h(v)\|_{0,e} \leqslant c_2\, h_e^{1/2}\, \|v\|_{1,\Delta(e)} \qquad \forall\, e \in \mathcal{E}_h\,, \tag{A.6}$$

where $\Delta(K) := \bigcup\{K' \in \mathcal{T}_h \ : \ \ K' \cap K \neq \varnothing\}$ *and* $\Delta(e) := \bigcup\{K' \in \mathcal{T}_h \ : \ \ K' \cap e \neq \varnothing\}$.

B Preliminaries for efficiency

For the efficiency analysis, we apply the localization technique based on bubble functions, along with inverse and discrete trace inequalities. For the former, given $K \in \mathcal{T}_h$, we let K be the usual element-bubble function (cf. [39, eq. (1.5) and Remark 3.2]), which satisfies

$$\psi_K \in \mathrm{P}_{n+1}(K)\,, \quad \mathrm{supp}(\psi_K) \subset K\,, \quad \psi_K = 0 \quad \text{on} \quad \partial K\,, \quad \text{and} \quad 0 \leqslant \psi_K \leqslant 1 \quad \text{in} \quad K\,. \tag{B.1}$$

The specific properties of ψ_K to be employed in what follows, are collected in the following lemma, for whose proof we refer to [39, Lemma 3.3].

Lemma B.1 *Let k be a non-negative integer, and let $\mathrm{p}, \mathrm{q} \in (1, +\infty)$ conjugate to each other, i.e. $1/\mathrm{p} + 1/\mathrm{q} = 1$, and $K \in \mathcal{T}_h$. Then, there exist positive constants c_1, c_2 and c_3, independent of h and K, but depending on the shape-regularity of the triangulations (minimum angle condition) and k, such that for each $u \in \mathrm{P}_k(K)$ there hold*

$$c_1 \, \|u\|_{0,\mathrm{p};\, K} \leqslant \sup_{0 \neq v \in \mathrm{P}_k(K)} \frac{\displaystyle\int_K u \, \psi_K \, v}{\|v\|_{0,\mathrm{q};\, K}} \leqslant \|u\|_{0,\mathrm{p};\, K} \, , \tag{B.2}$$

and

$$c_2 \, h_K^{-1} \, \|\psi_K \, u\|_{0,\mathrm{q};\, K} \leqslant \|\nabla(\psi_K \, u)\|_{0,\mathrm{q};\, K} \leqslant c_3 \, h_K^{-1} \, \|\psi_K \, u\|_{0,\mathrm{q};\, K} \, . \tag{B.3}$$

We also make use of the following inverse inequality (cf. [26, Lemma 1.138]).

Lemma B.2 *Let k, l, and m be non-negative integers such that $m \leqslant l$, and let $\mathrm{p}, \mathrm{q} \in [1, +\infty]$, and $K \in \mathcal{T}_h$. Then, there exists $c > 0$, independent of h, K, p and q, but depending on k, l, m, and the shape regularity of the triangulations, such that*

$$\|v\|_{l,\mathrm{p};\, K} \leqslant c \, h_K^{m-l+n(1/\mathrm{p}-1/\mathrm{q})} \, \|v\|_{m,\mathrm{q};\, K} \qquad \forall \, v \in \mathrm{P}_k(K) \, . \tag{B.4}$$

Finally, proceeding as in [1, Lemma 3.10], that is, employing the usual scaling estimates with respect to a fixed reference element $\widehat{K}$, and applying the trace inequality in $\mathrm{W}^{1,\mathrm{p}}(\widehat{K})$, for a given $\mathrm{p} \in (1, +\infty)$, one is able to establish the following discrete trace inequality.

Lemma B.3 *Let $\mathrm{p} \in (1, +\infty)$. Then, there exists $c > 0$, depending only on the shape regularity of the triangulations, such that for each $K \in \mathcal{T}_h$ and $e \in \mathcal{E}(K)$, there holds*

$$\|v\|^{\mathrm{p}}_{0,\mathrm{p};\, e} \leqslant c \left\{ h_K^{-1} \, \|v\|^{\mathrm{p}}_{0,\mathrm{p};\, K} + h_K^{\mathrm{p}-1} \, |v|^{\mathrm{p}}_{1,\mathrm{p};\, K} \right\} \qquad \forall \, v \in \mathrm{W}^{1,\mathrm{p}}(K) \, . \tag{B.5}$$

References

[1] S. Agmon, *Lectures on Elliptic Boundary Value Problems*. Van Nostrand Mathematical Studies, No. 2, D. Van Nostrand Co., Inc., Princeton, N.J.-Toronto-London, 1965.

[2] M. Ainsworth and J. T. Oden, *A posteriori error estimators for the Stokes and Oseen equations*. SIAM J. Numer. Anal. 34 (1997), no. 1, 228–245.

[3] M. Álvarez, E. Colmenares and F. A. Sequeira, *A posteriori error analysis of a semi-augmented finite element method for double-diffusive natural convection in porous media*. Numer. Methods Partial Differential Equations 40 (2024), no. 4, Paper No. e23090, 48 pp.

[4] M. Álvarez, G. N. Gatica and R. Ruiz-Baier, *A posteriori error analysis for a viscous flow-transport problem*. ESAIM Math. Model. Numer. Anal. 50 (2016), no. 6, 1789–1816.

[5] M. Álvarez, G. N. Gatica and R. Ruiz-Baier, *A posteriori error analysis of a fully-mixed formulation for the Brinkman-Darcy problem*. Calcolo 54 (2017), no. 4, 1491–1519.

[6] A. J. Bustos, S. Caucao and G. N. Gatica, *Mixed-primal and fully-mixed formulations for the convection-diffusion-reaction system based upon Brinkman–Forchheimer equations*. Comput. Math. Appl. 207 (2026), 222–249.

[7] J. Camaño, S. Caucao, R. Oyarzúa, and S. Villa-Fuentes *A posteriori error analysis of a momentum conservative Banach spaces based mixed-FEM for the Navier–Stokes problem*. Appl. Numer. Math. 176 (2022), 134–158.

[8] J. Camaño, C. Muñoz and R. Oyarzúa, *Numerical analysis of a dual-mixed problem in non-standard Banach spaces*. Electron. Trans. Numer. Anal. 48 (2018), 114–130.

[9] C. Carstensen, *A posteriori error estimate for the mixed finite element method*. Math. Comp. 66 (1997), no. 218, 465–476.

[10] C. Carstensen and G. Dolzmann, *A posteriori error estimates for mixed FEM in elasticity*. Numer. Math. 81 (1998), no. 2, 187–209.

[11] S. Caucao, G. N. Gatica, L. F. Gatica, *A posteriori error analysis of a mixed finite element method for the stationary convective Brinkman–Forchheimer problem*. Appl. Numer. Math. 211 (2025), 158–178.

[12] S. Caucao, G. N. Gatica and J. P. Ortega, *A posteriori error analysis of a Banach spaces-based fully mixed FEM for double-diffusive convection in a fluid-saturated porous medium*. Comput. Geosci. 27 (2023), no. 2, 289–316

[13] S. Caucao, G. N. Gatica, R. Oyarzúa, and F. Sandoval, *Residual-based a posteriori error analysis for the coupling of the Navier–Stokes and Darcy–Forchheimer equations*. ESAIM Math. Model. Numer. Anal. 55 (2021), no. 2, 659–687.

[14] S. Caucao, G. N. Gatica, R. Oyarzúa, and P. Zúñiga, *A posteriori error analysis of a mixed finite element method for the coupled Brinkman-Forchheimer and double-diffusion equations*. J. Sci. Comput. 93 (2022), no. 2, Paper No. 50.

[15] S. Caucao, D. Mora, and R. Oyarzúa, *A priori and a posteriori error analysis of a pseudostress-based mixed formulation of the Stokes problem with varying density*. IMA J. Numer. Anal. 36 (2016), no. 2, 947–983.

[16] S. Caucao, R. Oyarzúa and S. Villa-Fuentes, *A posteriori error analysis of a momentum and thermal energy conservative mixed FEM for the Boussinesq equations*. Calcolo 59 (2022), no. 4, Paper No. 45.

[17] S. Caucao and I. Yotov, *A Banach space mixed formulation for the unsteady Brinkman–Forchheimer equations*. IMA J. Numer. Anal. 41 (2021), no. 4, 2708–2743.

[18] S. Caucao and P. Zúñiga, *A posteriori error analysis of a mixed FEM for the coupled Brinkman–Forchheimer/Darcy problem*. East Asian J. Appl. Math., to appear.

[19] A. O. Celebi, V. K. Kalantarov and D. Ugurlu, *On continuous dependence on coefficients of the Brinkman–Forchheimer equations*. Appl. Math. Lett. 19 (2006), no. 8, 801–807.

[20] P. Clément, *Approximation by finite element functions using local regularisation*. RAIRO Modl. Math. Anal. Numr. 9 (1975), 77–84.

[21] E. Colmenares, G. N. Gatica and R. Oyarzúa, *Analysis of an augmented mixed-primal formulation for the stationary Boussinesq problem*. Numer. Methods Partial Differ. Equ. 32 (2016), no. 2, 445–478.

[22] E. Colmenares, G. N. Gatica and R. Oyarzúa, *A posteriori error analysis of an augmented mixed-primal formulation for the stationary Boussinesq model*. Calcolo 54 (2017), 1055–1095.

[23] J. K. Djoko and P. A. Razafimandimby, *Analysis of the Brinkman–Forchheimer equations with slip boundary conditions*. Appl. Anal. 93 (2014), no. 7, 1477–1494.

[24] C. Domínguez, G. N. Gatica and S. Meddahi, *A posteriori error analysis of a fully-mixed finite element method for a two-dimensional fluid-solid interaction problem*. J. Comput. Math. 33 (2015), no. 6, 606–641.

[25] S. Du and X. Xie, *On residual-based a posteriori error estimators for lowest-order Raviart-Thomas element approximation to convection-diffusion-reaction equations*. J. Comput. Math. 32 (2014), no. 5, 522–546.

[26] A. Ern and J.-L. Guermond, *Theory and practice of finite elements*. Applied Mathematical Sciences, 159. Springer-Verlag, New York, 2004.

[27] G. N. Gatica, *A simple introduction to the mixed finite element method. Theory and applications*. SpringerBriefs in Mathematics. Springer, Cham, 2014.

[28] G. N. Gatica, L. F. Gatica, and F. Sequeira, *A priori and a posteriori error analyses of a pseudostress-based mixed formulation for linear elasticity*. Comput. Math. Appl. 71 (2016), no. 2, 585–614.

[29] G. N. Gatica, B. Gómez-Vargas, and R. Ruiz-Baier, *A posteriori error analysis of mixed finite element methods for stress-assisted diffusion problems*. J. Comput. Appl. Math. 409 (2022), Paper No. 114144.

[30] G. N. Gatica, C. Inzunza, R. Ruiz-Baier, and F. Sandoval, *A posteriori error analysis of Banach spaces-based fully-mixed finite element methods for Boussinesq-type models*. J. Numer. Math. 30 (2022), no. 4, 325–356.

[31] G. N. Gatica, A. Márquez, and M. A. Sánchez, *Analysis of a velocity-pressure-pseudostress formulation for the stationary Stokes equations*. Comput. Methods Appl. Mech. Eng. 199 (2010), 1064–1079.

[32] F. Hecht, *New development in FreeFem++*. J. Numer. Math. 20 (2012), 251–265.

[33] F. Hecht, *FreeFem++*. Third edition, Version 3.58-1. Laboratoire Jacques-Louis Lions, Université Pierre et Marie Curie, Paris, 2018.

[34] T. Sayah, *A posteriori error estimates for the Brinkman-Darcy-Forchheimer problem*. Comput. Appl. Math. 40 (2021), no. 7, Paper No. 256.

[35] T. Sayah, G. Semaan and F. Triki, *A posteriori error estimates for Darcy-Forchheimer's problem*. Comput. Methods Appl. Math. 23 (2023), no. 2, 517–544.

[36] T. Sayah, G. Semaan and F. Triki, *Finite element methods for the Darcy–Forchheimer problem coupled with the convection-diffusion-reaction problem*. ESAIM Math. Model. Numer. Anal. 55 (2021), no. 6, 2643–2678.

[37] F. Triki, T. Sayah and G. Semaan, *A posteriori error estimates for Darcy-Forchheimer's problem coupled with the convection-diffusion-reaction equation*. Int. J. Numer. Anal. Model. 21 (2024), no. 1, 65–103.

[38] R. Verfürth, *A posteriori error estimators for convection-diffusion equations.* Numer. Math., 80 (1998), no. 4, 641–663.

[39] R. Verfürth, *A Review of A Posteriori Error Estimation and Adaptive Mesh-Refinement Techniques.* Wiley Teubner, Chichester, 1996.

[40] R. Verfürth, *Robust a posteriori error estimates for stationary convection-diffusion equations.* SIAM J. Numer. Anal. 43 (2005), no. 4, 1766–1782.

Centro de Investigación en Ingeniería Matemática (CI^{2}MA)

PRE-PUBLICACIONES 2026

2026-04 Akbar Davoodi, Diana Piguet, Hanka Rada, Nicolás Sanhueza-Matamala: *The asymptotic version of the Erdős–Sós conjecture and beyond*

2026-05 Rodrigo Abarca Del Rio, Fernando Campos, Cristóbal Caro-Ramírez, Jean François Cretaux, Daniel Moreira, Alfredo Ribeiro Neto, Jonas Felipe Santos De Souza, Mauricio Sepúlveda: *First insights into the performance of the SWOT Level 2 River Single-Pass Vector Data Product in rivers with complex morphology: application to the Bíobío River basin, Chile*

2026-06 Juan José Maulén, Fernando Roldán, Cristian Vega: *Relaxed and inertial nonlinear Forward-Backward algorithm*

2026-07 Luis Briceño-Arias, Fernando Roldán: *Optimal leveraging of smoothness and strong convexity for Peaceman-Rachford splitting*

2026-08 Fahim Aslam, Jianghao Hao, Iqra Kanwal, Mauricio Sepúlveda: *Stability and finite-time blow-up for a fractionally damped nonlinear plate equation: numerical and analytical insights*

2026-09 Fahim Aslam, Zayd Hajjej, Jianghao Hao, Iqra Kanwal, Mauricio Sepúlveda, Rodrigo Véjar: *Stability and blow-up for a suspension bridge plate model with fractional damping and memory*

2026-10 Aníbal Coronel, Fernando Huancas, Mauricio Sepúlveda: *Identification of a power-like reaction term in a reaction-diffusion SIS model*

2026-11 Esteban Henriquez, Manuel Solano: *An unfitted HDG method for a distributed optimal convection-diffusion control problem*

2026-12 Sergio Caucao, Gabriel N. Gatica, Luis F. Gatica, Cristian Inzunza: *A priori and a posteriori error analysis of a mixed FEM for stationary convective Brinkman-Forchheimer flows with variable porosity*

2026-13 Jessika Camaño, Ricardo Oyarzúa, Katherine Rojo, Segundo Villa-Fuentes: *A mixed finite element method based on pseudostress and stream-function for the Navier–Stokes problem in 2D*

2026-14 Raimund Bürger, Cipriano Escalante, Enrique D. Fernández Nieto, Jorge Moya: *A two-dimensional multilayer shallow water model of tsunami-forest interaction*

2026-15 Alonso J. Bustos, Sergio Caucao: *A posteriori error analysis of two mixed formulations for a coupled Brinkman–Forchheimer and convection-diffusion-reaction system*

Para obtener copias de las Pre-Publicaciones, escribir o llamar a: Director, Centro de Investigación en Ingeniería Matemática, Universidad de Concepción, Casilla 160-C, Concepción, Chile, Tel.: 41-2661324, o bien, visitar la página web del centro: `http://www.ci2ma.udec.cl`



Centro de Investigación en
Ingeniería Matemática (CI²MA)
Universidad de Concepción

Casilla 160-C, Concepción, Chile
Tel.: 56-41-2661324/2661554/2661316
http://www.ci2ma.udec.cl